TRANSPORTATION RESEARCH RECORD 678

Tolerable Movement of Bridge Foundations, Sand Drains, K-Test, Slopes, and Culverts

TRANSPORTATION RESEARCH BOARD

COMMISSION ON SOCIOTECHNICAL SYSTEMS
NATIONAL RESEARCH COUNCIL

NATIONAL ACADEMY OF SCIENCES
WASHINGTON, D.C. 1978

Transportation Research Record 678
Price $4.00

modes
1 highway transportation
3 rail transportation
4 air transportation

subject area
63 soil and rock mechanics

Transportation Research Board publications are available by ordering directly from the board. They may also be obtained on a regular basis through organizational or individual supporting membership in the board; members or library subscribers are eligible for substantial discounts. For further information, write to the Transportation Research Board, National Academy of Sciences, 2101 Constitution Avenue, N.W., Washington, DC 20418.

Notice

The papers in this Record have been reviewed by and accepted for publication by knowledgeable persons other than the authors according to procedures approved by a Report Review Committee consisting of members of the National Academy of Sciences, the National Academy of Engineering, and the Institute of Medicine.

The views expressed in these papers are those of the authors and do not necessarily reflect those of the sponsoring committee, the Transportation Research Board, the National Academy of Sciences or the sponsors of TRB activities.

To eliminate a backlog of publications and to make possible earlier, more timely publication of reports given at its meetings, the Transportation Research Board has, for a trial period, adopted less stringent editorial standards for certain classes of published material. The new standards apply only to papers and reports that are clearly attributed to specific authors and that have been accepted for publication after committee review for technical content. Within broad limits, the syntax and style of the published version of these reports are those of the author(s).

The papers in this Record were treated according to the new standards.

Library of Congress Cataloging in Publication Data
National Research Council. Transportation Research Board.
Tolerable movement of bridge foundations, and sand drains, K-test, slopes, and culverts.

(Transportation research record; 678)

1. Bridges–Foundations and piers–Addresses, essays, lectures. 2. Sand drains–Addresses, essays, lectures. 3. Culverts–Addresses, essays, lectures. 4. Roads–Embankments–Addresses, essays, lectures. 5. Soil mechanics–Addresses, essays, lectures. I. Title. II. Series.
TE7.H5 no. 678 [TG320] 380.5'08s [625.7'32] 79-14181
ISBN 0-309-02823-X

Sponsorship of the Papers in This Transportation Research Record

GROUP 2–DESIGN AND CONSTRUCTION OF TRANSPORTATION FACILITIES
Eldon J. Yoder, Purdue University, chairman

Soil Mechanics Section
Lyndon H. Moore, New York State Department of Transportation, chairman

Committee on Embankments and Earth Slopes
Raymond A. Forsyth, California Department of Transportation, chairman
Thomas A. Bellatty, Bruce N. Bosserman, A. Alexander Fungaroli, David S. Gedney, Wilbur M. Haas, Larry G. Hendrickson, William P. Hofmann, Robert D. Holtz, Henry W. Janes, Charles C. Ladd, Richard E. Landau, Harry E. Marshall, Glen L. Martin, Jerry R. Masters, R. M. Mattox, Frank H. McGuigan, Lyndon H. Moore, Melvin W. Morgan, Lyle K. Moulton, Gerald P. Raymond, Dwight A. Sangrey, Walter C. Waidelich, William G. Weber, Jr.

Committee on Foundations of Bridges and Other Structures
Clyde N. Laughter, Wisconsin Department of Transportation, chairman
Arnold Aronowitz, William Bootz, Michael Bozozuk, Bernard E. Butler, Ronald G. Chassie, Harry M. Coyle, Gerald F. Dalquist, M. T. Davisson, Frank M. Fuller, Stanley Gordon, Bernard A. Grand, Robert J. Hallawell, T. J. Hirsch, W. Kenneth Humphries, Hal W. Hunt, Henry W. Janes, Philip Keene, G. A. Leonards, R. M. Mattox, Alex Rutka, John L. Walkinshaw, James Doyle Webb

Committee on Subsurface Soil-Structure Interaction
Raymond J. Krizek, Northwestern University, chairman
John F. Abel, Mike Bealey, Robert M. Clementson, Hameed A. Elnaggar, Delon Hampton, John G. Hendrickson, Jr., Michael G. Katona, J. Neil Kay, G. A. Leonards, Don A. Linger, George W. Ring III, Ernest T. Selig, Corwin L. Tracy, Harry H. Ulery, Jr.

Soil and Rock Properties and Geology Section
David L. Royster, Tennessee Department of Transportation, chairman

Committee on Soil and Rock Properties
William F. Brumund, Golder Associates, chairman
Richard E. Goodman, James P. Gould, Ernest Jonas, Charles C. Ladd, G. A. Leonards, John D. Nelson, Douglas R. Piteau, Gerald P. Raymond, Hassan A. Sultan, David J. Varnes, J. Lawrence Von Thun, Harvey E. Wahls, John L. Walkinshaw, T. H. Wu

John W. Guinnee, Transportation Research Board staff

Sponsorship is indicated by a footnote at the end of each report. The organizational units and officers and members are as of December 31, 1977.

Contents

Tolerable Movements of Bridge Foundations

Philip Keene, Consultant, Middletown, Connecticut

As many aspects of bridge engineering knowledge expand, it is desirable to examine the question of tolerable movements of bridge foundations. It is a subject that has had comparatively little study in the past; this lack has sometimes produced unrealistic results, especially in costly overdesigns. A nationwide investigation of the matter has found differences in definitions and practices. The definition of tolerable movement of highway structure foundations is often complicated. It involves amount of movement, type of structure, effect on each part of structure, cost of alternative choices, effect on traveling public, subjective reasons, and apprehension during design. Case histories illustrate that large movements that cause some harm should be called tolerable if alternative choices are excessively costly or more undersirable. Small movements that result in substantial costs for remedial work should be called intolerable if the movements could have been easily avoided. In addition to the structural analyses to determine the effects of prediction foundation movements, the geotechnical work on which the predicted movements are based should in many cases be improved. Recommendations are given to aid in improving the geotechnical work.

In engineering literature, there have been many publications on tolerable movements of buildings, such as those listed in the bibliography of Feld's paper (1), but few publications, if any, on tolerable movements of highway bridges and other structures. This lack of information on highway structures spurred a 3-year survey by a Transportation Research Board subcommittee of the Committee on Foundations of Bridges and Other Structures. Interest in this aspect of bridge behavior is in keeping with the progressive developments in many other aspects of bridges, such as prestressed concrete girders, orthotropic superstructures, integral abutments, weathering steel, and cantilevered end spans, as well as the use of computers in stress analysis and other calculations.

Movements of buildings are a more serious problem than movements of highway structures. Buildings are usually more sensitive because of glass panels, doors, windows, elevators, and utility configurations, whose performance could be affected by stresses caused by movements. The load on the foundation is added gradually during the orderly process of construction. By contrast, highway bridges are generally constructed more easily and, where necessary, construction can be done in stages. Approach embankments (often the chief cause of movements) and the substructures can be built and allowed to move for several months before starting the superstructure, the most delicate part of the bridge. In the case of box culverts, the structure is rugged and can have expansion joints at frequent intervals; differential movements and minor cracks sometimes are never known by anyone except occasional maintenance workers.

DEFINITION OF TOLERABLE MOVEMENT

The two chief considerations in bridge design and construction are safety and economy. Tolerable movements of highway structures, because the concern is small movements, are seldom concerned with safety. Safety involves large movements that lead to structural failure and collapse of the structure or a major part of it. Tolerable movements, then, are concerned mainly with economy; that is, can the movements be tolerated in order to save expense in money or time or should a more costly design and construction be used in order to reduce or eliminate the movements? Costs for the more economical choice may include temporary overload of approach embankments, proper sequence of operations, and observation of movements during construction. Also, later maintenance may require adjustments or repairs to bearing plates, expansion rockers, bridge railing, bridge deck, and approach pavements and traffic detours during the repair work. Costs for the more expensive choice may include additional spans, piles, or a more expensive site. The selection of the best choice depends on many factors, which may vary with each structure. To be avoided is a wasteful choice; to quote the late O. J. Porter, the internationally known soils and foundations engineer (2, p. 139), "While we have had many mistakes due to inadequate foundations, we have also had many buried treasures of money due to using an expensive pile foundation where spread footings could be safely used."

The incentives to overdesign are probably well known. They include: (a) easier analyses and hence cheaper design payroll costs; (b) a safer product that causes no worries; and (c) construction costs that are borne by another group, the taxpayers. Also, if a consulting firm is paid for the design on a percentage of the construction cost (no longer commonly done), there might be a tendency to overdesign to increase the fee. It can be added that another incentive for conservatism may be in lack of confidence in the design geotechnical work or in the supervision and inspection during construction.

An example of the savings realized when a wasteful choice is rejected is the twin bridges carrying I-91 over Silas Deane Highway in Connecticut (3), built in 1961 (Figure 1). The design consultant wanted piles under all footings. His soils engineer predicted large settlements without piles, based on superficial investigations and unrealistic analyses. The consultant had been caught in controversy on two previous projects in a neighboring state (one concerned an incinerator near a swimming pool and the other concerned a low-cost housing development built partly on new fill). On neither project was he in error, but his association with them was very unpleasant and it motivated his conservative solutions.

On the Connecticut Interstate project, after some detailed supplemental investigations at the site by the state's soils engineers, the state ordered the omission of all piles and the use of a 1.5-m (5-ft) overload on the approach embankments with a 3-month waiting period prior to the construction of any substructure units. The results for the northbound bridge are shown in Figure 2. Results for the southbound bridge are similar. Settlements of the superstructure were insignificant. The same procedure was ordered at two other pairs of bridges on this project, with results almost identical to those for the Silas Deane bridges. The net savings for the three pairs of bridges was $250 000, a large amount in 1961. The above are included in the savings of over $4 million realized on 33 Connecticut bridges, described at a bridge conference in 1966 (4, 5).

The definition of tolerable movements depends on several factors that vary in degree and importance with conditions at each structure. In special cases, movements might be called harmful but tolerable because the alternative choices are more undesirable. The chief factors in defining tolerable movements are

1. Amount of movement—Bozozuk suggests in a paper in this Record that 10 cm (4 in) of vertical or 5 cm (2 in) of horizontal movement is the limit of tolerability. Obviously these limits are too low for some cases and too high for others.
2. Type of structure—This has many varieties due to the many types of structures, span lengths, and skew angles. For example, a bridge with short continuous spans and deep girders will tolerate less differential settlement than one with long continuous spans and shallow girders. Connecticut made a table showing theoretical stress increase in girders for two-span continuous bridges of various span lengths, girder depths, and differential settlements (Table 1). This table was given to those design consultants who wanted zero settlement. Another feature to be remembered is that a bridge with a severe skew is more affected by horizontal movements than one that has no skew.
3. Effect on each part of structure—A common example is an abutment and wing walls built and backfilled as an early operation and allowed to settle. After a waiting period, the superstructure is erected. Here the substructure could tolerate large settlements, but the superstructure could not.
4. Cost of alternative choices—Frequently there is a question between various designs over the matter of movements of the structure. One choice of design will result in appreciable movements and consequent maintenance of the structure and another choice will reduce or eliminate the movements but be more costly. If the former choice will give only moderately undesirable results and the latter is very expensive, it is obviously a waste of money to adopt the latter. Movements involved in the former are tolerable and should be lived with, and the reasons made clear to all concerned.
5. Effect on traveling public—This should always be kept in mind, as the project is built to serve the public. Examples of adverse effects are ugly cracks in concrete at conspicuous locations; poor rideability, especially at high speed; and inconvenience to traffic during maintenance on high-capacity facilities.
6. Subjective reasons—Often the designers do not wish to make detailed studies and calculations where movements might occur. This may be due to inertia or to avoid trouble. Consultants may also wish to reduce their design payroll costs or increase their fee payments by using the easier, more expensive design.
7. Apprehensions during design—Where the design engineer does not trust the accuracy of the soils engineer's predictions of probable movements or fears poor construction operations, he or she may label the predicted movements intolerable. Actually, the fear is that the movements may be much greater and hence intolerable. It may be added that settlement predictions that have a 25 percent variance from the actual settlement are good and predictions having a 50 percent variance are fair if conditions are not complicated. Predictions of horizontal movements are more difficult.

Figure 1. I-91 over Silas Deane Highway.

Figure 2. Foundation settlement: I-91 northbound over Silas Deane Highway.

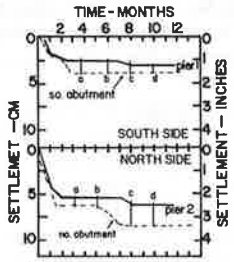

a. Overload removed
b. Pier + abutment complete
c. Steel erection complete
d. Bridge complete

Note: 1 cm = 0.39 in.

Table 1. Two-span continuous bridges: increase in fiber stress due to 5-cm (2-in) differential settlement.

Differential Settlement	Increase in Fiber Stress Due to 5-cm Differential Settlement (kPa)			
	0.9 m Girders		1.2 m Girders	
	At Pier	At Mid-Span	At Pier	At Mid-Span
Two 38-m spans				
5 cm at pier	9 900	4800	13 100	6 600
5 cm at abut	5 000	2500	6 600	3 300
Two 27-m spans				
5 cm at pier	19 300	9700	25 600	12 700
5 cm at abut	9 700	4800	12 800	6 300

Notes: 1 m = 3.3 ft; 1 cm = 0.39 in.
Girders have constant moment of inertia.

SURVEYS AND CASE HISTORIES

Thirty-five states and Canadian provinces responded to the questionnaire issued by the TRB subcommittee. Ohio's contribution was its massive 1961 survey of 1525 bridges and its 1975 follow-up on 79 bridges; these are the subject of a paper in this Record by Grover of the Bureau of Bridges, Ohio Department of Transportation. The 19 reporting states west of the Mississippi River are covered by Walkinshaw's paper in this Record.

The remaining 14 reporting states east of the Mississippi and the Canadian provinces cover a total of 42 bridges. About one-half of these had intolerable movements. About two-thirds had simple spans and one-third had continuous spans. The embankment at one or both abutments was nearly always the prime cause of intolerable movements. Such movements were due to causes such as settlement of embankment, with drag down if piles were used, lateral pressure against abutment (and piles), and lateral movement of adjacent pier due to substantial lateral movement of the foundation soil.

However, remember that some bridges labeled with intolerable movements may have had harmful movements that actually were tolerable. As stated previously, these cases would exist where alternative choices of design and construction would be excessively costly in money

Figure 3. Profile of centerline of CT-15 Expressway over Silver Lake.

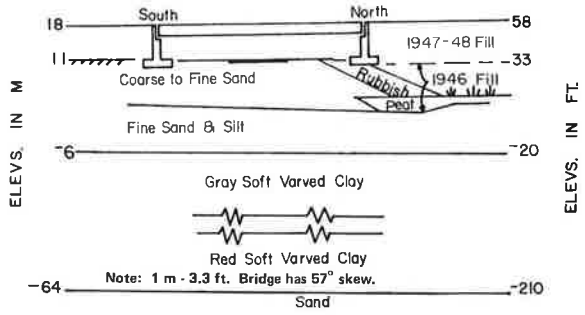

Figure 4. Shims under girder base plate.

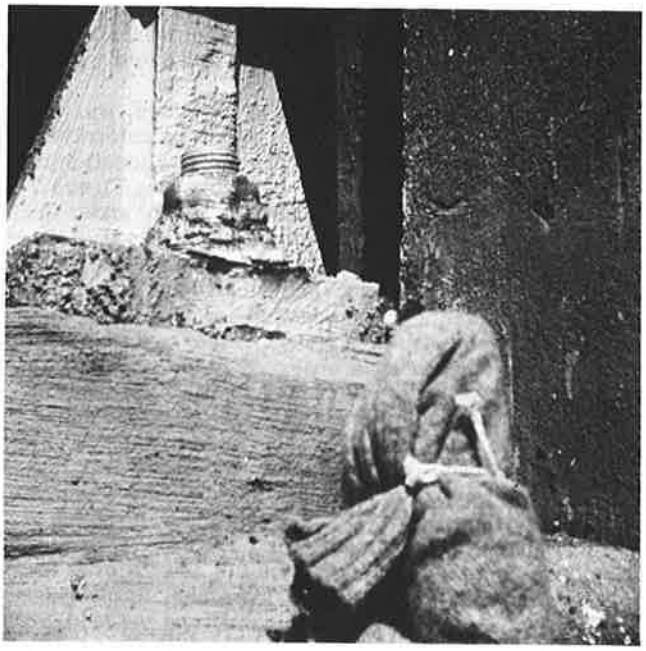

Figure 5. Tilt of rocker due to span shortening.

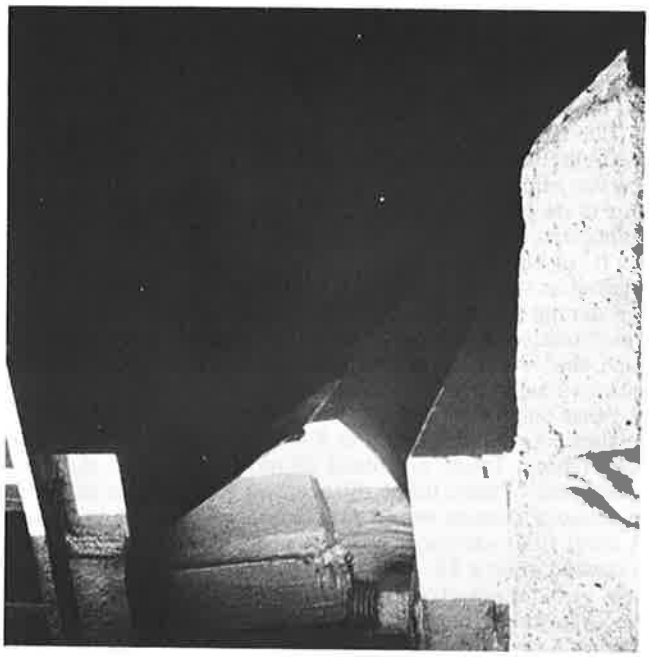

or time, very disruptive to neighboring property or local street systems, or highly displeasing aesthetically. In such cases the movements are harmful, but must be tolerated.

Of the 45 structures reported by Connecticut, 7 of the more significant ones will be described. The first 4 of these and the last 1 had rather harmful movements but are tolerable because of unusual factors. The other

Figure 6. I-84 over Hockanum River.

Figure 7. Conventional versus modern foundation treatment.

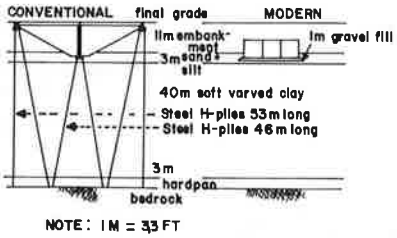

Figure 8. Profile of CT-2 Expressway over Willow Brook and Willow Street Extension.

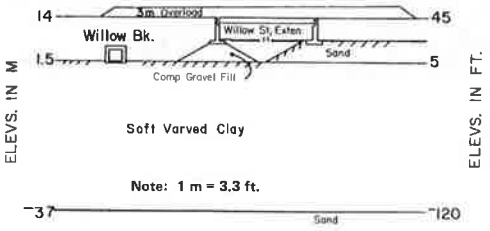

Figure 9. CT-15 Expressway over Folly Brook Boulevard.

2 should be considered not tolerable.

CT-15 Expressway over Silver Lane, East Hartford, was built in 1946 to 1948. The rubbish and peat shown in Figure 3 at the north abutment were removed and replaced by compacted gravel fill and the lower half of the embankment was placed. One year later the bridge was built and the final 7 m (24 ft) of embankment was placed. Settlement of the substructure before erecting the girders was 10 to 15 cm (4 to 6 in) in the north abutment and 2.5 cm (1 in) in the south abutment. Shims were placed under the north ends of the girders to bring them up to plan elevation. Figure 4 shows the largest shimming. A survey made 24 years later showed that the north ends of the girders had settled an additional 23 to 36 cm (9 to 14 in) and the south had settled 15 to 23 cm (6 to 9 in). Also, the span has lengthened 4 cm (1.5 in) at its east end and shortened 1 cm (0.5 in) at its west end (Figure 5). The abutments have a few hairline cracks. The greater vertical and horizontal movements were at the east end because of much more fill at the obtuse (skew) angle of the north abutment and northeast wing wall and the 16-m (54-ft) fill behind the north abutment. Short piles would have been ineffective to stop or reduce movements and long piles, over 76 m (250 ft) long, driven through the clay would have been extremely costly. Also, the omission of piles allowed the abutments to settle with the approach fill and avoid a bump at each end of the bridge deck.

Figure 10. Charter Oak Bridge over Connecticut River.

Figure 11. CT-185 bridge over Farmington River.

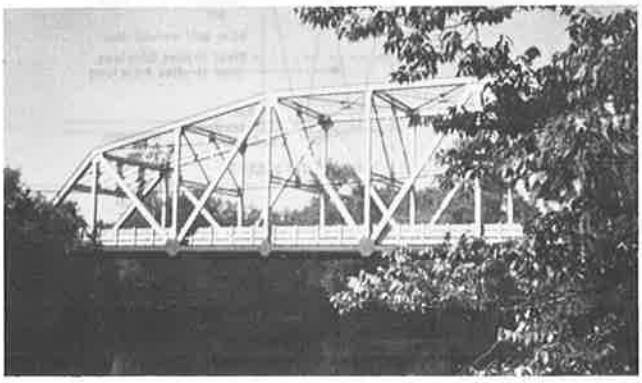

Figure 12. Pile-load test results at bridge over Farmington River.

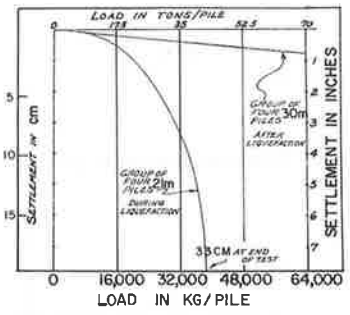

Notes: 1 cm = 0.39 in, 1 kg = 0.001 ton.

Figure 13. Lateral and vertical movements of abutments.

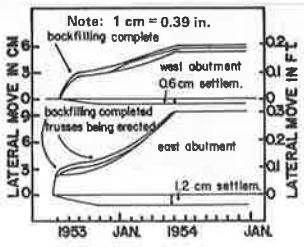

I-84 over Hockanum River, East Hartford, was built in 1963 (Figure 6). As the river was to be relocated, the embankment was placed across the new location to grade and allowed to settle for 6 months (see Figure 7). At that time, settlements were 36 cm (14 in) under the expressway and 18 cm (7 in) under the midslope of the embankment. Then excavation was made for the triple-box culvert, and it was built and backfilled. The box settled 20 cm (8 in) under the pavement and 10 cm (4 in) at the ends. These settlements were 20 percent greater than predicted. No distress is observed in the structure. Piles would have had a net cost of $200 000 at that time.

CT-2 Expressway over Willow St. Extension and Willow Brook, East Hartford, was built in 1959 to 1960 (Figure 8). First, the Willow Brook box culvert, 192 m (630 ft) long, was built. Then the embankment was placed across the entire site to final grade plus 3 m (10 ft) overload and allowed to settle for 6 months. This produced settlements of 33 and 25 cm (13 and 10 in) at the north and south bridge abutment locations, respectively. Finally the bridge site was excavated, and the bridge was built and backfilled. The north and south abutments have settled 28 and 20 cm (11 and 8 in), respectively, with only a few hairline cracks in them. The box culvert settled 51 cm (20 in) under the expressway centerline and 20 cm (8 in) at 61 m (200 ft) left and right. It had no damage except faulting of 1 to 2 cm (0.5 to 1 in) at several expansion joints. The settlements were about 25 percent greater than predicted. The net saving by the omission of piles was $420 000 at that time.

CT-15 Expressway over Folly Brook Boulevard, Wethersfield, was built in 1941. This is a two-span continuous rigid-frame bridge with a 45° skew (Figure 9). The pier is on piles that straddle an old brick sewer. The abutments are on 2 m (7 ft) of desiccated clay overlying 7 m (23 ft) of soft varved clay. Piles for the abutments were deleted at the start of construction due to the steel shortage during World War II. Four months after the bridge was completed and approach embankments were placed, each abutment had settled 2.5 cm (1 in) at the end that had an acute angle with the wing wall and 4 cm (1.5 in) at the end that had an obtuse angle. Thrity-five years later, settlements were 4 and 5 to 8 cm (1.5 and 2 to 3 in), respectively. These are about 35 percent greater than predicted. These large differential settlements of the continuous frames would result in a substantial increase in steel fiber stress, but fortunately the settlements have occurred over a 35-year period. Consequently, plastic flow in the steel girders relieves much of the effect of the differential movement. The abutment walls have opened 1 cm (0.5 in) or less at expansion joints and each

has moved forward about 2.5 cm. These movements are not very harmful and are tolerable. However, if deletion of the piles at the abutments had been foreseen during design, the embankment would have been placed first and allowed to settle to avoid a potentially intolerable situation.

It may be of interest to describe the compressibility of the soft varved clays under the foundations of these structures. These clays are part of glacial Lake Connecticut deposits. Their natural water content is approximately 50 percent and their resistance (N) in the standard penetration test is 2 to 4 blows/30 cm (12 in). However, they have been preconsolidated (overconsolidated) in their past history to about 1.5 to 2.5 kg/cm^2 (1.5 to 2.5 tons/ft^2) in excess of today's overburden load. This overconsolidation is indicated by laboratory consolidation tests on undisturbed samples and in part by geological studies. Consequently all or most of the compression in these varved clays, due to the project loads, is in the recompression phase and therefore the settlements are much less than if the clays had not been preconsolidated.

Turning to cases of movements that are largely or entirely horizontal, Charter Oak Bridge is over the Connecticut River, Hartford (Figure 10). Two cases occurred, one in 1941 and one in 1946, both due to lateral pressures against piers founded on long piles driven through soft varved clay. The first case involved piers 9 and 10, which moved away from each other 2.5 and 7.5 cm (1 and 3 in), respectively, due to a dike fill 8 m (25 ft) high placed between these piers. The resulting 10-cm (4-in) increase in span length required considerable adjustment of the girders when erected the next year; the girders for this span are barely seated on pier 10. The other case involved a roadway fill 5 m (15 ft) high placed some years later between piers 3 and 4. They moved about 2.5 cm each, causing the joint at the expansion pier 4 to open 5 cm (2 in). This became a hazard in cold weather—sufficiently so to be photographed for a front-page article in the evening newspaper. To resist any further movements, sloping steel raker piles were installed at both piers. Both of these cases can be considered not tolerable, as they involved harmful movements that could have been avoided by counterweight fills placed on the opposite side of each pier without difficulty.

The final case history concerns a Farmington River bridge in Simsbury built in 1953. This is a 69-m (224-ft) single-span through-truss bridge carrying CT-185 over the river (Figure 11). The soil below the footings is 6 m (20 ft) of brown silt and fine sand overlying 42 m (140 ft) of fairly firm brown silt; below this is sand. The structure is supported on 27-m (90-ft) cast-in-place concrete piles in Monotube shells. To simulate possible liquefaction of the soil, the four test piles, before they were loaded as a group, were surrounded by 27 other piles. Liquefaction occurred and was dissipated in 2 weeks after the 31 piles were driven. Figure 12 shows the results of load tests made during liquefaction and after it was gone. As seen in Figure 13, the abutments settled 0.5 to 1 cm (0.25 to 0.5 in) and moved toward the river 6 to 9 cm (2.5 to 3.5 in), chiefly by translation (not rotation). This shortening of the span by 15 cm (6 in) was anticipated in design. Figure 13 shows that 7.5 cm (3 in) of shortening occurred before the superstructure was erected and 7.5 cm after its erection. Some years later, at the expansion end of each truss, the rocker base was shifted 6 cm to make the rocker plumb at mean temperature. This was because the rocker system had not been designed for an excessive tilting of the rockers. Figures 14 and 15 show the results after these adjustments. It appears that the movements were slightly

Figure 14. Shift of rocker base.

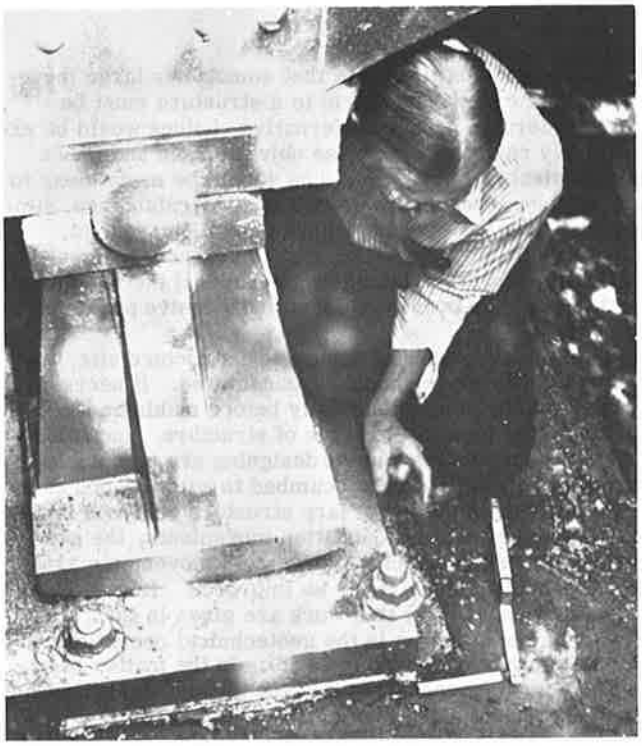

Figure 15. Tilt of rocker.

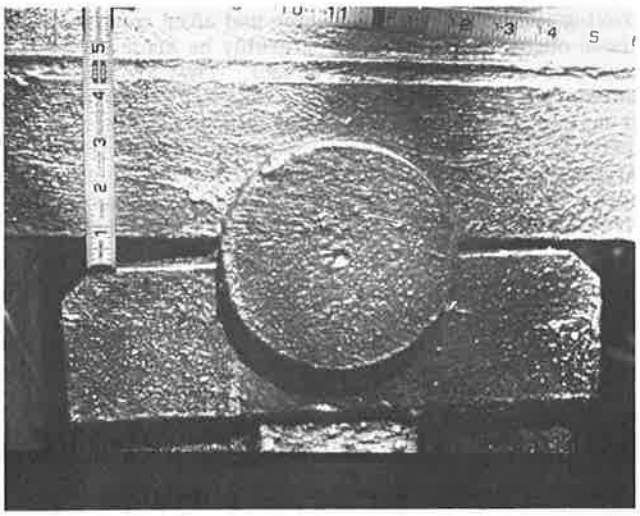

harmful but tolerable. The cost of shifting the two rocker supports was small and probably much less than that for adding a short span with stub (perched) abutment at each end of the bridge.

SUMMARY AND CONCLUSIONS

The definition of tolerable movement is often complicated by several factors, including

1. Amount of movement,
2. Type of structure,
3. Effect on each part of structure,
4. Cost of alternative choices,

5. Effect on traveling public,
6. Subjective reasons, and
7. Apprehension during design.

Case histories illustrate that sometimes large movements that cause some harm to a structure must be called tolerable because alternative choices would be excessively costly or otherwise objectionable and hence less desirable. Such situations should be made clear to all persons concerned, to avoid misunderstandings. Similarly, some cases occur where a small movement, which results in substantial cost to correct the resulting difficulty, should be labeled intolerable if the movement could have been prevented by an inexpensive provision in the design.

In the early stages of design at a structure site, the factors listed above should be considered. If necessary they should be studied carefully before making a decision on the location and type of structure. Incentives to avoid such studies by overdesigning are commonly known but should not be succumbed to without good cause.

In addition to the necessary structure analyses to determine the effects of foundation movements, the geotechnical work on which the predicted movements are based should in many cases be improved. Recommended ways of strengthening this work are given in Goughnour's report on the situation in the geotechnical operations in the state highway departments (6). In the matter of organization, he emphasizes that the geotechnical functions of a department should be combined in one unit, to provide for unified control of personnel and equipment that are involved with the same basic geotechnical problems.

In the geotechnical work, probably the greatest need in predicting structure foundation movements is in improving field observations during and after construction. These observations should preferably be made by the geotechnical engineering personnel. They are much more concerned with the results than are construction or maintenance personnel. They will use the data directly to learn how accurate (or inaccurate) their predictions were and to strengthen their knowledge of their work. Field observations could include readings on the structure units, settlement platforms, deeper settlement devices (such as Borros anchors), piezometers, and inclinometers, all based, of course, on proper bench marks and reference points.

ACKNOWLEDGMENTS

The following members of the Connecticut Department of Transportation were helpful in reviewing this paper: J. L. Petroski of Soils and Foundations, M. Q. Johnson of Bridge Design, and J. F. Cavanaugh of Bridge Maintenance. In preparing for the symposium of which this paper is a part, the members of the Subcommittee on Tolerable Movements of Highway Structures were most helpful in obtaining and tabulating information from the questionnaires sent to the states and Canadian provinces. They also contributed substantially through their ideas toward presentation in this symposium.

REFERENCES

1. J. Feld. Tolerance of Structures to Settlement. Specialty Conference on Design of Foundations for Control of Settlement, SM and F Div., ASCE, Evanston, IL, 1964, Vol. 90, SM5, p. 555.
2. O. J. Porter. Discussion of: The Use of Soil Mechanics in the Design and Construction of Bridge Foundations. Proc., Annual Convention, Association of Highway Officials of North Atlantic States, 1953.
3. P. Keene. Non-Engineering Elements in Factors of Safety in Soil and Foundation Engineering. HRB, Highway Research Record 269, 1969, pp. 1-6.
4. Science Cuts Bridge Costs. Hartford Times, Dec. 21, 1966.
5. Savings Cited on Bridges With New Techniques. Hartford Courant, Dec. 22, 1966.
6. R. D. Goughnour. Soil Management Studies in the State Highway Departments. Federal Highway Administration, Highway Focus, Vol. 8, No. 4, Dec. 1976, pp. 1-10.

Publication of this paper sponsored by Committee on Foundations of Bridges and Other Structures.

Survey of Bridge Movements in the Western United States

John L. Walkinshaw, Office of Construction and Maintenance, Federal Highway Administration, San Francisco

The design of bridge superstructures is usually based on the assumption that less than 25 mm (1 in) of movement will occur within the substructure. Consequently, the foundation engineer must find soils at a proposed site of sufficient bearing capacity to limit movement to this small value. Often the movement criteria will dictate the size or depth of the foundation, thereby increasing its cost needlessly if the criteria established are too strict. The purpose of this survey is to document field performance of various structures that have moved and obtain an evaluation as to the acceptability of these movements by various state highway agencies. The 35 structures reported in this paper include 54 movements of structural elements. Sixty percent of these represent movements at the abutments and 40 percent represent movements at piers. Although some very large vertical movements were reported tolerable for some of the older structures, movements in excess of 63 mm (2.5 in) within the structure were usually considered objectionable from a rideability viewpoint. Horizontal movements in excess of 50 mm (2 in) usually caused structural distress that was considered harmful. Recommendations are made to improve reporting procedure and make use of available material. Emphasis is on more thorough involvement between designers and maintenence crews in solving movement problems.

This survey attempts to establish criteria that would define, from a practical viewpoint, tolerable movement of highway structures. Advances in our prediction techniques for soil movements based on new sampling, testing, and analysis techniques have often been undermined

by unrealistic design tolerances in the superstructures. The often heard, "We cannot tolerate more than one inch [25 mm]," from the structural engineer imposes an upper limit on movement that, on many occasions, leads to an overly conservative foundation design or undesirable superstructure characteristics, such as joints, which cause poor riding and difficult maintenance. Of interest for the survey are (a) horizontal and vertical movements of piers and abutments, (b) the type of structure, (c) the construction sequence, (d) the effects of the movements on the structural elements, and (e) an evaluation by the reporting agency of whether the observed movements are considered tolerable.

LITERATURE REVIEW

The design of structures based on static and stress analysis concepts has led to the development of standards or guidelines often used in the design of foundations. A review of the failure criteria in some of our most commonly used pile-load test procedures, for example, reveals usually low allowable movements of the pile head before the load test is stopped or declared a failure.

In the Standard Specifications for Highway Bridges of the American Association of State Highway and Transportation Officials (AASHTO) (1), a load test is considered to be a failure if after the continuous application of twice the design load for 48 h the net settlement of the pile head after unloading exceeds 6.35 mm (0.25 in). The standards of the American Society for Testing and Materials (ASTM) for static load tests for the years prior to 1969 gave little guidance as to failure criteria and generally only described a rather slow testing procedure to twice the proposed design load.

The drawbacks of some of these standard testing procedures prompted some agencies to research for quicker testing methods and different failure criteria in the early 1960s. The development of a quick test method by the Texas highway department is described by Fuller and Hay (2) and more recently promoted in a user's package form by Butler and Hay in a Federal Highway Administration (FHWA) implementation package (3). In this package, it is recommended that the piles or drilled shafts be loaded to plunging failure. Interpretation of the results of these tests is then based on the intersection of two tangents to the load-settlement curve and the safe design load found by applying an appropriate safety factor. With this information and a good knowledge of the subsurface conditions, economical and safe foundations can be designed.

Some of this pile-load test research work has led to the establishment of new standards and failure criteria as published in ASTM D1143-74 (4). Under article 4.5, which describes the constant rate of penetration test, it is recommended that the load required be held to achieve the specified penetration rate until the total penetration is at least 15 percent of the average pile diameter or diagonal dimension. Article 4.7 describes briefly the quickload test without any discussion of failure criteria, and article 4.8, which describes the settlement controlled method, states that the test is complete once the total pile-butt settlement equals 10 percent of the average pile diameter or diagonal dimension.

Note that none of the above failure criteria takes into account the length of the pile tested or its material composition. More work is needed in this area to provide a more engineered approach to interpretation of pile-load tests. Also of concern (as will be seen from the results of the survey) should be the lateral forces that are imposed on the foundations by the structure and surrounding soil. Again, structural analysis can give us good estimates of the lateral loads imposed by the superstructure, but many unknowns still exist as to the lateral loads generated by lateral movements of consolidating soils, for instance.

Some case histories in the literature show that excessive moments can be introduced into pile foundations due to consolidation of an adjacent embankment. Such a case is described in the proceedings of the 5th International Soil Mechanics and Foundation Engineering (ISMFE) conference (5) and followed up in the 6th ISMFE conference proceedings by Heyman (6). In the proceedings of the 8th ISMFE conference (7), another case history describes measurements made on piles subjected to both negative skin friction and lateral soil pressures. It is stated that the degree of consolidation of the soft layer had practically no effect on the magnitude of the maximum negative skin-friction load measured, which reached 54 Mg (60 tons) for some piles. On the other hand, the degree of consolidation was of great importance in reducing the maximum movement occurring in the foundation piles.

An example of another case history that supports the above conclusions was reported by Nicu, Antes, and Kessler (8) on a structure in Allamuchy, New Jersey. There one of the abutments was monitored during construction and backfilling operations and compared to the other abutment, which was backfilled at a slower rate. Considerably less lateral movement of the abutment occurred after some consolidation of the soft layer. This demonstrated clearly the value of this method in reducing horizontal movements.

In 1972, Marche and LaCroix (9) published their analysis of the stability of abutments founded on piles driven through soft soil layers for 15 different structures. These structures included some of the above case histories and some reported by Stermac, Devata, and Selby (10). Their results describe the influence of the type of abutment on the direction of movement relative to the superstructure, the relative stiffness of the pile-soil system, and the degree of loading imposed by the embankment.

Generally, movements became large if the embankment loading produced an increase of stress larger than three times the undrained shear strength of that soil at the surface of the consolidating layer. Documented failure occurred when the loading approached 5.14 times the undrained shear strength. Recommended solutions to this problem consist principally of either reduction of the load at the abutment by the use of lightweight fill or preconsolidation of the soft layer. Alternatively, from a structural standpoint, designing the structure to accommodate the anticipated movement may, in some cases, be more economical than to try and prevent it.

FIELD SURVEY

In September 1975 a survey questionnaire was sent to the highway departments of the 17 states shown in Figure 1. The information requested was to be completed on a prepared form from case histories documented in the agency's files.

As a guideline, the following definition of intolerable movement was given in the questionnaire: Movement is not tolerable if damage requires costly maintenance or repairs and a more expensive construction to avoid this would be preferable. Ten states gave information on a total of 35 structures; six states replied that this information was not documented in their files.

A list of the reported movements is given in Table 1. These represent movements of 54 structural elements, abutments, or piers in 35 highway bridges. These movements were divided into three classifications: (a) toler-

Figure 1. States surveyed.

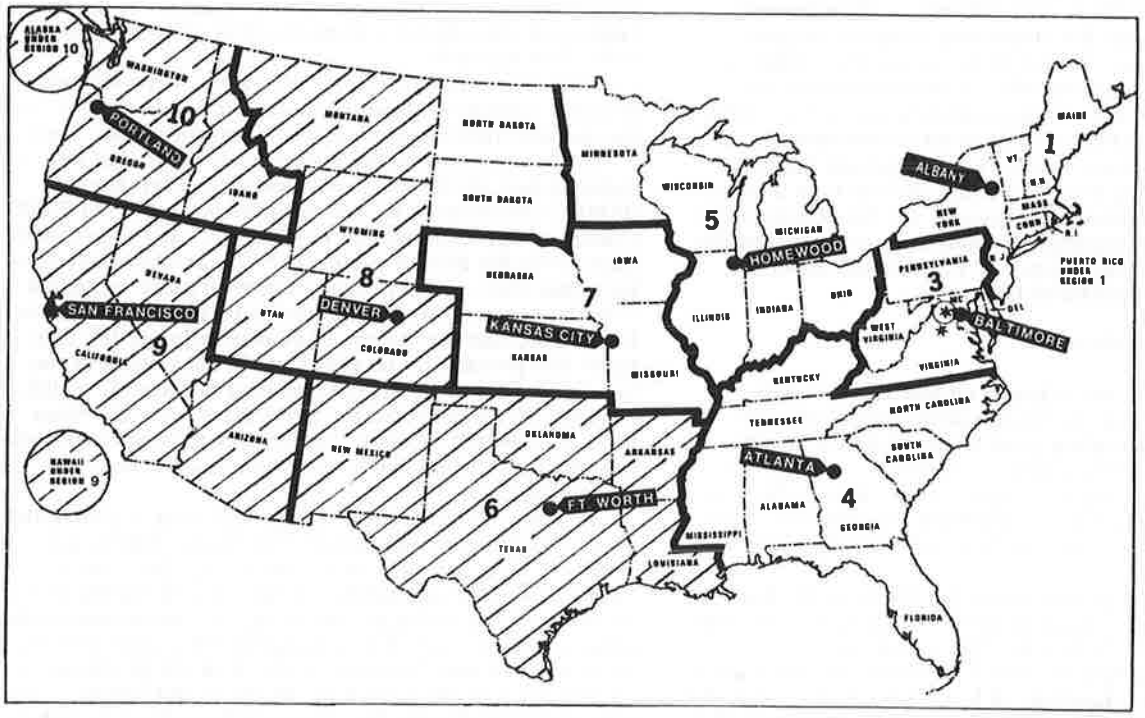

Table 1. Movements of structural elements reported.

	Simple Span				Continuous			
	Abutments (mm)		Piers (mm)		Abutments (mm)		Piers (mm)	
Movement	Vertical	Horizontal	Vertical	Horizontal	Vertical	Horizontal	Vertical	Horizontal
Tolerable								
1 Direction	125, 50, 25 450, 25	38	63,[a] 150 63	50	125, 50		75 to 88, 88, 25, 38, 38 13	25
2 Directions	25	50			13, 75	25, 25		
Intolerable, poor riding								
1 Direction	225, 225 300				200		63, 150	
2 Directions	125	25			450	87		
Intolerable, structural damage								
1 Direction		75	50,[a] 350, 75 to 125		50 to 125, 25 to 50, 150, 200 to 250	50, 50, 75 163	50 to 75[a]	
2 Directions	600, 50 400, 425	13, 75, 25, 63	600,[a] 100 225	150, 25, 25	63, 38	200, 50	13	25 to 88

Note: 1 mm = 0.04 in.

[a] Vertical heave.

able movements, (b) intolerable movements but only poor riding characteristics were cited, and (c) intolerable movements that resulted in structural damage. Each of these classifications was subdivided into one-direction and two-direction movements to indicate structural elements for which only vertical or horizontal movement occurred and others where both occurred. When both occurred, each structural element is represented by two numbers, one in the vertical column and one in the horizontal column, and listed in sequential order in each column. When differential movement was reported, the range is shown. Not all vertical movements were down, but significant heaves are also included in this table. Most of these unusual movements were due to frost or ice action on the foundations.

A review of the data shows a surprising range of values in each classification. Tolerable movements were reported for 11 abutments and 12 piers. Vertical displacements in this group varied from 13 to 450 mm (0.5 to 18 in) and horizontal movements were limited to a maximum of 50 mm (2 in). Much less movement was tolerable when both occurred together and the maximum reported was for an abutment that settled 75 mm (3 in) and moved horizontally 25 mm (1 in).

The second classification—intolerable movements, poor riding—was chosen in an attempt to define a consumer-related measure of tolerability. Eight elements are in this category; six were vertical settle-

Figure 2. Condition items of FHWA survey inventory and appraisal sheet.

CONDITION	MATERIAL	CONDITION ANALYSIS	RATING (9-0)
58 Deck			
59 Superstructure			
60 Substructure			
61 Channel & Channel Protection			
62 Culvert & Retaining Walls			
63 Estimated Remaining Life		65 Approach Roadway Alignment	
64 Operating Rating		66 Inventory Rating	

Figure 3. Structure condition rating system.

Recording and Coding Guide - July 1972		Commentary on July 1972 Coding Guide		BIT Course Coding	
		Unabridged	Abridged		
9	New condition	New condition	New condition	Good	The item is in new or good condition with no repairs necessary
8	Good condition - no repair necessary	No repair necessary. No sign of distress or deterioration	Good condition - no repair necessary		
7	Minor items in need of repair by maintenance forces	A defective or deteriorated secondary member, that will not progress to a serious defect if not repaired within a reasonable period of time. Most preventative maintenance is in this category.	Minor items in need of repair	Fair	The item is still performing the function for which it was intended. A minor or major item is in need of minor repair
6	Major items in need of repair by maintenance forces	A defective or deteriorated main supporting member or support system vital to the structural integrity of the bridge. Includes any progressive deterioration that can be arrested by maintenance repairs such as concrete cracking that can lead to rebar corrosion and steel cracks and corrosion that can lead to possible failure.	Major items in need of repair		
5	Major repair - contract needs to be let	Same as 6 except that the extent of deterioration is greater and repair could require complicated and/or extensive procedures.	Major rehabilitation needed	Poor	The item is still performing the function for which it was intended but at a minimum level. The item concerned is in need of major repair
4	Minimum adequate to tolerate present traffic, immediate rehabilitation necessary to keep open	The structure can marginally support loads from unrestricted legal load and posting should be considered. Continued observation indicates that failure is not progressive under restricted loading. This rating is relative to the class of loading using the bridge. This rating applies only to major components or elements.	Marginally adequate to tolerate unrestricted legal loads - consider restricting traffic and/or posting for less than maximum legal loads		
3	Inadequacy to tolerate present heavy load - warrants closing bridge to trucks	Major structural element deteriorated or damaged so as to reduce its capability of carrying trucks. Allow light loads only if stress check warrants and continued observation indicates failure is not progressive under these light loads.	Inadequate to tolerate legal loads. Post for light loads		
2	Inadequacy to tolerate any live load - warrants closing bridge to all traffic	Major structural element deteriorated or damaged so as to reduce its capability of carrying any loads. Stress check indicates structure cannot support any live load. Bridge should be closed.	Inadequate to tolerate any live load. Warrants closing bridge to all traffic	Critical	The item is not performing the function for which it was intended
1	Bridge repairable, if desirable to reopen to traffic	Bridge closed. Inspection indicates that bridge can be reopened with a complete rehabilitation.	Bridge closed. Complete rehabilitation needed to reopen		
0	Bridge conditions beyond repair - danger of immediate collapse	Bridge closed. Inspection indicates that bridge conditions are beyond repair and in danger of immediate collapse. Keep bridge closed.	Bridge closed. Bridge conditions beyond repair. Danger of immediate collapse.		

ments only, which varied from 63 to 300 mm (2.5 to 12 in). The other two are abutments where two-directional movements reached a maximum of 450 mm (18 in) vertically and 87 mm (3.5 in) horizontally. However, of more significance is the lowest value of vertical settlement reported intolerable from a rideability viewpoint. In this case it is 63 mm. This is a reasonable value because more than half of the tolerable vertical movements are at or below this displacement.

The third classification includes the remaining 23 structural elements reported. For each of these, some form of structural damage occurred as a result of the movements. In this group, vertical displacements varied from 13 to 600 mm (0.5 to 24 in), including some cases of vertical heave that equaled the maximum value reported. One-half of the displacements in this classification involved two directions. Horizontal movements were in many cases the cause of the damage to the structure. These ranged from 25 to 200 mm (1 to 8 in). Most of them were 50 mm (2 in) or more. This last value appears to be an upper value of tolerability, especially when movement is toward the deck and reduces the clearance for temperature expansion.

A review of the possible influence of the construction sequence on the movement of the abutments showed that 21 of the 27 abutments for which the construction sequence was known were built by first building the embankment, then the substructure, and then the superstructure. Of these movements, 10 were vertical only, 5 were horizontal only, and 6 were a combination of both.

The majority of the embankments were between a height of 3.6 and 7.1 m (12 to 30 ft) but otherwise varied from a low of 1.2 m (4 ft) to a high of 21.3 m (70 ft).

A review of the boring information made available for many of the structures showed that at nearly every site a layer of loose fine sand, sandy silt, or silty clay existed beneath the bridge approaches prior to construction. Only three sites described soft clays from which long-term consolidation problems could be anticipated.

It appears that the possibility of consolidation was recognized because 23 of the 32 abutments were on pile foundations. However, only eight movements were considered tolerable, so the piles were probably underdesigned for either the lateral loads or negative skin friction loads applied to them by the embankment. Unfortunately, it is not known how many construction projects included waiting periods between the bridge approach construction and bridge foundation construction. It seems that in most of these cases it was insufficient.

Following the receipt of these data and looking for a way to expand the number of case histories submitted, I became aware of the Structure Inventory and Appraisal of the Nation's Bridges program. This inventory was initiated by FHWA in 1972 in order that an accurate report might be made to Congress on the number and condition of the nation's bridges. Each state was requested to inventory all the bridges carrying and going over federal-aid highways. However, complete inspection was not mandatory. In July 1972 a recording and coding guide (11) was provided to the states as an example of the data base needed for the final report. Clarification of some items in the recording guide was made in July 1977 (12) as part of this continuing program. The data collected for each structure are summarized and reported to the FHWA in a structure inventory and appraisal (SI&A) sheet.

An extract of the SI&A sheet, which rates the condition of the structure, is shown in Figure 2. The rating system used for items 58 through 62, plus item 65, is shown in Figure 3. As can be seen from Table 1, this type of rating system does not allow the reviewer to determine if any down rating of the substructure (item 60) is due to movement or to other causes. This is unfortunate, because this type of information would be of interest to the foundation engineer for future designs.

RECOMMENDATIONS

Although this survey was limited in scope, it points out some important facts about the difficulties that exist in determining tolerable movements for various structures designed. Accurate movement data are difficult to obtain. Some agencies claim that this information is not kept in their files or are unwilling to part with this information. Some states, on the other hand, have quantities of data in their maintenance files but, because the bridge is complete from a construction point of view, design information must be obtained from one or more other offices within the agency.

Another problem is the reliance that one has to make on the memory of a few individuals to locate case histories of structures with movement. The ones that are remembered are usually only those structures that have had major movements, which caused some kind of structural distress. It would appear beneficial to develop a classification and retrieval method so that the designer can evaluate the performance of previous designs. In this age of rapidly rising construction costs it is important that geotechnical engineers and designers have all the information needed to design a safe and economical foundation without costly overdesign to take care of uncertainties.

From the values reported in the survey, horizontal movements were the most critical. Structural distress was usually reported if 50 mm (2 in) or more occurred. Vertical movements were reported tolerable up to some very high values but poor riding characteristics were mentioned once the settlement exceeded 63 mm (2.5 in) within the structure or approaches, for high-design roadways. Detrimental movements of smaller magnitude were reported when both horizontal and vertical displacements occurred simultaneously. These values appear to be reasonable limits for many structures as tolerable movements.

Since a large percentage of the abutment movements reported were founded on piles installed through in-place embankments, a closer look at probable embankment movements should be made during the investigation and design stage of the bridge approaches. Very little settlement of the embankment relative to the pile is needed to impose large negative friction loads and bending moments on the piles.

When the abutments are founded on piles installed through a thick layer of soft deposits, the geometry of the abutment will have an influence on the direction of the horizontal movements. Appropriate design features should be incorporated in the design to minimize damage to these structural elements.

Geotechnical engineers and designers should be involved early in monitoring of movements detected by bridge inspections. Field instrumentation installed at an early stage to detect direction and depth of movement provides invaluable information to the engineer for the design of correction schemes if necessary.

ACKNOWLEDGMENT

I wish to express appreciation to the agencies and their engineers who provided the data presented here. Their time and efforts made the preparation of this paper possible.

REFERENCES

1. Standard Specifications for Highway Bridges—with current revisions. AASHTO, 11th ed., Washington, 1973.
2. F. M. Fuller and H. E. Hay. Pile Load Tests Including Quick-Load Test Method, Conventional Methods, and Interpretations. HRB, Highway Research Record 333, 1970, pp. 74-86.
3. H. D. Butler and H. E. Hay. The Texas Quick-Load Method for Foundation Load Testing—User's Manual. Federal Highway Administration Implementation Package 77-8, March 1977.
4. Annual Book of ASTM Standards. ASTM, Philadelphia, 1975, pp. 178-189.
5. L. Heyman and L. Boersma. Bending Movements in Piles Due to Lateral Earth Pressure. Proc., 5th International Conference on Soil Mechanics and Foundation Engineering, Vol. 2, 1961, pp. 425-429.
6. L. Heyman. Measurement of the Influence of Lateral Earth Pressure on Pile Foundations. Proc., 6th International Conference on Soil Mechanics and Foundation Engineering, 1965, pp. 257-260.
7. W. T. Heijnen and P. Lubking. Lateral Soil Pressure and Negative Skin Friction on Piles. Proc., 8th International Conference on Soil Mechanics and Foundation Engineering, 1973, pp. 143-147.
8. N. D. Nicu, D. R. Antes, and R. S. Kessler. Field Measurements on Instrumented Piles Under an Overpass Abutment. HRB, Highway Research Record 354, 1971, pp. 90-99.
9. R. Marche and Y. LaCroix. Stabilité des Culées de Pontes Etablies Sur de Pieux Traversant une Couche Molle. Canadian Geotechnical Journal, Vol. 9, No. 1, 1972, pp. 1-24.
10. A. G. Stermac, M. Devata, and C. G. Selby. Unusual Movements of Abutments Supported on End-Bearing Piles. Canadian Geotechnical Journal, Vol. 5, No. 2, 1968, pp. 69-79.
11. Recording and Coding Guide for the Structure Inventory and Appraisal of the Nation's Bridges. Federal Highway Administration, Transmittal 123, Vol. 20, Appendix 54, July 1972.
12. Commentary on Recording and Coding Guide for the Structure Inventory and Appraisal of the Nation's Bridges, July 1972. Federal Highway Administration, April 1977.

Discussion

Jack H. Emanuel, University of Missouri, Rolla

This paper, as well as the one by Grover in this Record, is an excellent presentation that provides an interesting account of the variability in the movement of piers, abutments, and approach slabs and in the relative effects of the magnitude of vertical and horizontal movements on ridability.

The effect of these movements on the bridge superstructure is of real concern to structural engineers. Differential vertical movements of piers and abutments may induce large support reactions and internal stresses. Differential horizontal movements require expansion supporting devices as well as deck expansion devices. The failure of these devices to function as intended in their design requires consideration of induced stresses. Many cases of abutment movement have resulted from the growth of approach slabs, the compaction or settlement of the approach fill, or the freezing of support or expansion devices.

The approaches of a number of bridges in California have been studied by Jones (13), who reported that more approach patching is required for closed-abutment bridges than for open-end structures. Examples of typical approach slab action and approach slab-pavement interaction are given by Strom (14).

A study of the annual movement of approximately 231 expansion joints (80 structures) in various climatic environments was made over a 3-year period by Stewart (15). His conclusions include (a) structures with regular expansion facilities at the abutments will have a higher average movement per unit length than will those that have no abutment expansion facilities; the larger the number of expansion joints in a structure, the less significant is abutment expansion; and (b) uniformly spaced expansion joints on long structures do not necessarily have the same movement.

In an effort to eliminate the settlement of approach slabs and the excessive movement of abutments (conditions that frequently result in broken abutment backwalls or the closing of expansion devices), many states have experimented with granular backfills, predrilling for piling, and stub abutments (16).

The general failure of expansion supporting devices to function as intended becomes apparent when they are observed in the field. During the summer of 1961, I conducted field observations of the behavior of bridge supporting and expansion devices on bridges located in Iowa, Kansas, and Nebraska (16). General limitations for observation were that the bridges should have three or more spans, either simply supported or continuous. The span lengths were usually 15.2 m (50 ft) or more. Of the 83 bridges tabulated, 39 had irregularities. Many of them had floor expansion devices that either had closed tight or had much less provision for further expansion than designed for at the observed temperature. Shifting of abutments, spalling and cracking of abutment backwalls, inconsistent rocker movement, cracked concrete bearing seats, and extrusion of asphaltic expansion joints were common observed irregularities. However, there appeared to be no direct relation between abutment movement and the age of the structure, type of approaches, or type of supporting or expansion devices. From the bridges observed, no definite trend or regularity of pattern could be isolated nor could a prediction be made as to which irregularity will occur or when it will occur. For example, both closed and open floor expansion devices were observed on bridges with concrete, asphalt, and gravel approaches. Similarly, evidence of abutment movement and irrational rocker movement was observed for all types of approaches and heights of approach fill. There were irregularities in both old and relatively new bridges.

To eliminate the problems of expansive supporting devices, one state highway department (circa 1950) began tying the superstructure to flexible piers and stub abutments. In 1934, a three-span, 57.9-m (190-ft), continuous steel beam bridge was constructed that utilized this type of construction. A single row of vertical piling with a concrete cap was used at the ends of the bridge, and a separate retaining wall was spaced 1.9 cm (0.75 in) at 27°C (80°F) from the end of the bridge. The concrete center piers rested on two vertical rows of piling. No roadway expansion device other than mastic was used. The bridge, which had had no maintenance except an occasional painting of structural members, had been subject to almost yearly flooding, and had supported a great

increase in traffic over the years, was in very good condition when observed in 1961 (16). Interest in and use of superstructures tied to flexible piers and stub abutments has continued to grow and is essentially limited only by the lack of suitable design criteria (17, 18, 19, 20).

Preboring for abutment piling is now commonly used. The paper reports that the possibility of consolidation apparently was recognized because 23 of the 32 (reported) abutments are on pile foundations. It is unfortunate that the respondents did not identify whether or not the pilings were prebored so that a comparison of abutment movement could be made. It also would be interesting to know whether the abutments are rigid high abutments or the spill-through type. It is believed that the influence of preboring, type of abutment, and superstructure-substructure interaction (connection), if known, would be reflected in modifications to Walkinshaw's recommendations.

In structural considerations, the effects of differential vertical movement and the restraint of horizontal movement should be compared and interrelated to thermally induced stresses [which may be significant (21, 22, 23)] in addition to the live-load stresses. Such analyses can be readily calculated by any highway bridge design group.

REFERENCES

13. C. W. Jones. Smoother Bridge Approaches. Civil Engineering, American Society of Civil Engineers, Vol. 29, No. 6, June 1959, pp. 407-409.
14. J. Strom. Maintenance of Bridge Expansion Joints. Univ. of Arkansas Engineering Experiment Station Bulletin 24, March 1957.
15. C. F. Stewart. Annual Movement Study of Bridge Deck Expansion Joints. California Division of Highways, R&D Rept. 2-69, June 1969.
16. J. H. Emanuel and C. E. Ekberg, Jr. Problems of Bridge Supporting and Expansion Devices and an Experimental Comparison of the Dynamic Behavior of Rigid and Elastomeric Bearings. Iowa Engineering Experiment Station, Iowa State Univ., Special Rept., Proj. 547-S, Sept. 1965.
17. C. E. Ekberg, Jr., and J. H. Emanuel. Current Design Practice for Bridge Bearings and Expansion Devices. Engineering Research Institute, Iowa State Univ., Proj. 547-S, 1967.
18. J. H. Emanuel and others. An Investigation of Design Criteria for Stresses Induced by Semi-Integral End Bends: Phase I—Feasibility Study. Missouri Cooperative Highway Research Program, Univ. of Missouri, Rolla, Final Rept. 72-9, 1973.
19. J. H. Emanuel and others. Current Design Practice for Bridge Superstructures Connected to Flexible Substructures. Department of Civil Engineering, Univ. of Missouri, Rolla, Civil Engineering Study 73-3, Structural Series, 1973.
20. J. D. Reynolds and J. H. Emanuel. Thermal Stresses and Movements in Bridges. Journal of the Structural Division, ASCE, Vol. 100, No. ST1, Proc. Paper 10275, Jan. 1974, pp. 63-78.
21. J. H. Emanuel and J. L. Hulsey. Thermal Stresses and Deformations in Nonprismatic Indeterminate Composite Bridges. TRB, Transportation Research Record 607, 1976, pp. 4-6.
22. J. H. Emanuel and D. J. Wisch. Thermal Stresses Induced in a Composite Model Bridge Structure. Missouri Cooperative Highway Research Program, Univ. of Missouri, Rolla, Study 75-2, Final Rept., 1977.
23. J. H. Emanuel and J. L. Hulsey. Temperature Distributions in Composite Bridges. Journal of the Structural Division, ASCE, Vol. 104, No. ST1, Proc. Paper 13474, Jan. 1978, pp. 65-78.

Publication of this paper sponsored by Committee on Foundations of Bridges and Other Structures.

Movements of Bridge Abutments and Settlements of Approach Pavements in Ohio

Raymond A. Grover, Ohio Department of Transportation

The Ohio Department of Transportation experienced intolerable movements of bridge abutments and adjacent approach slabs within a short time after construction of a new highway facility. Two accurate field surveys measured the extent and magnitude of the settlements against the data on embankment heights, subsoil conditions, type of abutment design, and other conditions. The first study, in 1961, indicated that 90 percent of the surveyed bridge abutments had settlements of 10 cm (4 in) or less and only 20 percent of the settlements were 2.5 cm (1.0 in) or less. In most cases, the abutments were supported on spread footings, without piles, in the approach embankment. Major revisions were incorporated in the design and construction specifications. The two most important ones were the use of piles at the abutments and the increase of compaction requirements for the embankments. The second survey was conducted in 1975 to evaluate the revised policies. These data indicated that 70 percent of the surveyed bridge abutments had no measurable settlements and 20 percent had minor settlements even though supported by piling. Generally, the measured settlements were within tolerable limits. In 1961, the average approach slab settlement was 6.5 cm (2.5 in) and in 1975, the average approach slab settlement was 5.0 cm (2.0 in).

By the end of 1960, the Ohio Department of Transportation had completed a large portion of their Interstate highway system as well as the construction of other major highway facilities. This construction program included hundreds of kilometers of new highways and hundreds of new bridges. Over 90 percent of the bridges were steel beams or girders of multiple spans with continuity over the piers, as shown in Figure 1.

Within 1 to 3 years after construction intolerable movements (vertical settlements and horizontal displace-

Figure 1. Steel beam bridge—continuous over piers.

ment) occurred at many bridge abutments and the adjacent approach pavements. The movements were considered intolerable because of the magnitude of the vertical settlements and the resulting dangerous and uncomfortable riding characteristics to the trucking industry and the private automobile. These settlements also caused an undesirable increase in the stresses of the superstructure, particularly over the pier area nearest the abutment. The horizontal movements decreased the efficiency of the temperature expansion joints at the abutments, often to a value of zero. When the expansion joints closed completely, additional compression stresses were transmitted to the superstructure, physical damage occurred to the abutment backwall, beam or girder bearing devices were distorted, and approach slabs were cracked. Maintenance costs and problems such as these so soon after construction of the highway were a serious concern.

The most extreme example of vertical settlement occurred on a structure where the approach embankment height was 17 m (58 ft), the overburden soils were soft wet silts and clays that had a thickness of 3 m (10 ft), and the underlying bedrock was a hard shale. The plans required the removal of all soil overburden such that the embankment would be built and supported directly on the shale bedrock. The plan requirements were fulfilled and the embankment fill was constructed of materials from an adjacent shale and sandstone roadway cut section. The bridge abutment was supported by spread footings (no piles) seated in the approach embankment. Before completion of the construction project, the abutment bearings needed to be shimmed 4 cm (1.5 in) due to consolidations within the rock embankment. During the next 15 years, the settlements continued; total accumulated amounts were more than 30 cm (12 in) in the roadway pavement and the bridge abutment. Three maintenance projects were needed in this time period to correct the settlements and repair the abutment (the last project removed the damaged abutment and rebuilt a new abutment supported on caissons drilled through the embankment into bedrock). This experience is objectionable and expensive.

In general, the field construction procedures for all projects were in reasonable conformance with the plan and specification criteria. This included the construction of the embankment, the controlled rates of embankment construction, the specified waiting periods between the completion of the embankment and the construction of the abutment, and the time relation between placing superstructure concrete versus the concrete abutment backwall.

STATEWIDE SURVEY: 1961

To define the extent and causes of the problem more clearly, a statewide survey was conducted in 1961 (1). The survey included accurate measurements of actual vertical settlements, lateral movements, abutment damage, and condition of expansion joints where significant settlements had occurred at bridges completed between the years 1955 and 1960.

The 12 district offices conducted the survey and no criteria were given to define significant settlement. Probably, noticeable or undesirable responses to a person riding in an automobile over the bridge approach area determined which bridges in the district would be included in the survey. In other words, the riding characteristics were probably tolerable or intolerable to a particular individual.

The existing (measured) roadway approach and bridge profiles were compared with the plan profiles to determine the amounts of settlement. These data were related to embankment heights, existing subsoil conditions, length of waiting periods, type of abutment design (piles, no piles, pile type), amounts of lateral movements, or other unusual conditions. Figures 2, 3, and 4 show typical data and plotted survey profiles.

During this 5-year period, Ohio constructed over 1500 bridges. The abutments of approximately 500 of these bridges were located in a roadway approach embankment that had a height of 5.5 m (18 ft) or more. The survey reported 75 bridges that had significant settlements, but profiles were furnished for only 68 bridge sites (133 abutments); most of the abutments were located in embankment fills of more than 5.5 m (18 ft) in height. Figure 5 shows these data and whether the abutments were designed with or without piles.

At the time of the 1961 survey, about 90 percent of the 133 abutments were below plan grade by 10 cm (4 in) or less and about 20 percent were below plan grade by 2.5 cm (1.0 in) or less.

Prior to the survey, steel shims had been placed at 28 of 133 abutments under the abutment bearing devices to correct settlements that occurred during or shortly after construction. Figures 6 and 7 show the two common bearing devices used in Ohio, one consisting of sliding steel bars and the other consisting of a fabricated rocker, but the sliding device has been shimmed 6.5 cm (2.5 in). When the bearing devices were shimmed, an unsightly differential displacement between the abutment and the superstructure was the end result, as pictured in Figure 8.

Often when vertical settlements occur at the abutments, the abutments will also have horizontal displacements. These horizontal movements will be toward the superstructure. In certain instances, especially when the abutments are supported on spread footings, the horizontal movements will be so severe that the steel beams will contact the concrete abutment backwall, and the backwall will sustain structural damage. When long-term and significant settlements are anticipated during the design stages but will not occur until after the highway is opened for traffic, the steel beams in the end spans can be hinged to avoid superstructure damage from settlements. These hinges probably will not accommodate horizontal movements. Figure 9 indicates a bearing device that has moved 7.5 cm (6 in) vertically and 5 cm (2 in) horizontally.

For the 28 above-noted abutments, 15 had total settlements (including thickness of shims) of 10 cm (4 in) or less, 9 had total settlements of 10 to 30 cm (4 to 12 in), and 4 had total settlements of more than 30 cm (12 in). Below is a tabulation of settlements, which includes settlements corrected prior to the 1961 survey (1 cm = 0.4 in).

Amount Below Plan Grade in 1961 (cm)	Number of Abutments	Amount Below Plan Grade in 1961 (cm)	Number of Abutments
0 to 2.5	28	15.0 to 25.0	4
2.5 to 7.5	79		
7.5 to 15.0	22	Total	133

Total Settlement (includes shims) (cm)	Number of Abutments
0 to 2.5	0
2.5 to 7.5	9
7.5 to 15.0	9
15.0 to 30.0	6
Over 30.0	4
Total	28

The results from the survey clearly indicated the magnitude of the maintenance problems and the probability where the problems would occur. The maintenance costs and the number of areas requiring mainte-

Figure 2. Typical profile, embankment height 11 m.

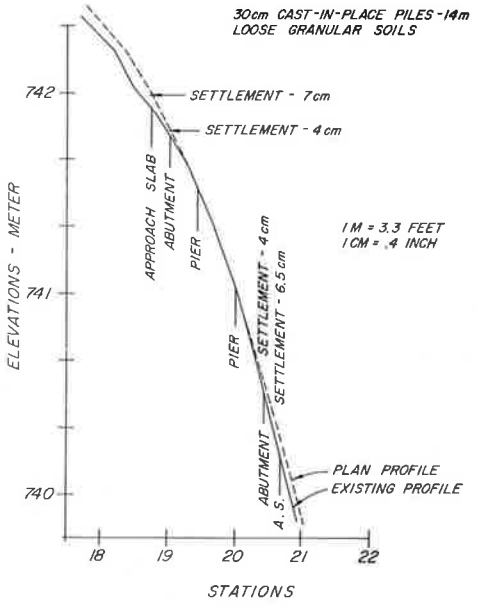

Figure 3. Typical profile, embankment height 5.5 m.

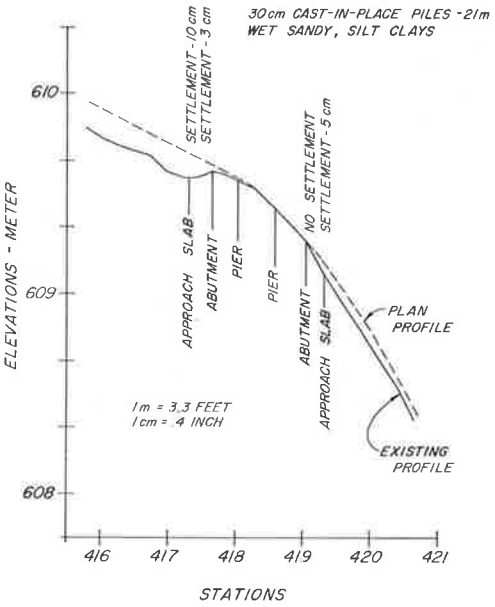

Figure 4. Typical profile, embankment height 12 m.

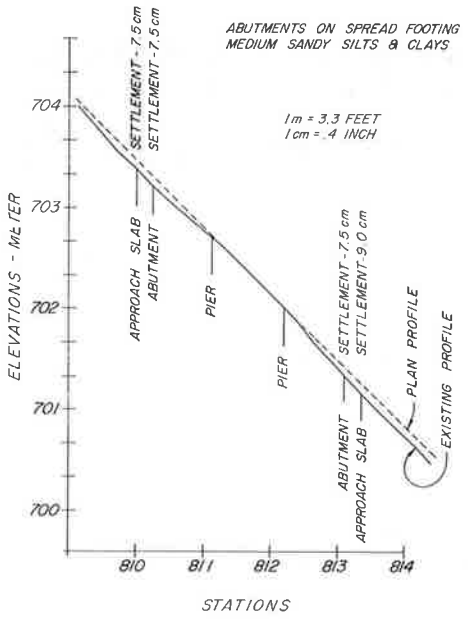

Figure 5. Bridges with measured settlements.

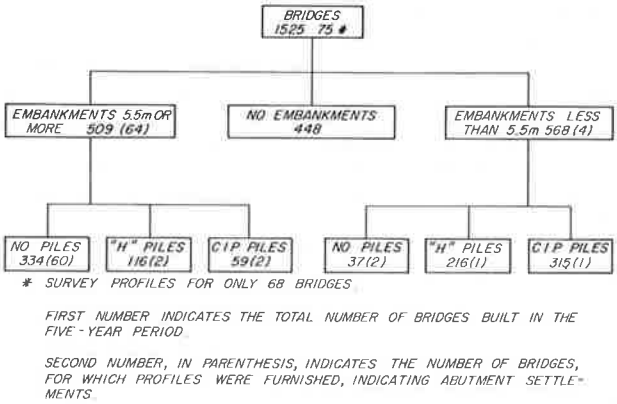

Note: 1 m = 3.3 ft.

Figure 6. Fabricated rocker bearing.

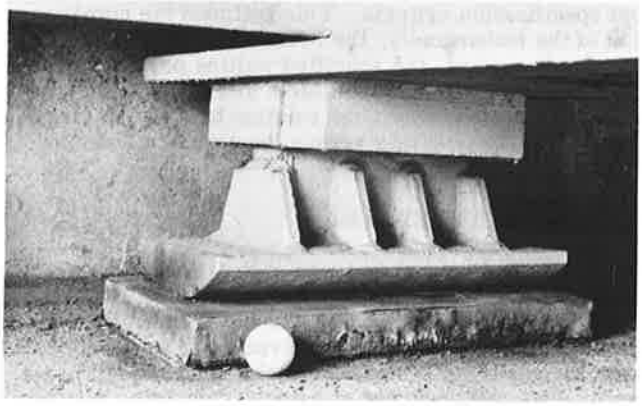

nance were extensive. Revisions to the construction specifications and design policies were mandatory. Several recommendations were offered to improve the design and construction procedures. The department adopted the most important ones.

The design revisions would dictate the use of piles at all abutments located in embankment fills. The piles must penetrate through the fill into a firm subsoil stratum even if preboring of holes was necessary. The plans would require a more positive lateral drainage system behind the abutment and a greater use of settlement platforms and piezometers for monitoring the approach embankment when the underlying soil strata were compressible with anticipated consolidations.

The revision to the construction specifications was to increase the compaction efforts in constructing the embankment. For soil, the compactive density would be based on a laboratory dry weight as high as 102 percent of AASHTO T99. For shale and rock materials, the required loose-layer thickness would not exceed 20 cm (8 in), the moisture content would be controlled, and each layer would have six coverages of a fully ballasted roller.

Figure 7. Sliding plate bearing.

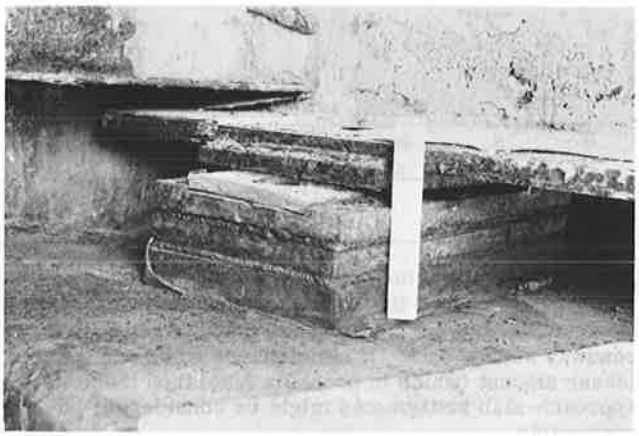

Figure 8. Differential displacement in curb and railing.

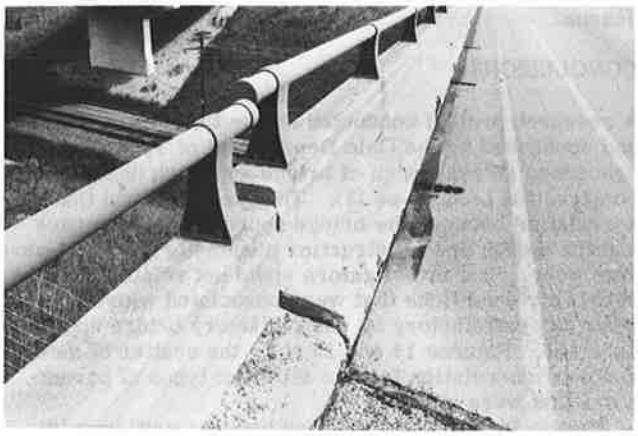

Figure 9. Horizontal and vertical movements.

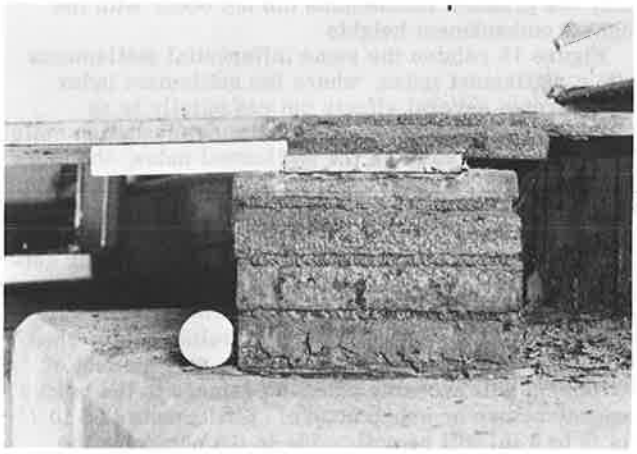

STATEWIDE SURVEY: 1975

In 1975, another survey of all parts of the state was conducted to evaluate the revised design and construction policies (2). Each district was requested to furnish a profile of several bridges and adjacent approach pavements whether or not settlements were noticeable. The given conditions were (a) the bridge should have been completed between 1964 and 1974, (b) the approach embankment height was 4.5 cm (15 ft) or more, (c) the abutments were supported by piles, and (d) the extent of lateral or rotational movements should be indicated.

Profiles for 79 bridges were submitted where the abutments were supported by either cast-in-place reinforced concrete piles or steel H-piles. For these 158 abutments, 71 percent had no measurable settlements and 19 percent had measurable settlements even though supported by piles. Of the 19 percent, 22 abutments were supported by friction piles and 8 were supported by steel H-bearing piles driven to bedrock. Only 6 percent of the abutments had settlements of more than 2.5 cm (1 in) and only one abutment had a settlement of more than 5 cm (2 in). In the 1961 survey, 55 percent of the abutments had settlements greater than 5 cm. An interesting observation should be carefully noted here but is seldom believed by most engineers: The use of piles at abutments located in a roadway embankment is not an assurance that there will be no settlement of the abutment. In Ohio, piles will considerably reduce the amount of abutment settlement versus an abutment design that does not include piles. Even when settlement of a pile-supported abutment occurs, the actual amount is probably within tolerable limits.

A phenomenon was measured in the 1975 survey that did not appear in the 1961 survey. At 10 percent of the abutments, the profiles showed that the existing field elevations were above plan grade from 1.0 to 4.0 cm (0.5 to 1.5 in). No rational explanation can be offered to explain these data. Two districts noted the occurrence of a few rotational or lateral movements of approximately 5 cm (2 in). Figure 10 shows a comparison of abutment settlements between the 1961 and 1975 surveys.

The difference in performance of the two abutment types (supported by piles or spread footings) can also be seen by a comparison of Figures 11 and 12. Deviations from the 1:1 slope line indicates differential settlements between the abutment and the end of the approach slab. Differential settlements are more common for the pile-supported abutments—63 percent of the cases exceeded 2.5 cm (1 in). In the differential settlements for abutments supported by spread footings, only 31 percent of the cases exceeded 2.5 cm.

This aspect of fewer differential settlements may appear desirable from a rideability aspect but is unsatisfactory from other aspects such as total settlements, lateral movements, and maintenance costs. Although

Figure 10. Comparison of abutment settlements.

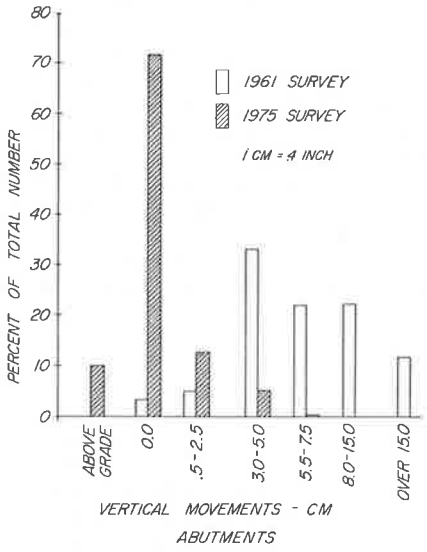

Figure 11. Performance of pile supported abutments.

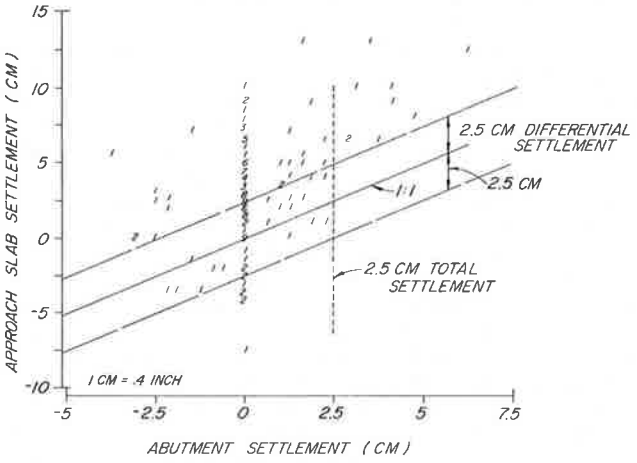

the differential settlements between the abutments on spread footings and the approach slabs were less than the abutments on pilings, the total settlements of the abutments on spread footings were of a much greater magnitude.

The improvement of the settlements at the end of the 158 approach slabs away from the abutments was not nearly as striking as the improvement of the abutment settlements. The data indicate that 10 percent of the approach slabs had no settlement in 1975 and 8 percent had no settlement in 1961. In 1975, 68 percent of the approach slabs had settlement from 2.5 to 7.5 cm (1 to 3 in); in 1961, 62 percent were in this range. In 1975, 12 percent of the approach slabs had settlements of more than 7.5 cm whereas in 1961, 31 percent had settlements of more than 7.5 cm. The 1975 survey measured a maximum approach-slab settlement of 14 cm (5.5 in), but the maximum measured amount was 23 cm (9 in) in 1961. Figure 13 shows a comparison of the approach-slab settlements for the two surveys.

The average approach-slab settlement was 5 cm (2 in) in 1975, but the average settlement was 6.5 cm (2.5 in) slabs having settlements of more than 2.5 cm (1 in), in the 1961 survey. With about 70 percent of the approach this may seem unreasonable. No assessments have

Figure 12. Performance of abutments on spread footings.

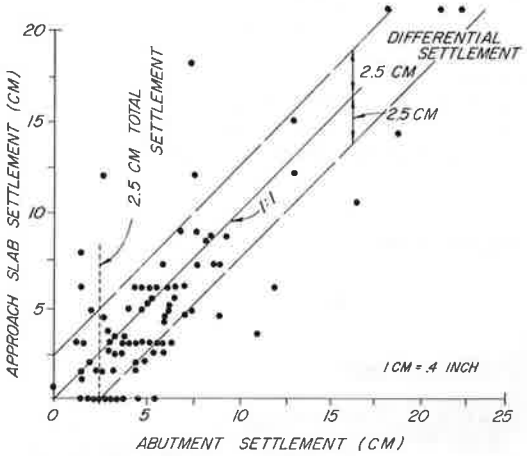

been made between the cost of plan requirements to significantly reduce the amount of approach-slab settlements versus the maintenance costs to repair these roadway settlements. If maintenance costs are the lesser amount (which is probably true) then these approach-slab settlements might be considered reasonable.

Like the abutments, 10 percent of the approach slabs were above the plan profile in the 1975 survey. Perhaps this phenomenon may be attributed to frost heave because the field measurements were made during the winter season.

CONCLUSIONS

A research project conducted by the University of Akron and sponsored by the Ohio Department of Transportation concerned an evaluation of bridge approach design and construction techniques (3). This project found that the correlation between the bridge approach performance and the design and construction parameters studied were very poor. The investigators could not relate with any reliability conditions that were associated with either generally satisfactory or unsatisfactory bridge approach behavior. Figures 14 and 15 show the scatter of data and poor correlation for two different types of parameters that were studied.

Figure 14 shows the relation between settlements (differential settlement between the end of the approach slab and the abutment) and the height of the approach embankment. There is no general correlation, and, in fact, the greatest settlements did not occur with the highest embankment heights.

Figure 15 relates the same differential settlements with a settlement index, where the settlement index incorporates several effects but essentially is an anticipated consolidation of the existing foundation soils. The greater the value of the settlement index, the more plastic the subsoils. The data of the graph are random: Nonplastic soils indicate settlement distress as great as that with cohesive soils.

After several years of observing and measuring settlements at bridge approaches, I believe that settlements of 2.5 cm (1 in) or less can be classified as tolerable and will hardly be noticed by the traveling public when tempered by an approach slab. Also, this amount of settlement will probably cause no damage to the bridge superstructure or substructure. Settlements of 5 to 7 cm (2 to 3 in) will be noticeable to the person in the

Figure 13. Comparison of approach slab settlements.

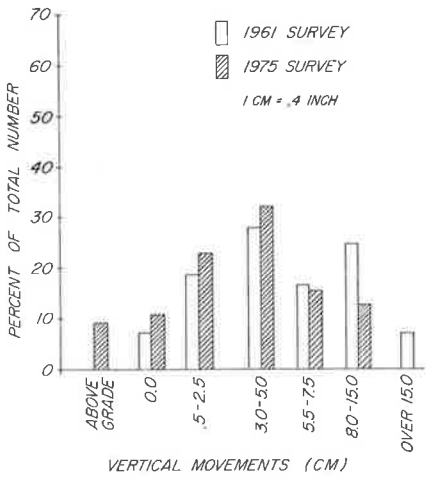

Figure 14. Differential settlements versus embankment height.

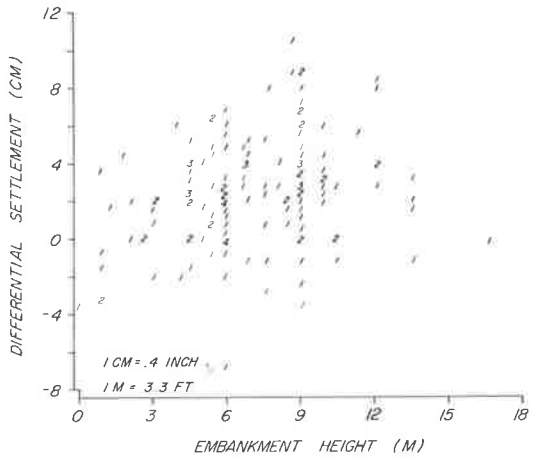

moving vehicle, but only minor damage, if any, will occur to the structure.

The vehicle response to settlements of 10 cm (4 in) or more will undoubtly be objectionable to a vehicle passenger and physical damage will likely occur in the bridge superstructure and abutments. Settlements of this amount should be classified as intolerable.

Little or no maintenance will be done and may not be necessary for settlements of 2 to 5 cm (1 to 2 in) or less.

Figure 15. Differential settlement versus settlement index.

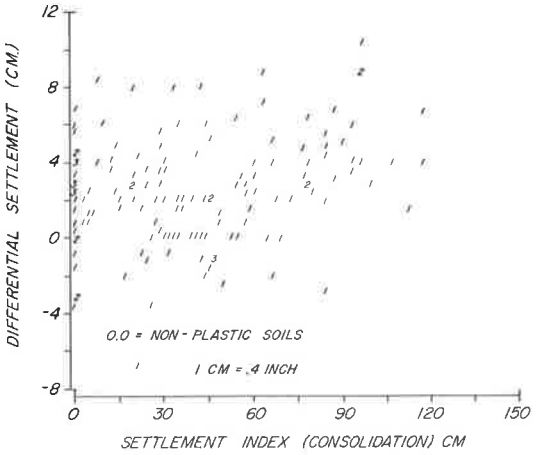

Maintenance may not be furnished for settlements of 7 to 10 cm (3 to 4 in) but should be considered desirable. For settlements of a greater magnitude, maintenance is probably necessary and likely to be completed.

ACKNOWLEDGMENT

These comments on tolerable or intolerable settlements and the related maintenance program are my own feelings and observations. They have no official status of my office or the Ohio Department of Transportation. I have no exact or precise documentation to either substantiate or refute my observations. I do believe rather strongly that this is an appropriate attitude toward tolerable or intolerable settlements.

REFERENCES

1. Report of Survey of Settlements in Bridge Substructures and Approach Pavements. Bureau of Bridges, Ohio Department of Highways, Sept. 1961.
2. Report of Survey of Vertical Movements in Bridge Abutments and Approach Pavements. Bureau of Bridges, Ohio Department of Transportation, Sept. 1975.
3. D. H. Timmerman. An Evaluation of Bridge Approach Design and Construction Techniques. Univ. of Akron. Ohio Department of Transportation, and Federal Highway Administration, Research Rept., Dec. 1976.

Publication of this paper sponsored by Committee on Foundations of Bridges and Other Structures.

Bridge Foundations Move

M. Bozozuk, Division of Building Research, National Research Council of Canada, Ottawa

The postconstruction performance of several hundred bridges in the United States and Canada was related to the measured movements of their foundations. The results, presented graphically, indicate the range of vertical and horizontal movements and consequently provide realistic information for the planning of remedial work and the practical design of new bridges. A classification of movements for bridge foundations is proposed.

In 1975 the Transportation Research Board Committee on Foundations of Bridges and Other Structures conducted a performance survey of existing bridges in the United States and Canada to determine the foundation movements that could be tolerated by a structure. A questionnaire, which was similar to one used in a 1967 survey, was sent to all highway departments, bridge departments, public works agencies, and research organizations in every state and province in these two countries. The following information was requested for each case: type of bridge, description of the foundations for the abutments and piers, description of the subsoils, the magnitude and description of foundation movements, the kind of maintenance required, and whether or not the movements were tolerable. The satisfactory response to the survey yielded a considerable amount of information covering most of the bridge, foundation, and soils combinations in North America.

SURVEY INFORMATION

On this continent there are literally thousands of bridges of all sizes, designs, and ages, which are supported on various foundations and soils. Only a limited number of meaningful measurements of foundation movements and assessments of the performances of the structures were obtained from the survey; however, it was clear from the answers given that where little maintenance was required, the performance was rated tolerable, no matter how little or great the movements. Where considerable maintenance or repairs were required, all movements were rated not tolerable. A detailed discussion of these movements is reported by Keene in a paper in this Record.

The engineering performance of the bridges was directly related to the extent and kind of movement to which the abutments, piers, and foundations were subjected after construction. As there were three basic foundations, the performance ratings were studied separately under the following headings:

1. Abutments and piers on spread footings—all footings placed on fills, natural ground, or bedrock.
2. Abutments and piers on friction piles—all friction piles including steel H, pipe, concrete, and wood, whether driven through fill or natural ground.
3. Abutments and piers on end-bearing piles—all piles bearing on rock or in a resistant soil formation.

In some cases movement was not recorded or was reported as zero. For presentation in figures in this report, zero movement, whether vertical or horizontal, was assumed to be equal to or less than 3 mm (0.01 ft).

Abutments and Piers on Spread Footings

Vertical and horizontal movements of about 120 abutments and piers and their rated performance with respect to whether they were tolerable or not tolerable are shown in Figure 1. Vertical settlements ranged from 0 to more than 1000 mm (3 ft), and the horizontal movements ranged from 0 to 510 mm (1.6 ft). Some of the movements were uniform; others were differential or rotational. About 28 percent of the cases were rated not tolerable.

The most common cause of movement was consolidation of earth fills and underlying foundation soils. Other causes included instability of embankment fills and valley slopes, soil creep, and active earth pressures behind abutments. Seasonal temperature variation was also listed as one of the causes. For example, Dillon and Edwards (1) report that abutments were affected by freezing of bridge bearings. As the bridge deck contracted in winter, the abutments were pulled together. In summer, the bearings behaved normally, but the subsequent expansion of the bridge deck did not push back the abutments. Over a number of years this process closed all expansion joints and caused heavy damage to the bridge.

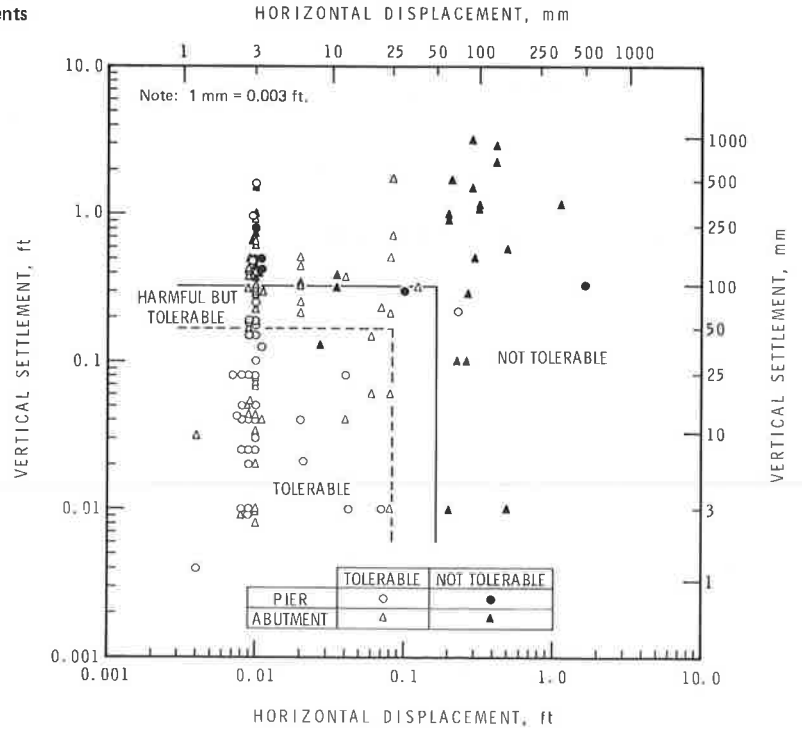

Figure 1. Engineering performance of bridge abutments and piers on spread footings.

Abutments and Piers on Friction Piles

About 60 cases involving friction piles were reported. Vertical and horizontal movements of abutments and piers and their effects on the performance of the bridges are plotted in Figure 2. The vertical settlements ranged from 0 to over 1220 mm (4 ft), and the horizontal displacements ranged from 0 to 460 mm (1.5 ft). In permafrost areas, vertical heaving of the piles of 50 to 1070 mm (0.17 to 3.5 ft) was observed due to frost action. About 40 percent of the cases were judged not tolerable and the remainder were tolerable. Some of the differential or rotational movements that were less than some of the tolerable ones were not tolerable; the tolerable movements were mainly uniform. The causes for these movements were instability of natural slopes, soil creep, settlement of embankment fills, and downdrag or negative skin friction.

Abutments and Piers on End-Bearing Piles

About 90 cases that describe the performance of abutments and piers on end-bearing piles were reported. The magnitude of the vertical and horizontal movements and their effects on the performance of the bridges are shown in Figure 3. Vertical settlements ranged from 0 to a maximum of 1100 mm (3.6 ft); the horizontal movements ranged from 0 to 550 mm (1.8 ft). About 60 percent of the cases were judged not tolerable. Some large movements were judged tolerable because they were uniform and did not interfere with the performance of the bridge, whereas some small differential or rotational movements were not tolerable.

The major causes for these movements were instability of natural slopes, soil creep (2), and consolidation of the compressible soils around piles due to the weight of embankment fills. When the subsoils consolidated, batter and vertical piles were forced to bend and caused the superimposed abutments and piers to settle, rotate, and translate horizontally (3). In numerous cases large settlements of the piles were attributed to downdrag or negative skin friction as the surrounding foundation soils consolidated around the piles. At one bridge site, negative skin friction was identified as the cause of failure of 17 end-bearing piles.

Large uniform settlements usually did not affect the performance of the bridges. For example, a bridge supported on end-bearing piles on bedrock was subjected to settlements of from 300 to 600 mm (1 to 2 ft). General subsidence of the underlying bedrock was caused by a solution of a thick salt formation 82 m (250 ft) thick at a depth of 426 m (1300 ft) at the site. This was responsible for large movements that were considered tolerable.

CLASSIFICATION OF BRIDGE FOUNDATION MOVEMENTS

Examination of the performance ratings of foundation movements plotted in Figures 1, 2, and 3 showed that horizontal movements affected the structures more than did the vertical movements. It was possible, nevertheless, to delineate the tolerable and not tolerable movements from which the proposed classification of bridge foundation movements was developed. It is shown on each of the figures and is given as follows:

Tolerable or acceptable:
$S_v < 50$ mm (0.16 ft)
$S_H < 25$ mm (0.08 ft)
Harmful but tolerable:
50 mm (0.16 ft) $\leq S_v \leq$ 100 mm (0.33 ft)
25 mm (0.08 ft) $\leq S_H \leq$ 50 mm (0.16 ft)
Not tolerable:
$S_v > 100$ mm (0.33 ft)
$S_H > 50$ mm (0.16 ft)

where

S_v = vertical movements (settlement or heave), and
S_H = horizontal movements.

To demonstrate how this classification applied to the performance ratings obtained from the field survey, all the cases plotted in Figures 1 through 3 were compared statistically in Tables 1 and 2 according to this classification.

In Table 1, 110 cases were assessed, covering spread footings, friction piles, and end-bearing piles where the abutment and pier movements were judged not tolerable. The percentage distribution of the field ratings for each of the foundations was relatively consistent with the proposed classification. When they were grouped, 85 percent agreed with the proposed classification, 12 percent came within the harmful but tolerable range, and 3 percent fell within the tolerable zone.

For the field-rated tolerable movements, the percentage distribution was different, but the agreement was satisfactory (Table 2). Of the 157 cases, 56 percent agreed with the proposed classification, 22 percent came within the tolerable but harmful range, and 22 percent fell into the not tolerable range. The results are shown in Figure 4.

The movements rated not tolerable in the field were in excellent agreement with the proposed classification, but agreement for the movements rated tolerable in the field was only satisfactory. The reason for the differences was that the performance of foundations was governed not only by the magnitude of the movements but also by the kind of movements. Large vertical and horizontal movements were acceptable if they were uniform, as shown by the statistical distribution of tolerable cases. On the other hand, vertical and horizontal movements can be very harmful and can damage the structures severely if they are differential or of a rotational nature. Most of the movements judged not tolerable were of the latter type, hence the good agreement with the classification. Since the engineering profession is more concerned with harmful or not tolerable movements, the proposed classification of foundation movements for bridges was considered satisfactory.

SUMMARY AND CONCLUSIONS

In 1975 a questionnaire circulated throughout the United States and Canada requested information on the engineering performance of all bridges whose abutments or piers were supported on either spread footings, friction piles, or end-bearing piles. The response to the survey showed that bridge foundations were affected by slope instability, consolidation of embankment fills and underlying subsoils, soil creep along valley slopes, frost action, and seasonal temperature variations. In addition, pile foundations were affected by soil settlements and negative skin friction or downdrag.

An analysis of the reported foundation movements and performance ratings showed that

1. Large vertical and horizontal uniform movements were often tolerated.
2. Differential or rotational movements were more damaging than uniform movements, and their effect on

the performance of the structure was often rated not tolerable.

3. Bridge structures were more sensitive to large horizontal movements than to large vertical movements.
4. Based on the available data, a classification of movements for bridge foundations was proposed that applied adequately to most of the cases reported in the survey.
5. All bridge foundations move.

ACKNOWLEDGMENTS

Appreciation is expressed to all those in the United States and Canada who took the time to answer the questionnaire and made their information available to the engineering profession. Many members of the TRB Committee on Foundations of Bridges and Other Structures helped collect this information and their assistance is gratefully acknowledged. This paper is a contribution from the Division of Building Research, National Re-

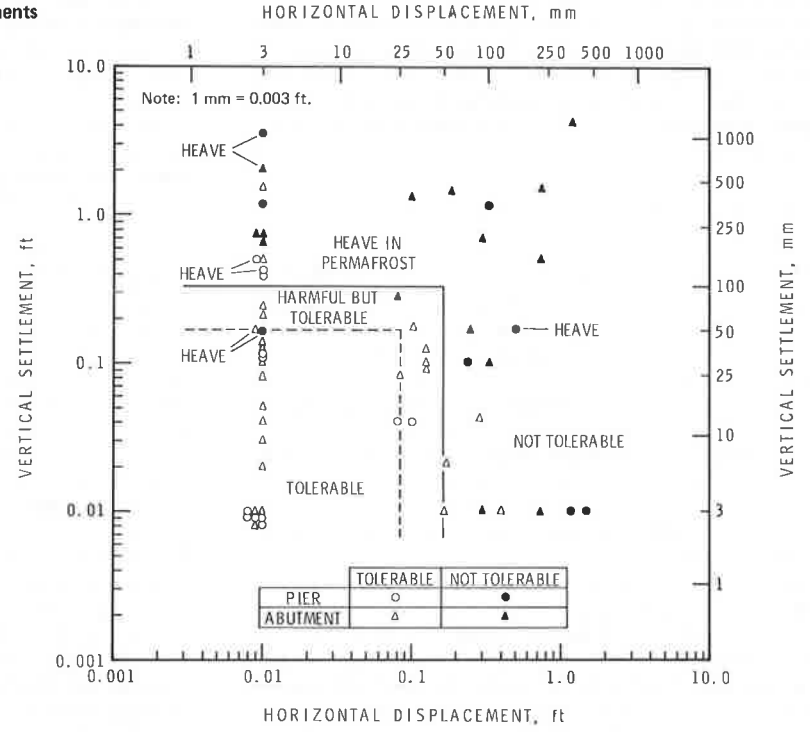

Figure 2. Engineering performance of bridge abutments and piers on friction piles.

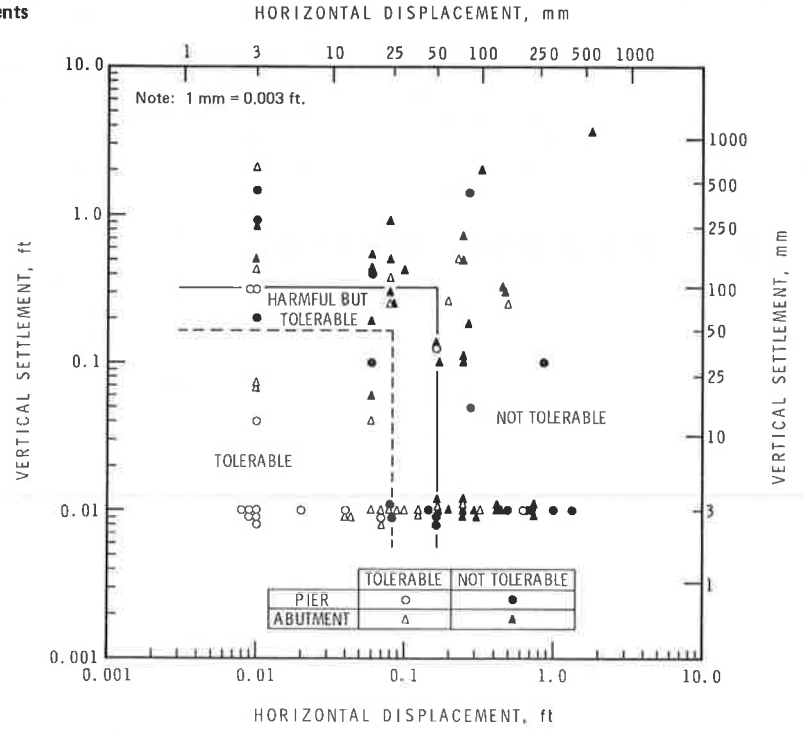

Figure 3. Engineering performance of bridge abutments and piers on end-bearing piles.

Table 1. Application of suggested classification for bridge foundation movements to field-rated not tolerable performance of bridges.

Type of Foundations for Piers and Abutments	Survey Points (number)	Classification of Bridge Foundation Movements: Not Tolerable Points (number)	Not Tolerable Distribution (%)	Harmful but Tolerable Points (number)	Harmful but Tolerable Distribution (%)	Tolerable Points (number)	Tolerable Distribution (%)
Spread footings	33	30	91	2	6	1	3
Friction piles	24	21	88	3	12	0	0
End-bearing piles	53	43	81	8	15	2	4
Total	110	94	85	13	12	3	3

Table 2. Application of suggested classification for bridge foundation movements to field-rated tolerable performance of bridges.

Type of Foundations for Piers and Abutments	Survey Points (number)	Classification of Bridge Foundation Movements: Not Tolerable Points (number)	Not Tolerable Distribution (%)	Harmful but Tolerable Points (number)	Harmful but Tolerable Distribution (%)	Tolerable Points (number)	Tolerable Distribution (%)
Spread footings	86	19	22	18	21	49	57
Friction piles	36	7	19	8	22	21	58
End-bearing piles	35	8	23	9	26	18	51
Total	157	34	22	35	22	88	56

search Council of Canada, and is published with the approval of the director of the division.

REFERENCES

1. R. M. Dillon and P. H. D. Edwards. The Inspection, Repair and Maintenance of Highway Bridges in London, Ontario. Engineering Institute of Canada, Engineering Journal, Vol. 44, No. 11, 1961, pp. 39-48.
2. M. Bozozuk. Mud Creek Bridge Foundation Movements. Canadian Geotechnical Journal, Vol. 13, No. 1, 1976, pp. 21-26.
3. A. G. Stermac, M. Devata, and K. G. Selby. Unusual Movements of Abutments Supported on End-Bearing Piles. Canadian Geotechnical Journal, Vol. 5, No. 2, 1968, pp. 69-79.

Figure 4. Assessment of foundation performance ratings.

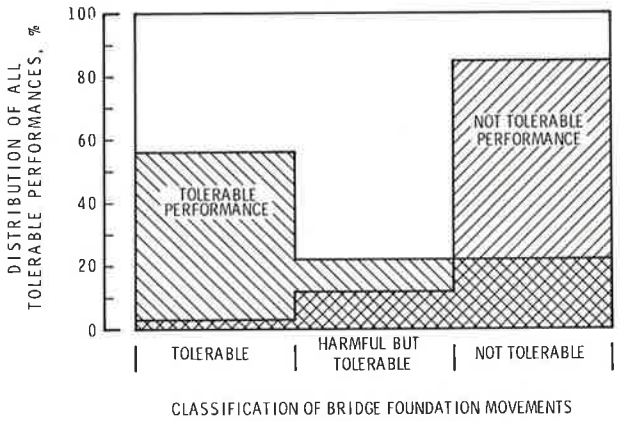

Discussion

A. G. Stermac, Materials Office, Ontario Ministry of Transportation and Communications

The author is to be complimented for his review, sorting, and tabulation of such a vast amount of information. It is certainly an interesting presentation.

When so many results start to form a pattern, one is tempted to draw certain conclusions. The author has obviously succumbed to this temptation and has suggested values beyond which bridge movements become harmful but still tolerable and beyond which they become not tolerable. What constitutes tolerable or intolerable movements of a bridge can be considered from a number of viewpoints, such as

1. Structural integrity,
2. Maintenance, and
3. Public perception of ride comfort.

There is no question that, by far, the most important consideration is the structural integrity of the bridge because it most directly affects the safety of the traveling public. It is, though, only the designer, the structural engineer, who can determine what type and amount of movement a particular bridge can safely tolerate.

It is well known that, basically, only differential movements will have a bearing on the structural integrity of a bridge. These, however, are a function of the bridge type, width, length, and span length. To lump all bridges together amounts to saying that all bridges are the same and behave in the same way. This, of course, is not the case. Not differentiating between uniform and differential movements and settlements amounts to saying that this does not matter. This also is not the case.

In view of the above, the value of criteria developed without reference to type, length, or width of bridges and type of movement or settlement is seriously questioned. The author's last conclusion that "all bridge foundations move" is also questioned since there is ample evidence that some did not.

Publication of this paper sponsored by Committee on Foundations of Bridges and Other Structures.

Sand Drain Theory and Practice

Richard E. Landau, West Hempstead, New York

The theoretical approach to the design of sand drain installations has often proved inadequate in the prediction of field performance. The divergence of field performance from designs based on data obtained from tests of undisturbed samples has been found to be greatest where displacement methods of sand drain installation are employed and least where nondisplacement techniques are used. The nondisplacement methods most commonly employed involve controlled jetting and augering systems. Nondisplacement methods are not equivalent with respect to the avoidance of subsoil disturbance; therefore, some divergence between designs based on undisturbed sample test data and field performance is still encountered. This paper reviews the basis for using sand drains and the background of the development of nondisplacement techniques and presents a systematic approach applicable to the evaluation of all installation methods. This approach is essential if the designer is to be provided with all tools necessary for the development of sand drain designs that have a reliable factor of safety when applied in construction, as the nondisplacement methods in use today do not produce comparable results in the field. The results of the Maine test section are reviewed to demonstrate how equivalent designs can be developed for specific methods of installation and specific types of soil.

Where stability problems or excessive residual primary settlements are anticipated, the use of sand drain stabilization should be considered either as an alternative to or in conjunction with preloading in the development of a feasible design. Other methods of construction should be considered and priced, and the final selection made on the basis of cost as well as on reliability of the design in producing the required result. Such intangibles as aesthetic and environmental effects during and after construction should be given due consideration.

The inconsistent performance of sand drain projects has often been related to an incomplete evaluation of factors involved in design (1). However, even where design theory (2) has been properly applied, it has been found that the effects of the installation procedure employed can be a determining factor in performance. This paper describes the use of empirically derived parameters in design to compensate for aspects of the installation procedure and discusses standardization of sand drain installation procedures as a means of minimizing the introduction of construction-related variables.

BACKGROUND

The history of sand drain stabilization is well documented (1) and need not be recounted. Typical displacement methods available are listed below. (1 cm = 0.39 in. Paper, Sandwick, and Fabridrains may be protected by U.S. patents.)

Descriptive Name	Usual Diameter (cm)	Backfill
Driven mandrel (closed end)	30 to 50	Placed at time of mandrel withdrawal
Paper drains (Kjellman method)	10 x 0.3	Drainage strip placed at time of mandrel withdrawal
Sandwick drains	Up to 15	Prepacked fabric filled with sand placed after hole is made by mandrel
Fabridrain	Up to 15	Fabric liner filled with sand placed at time of mandrel withdrawal

The first sand drain project specifically designed for installation of drains by nondisplacement methods that was successfully completed involved stabilization of sensitive varved silt and clay deposits, which supported the approach embankment of the State Street Bridge in East Hartford, Connecticut. This project, which involved use of the flight auger method, was the forerunner of many successful projects constructed in Connecticut (3) that involved similar soil conditions. The concept of nondisplacement as an element in sand drain stabilization design was later adopted by the New York State Department of Transportation for stabilizing highway embankment foundations on sensitive organic clay deposits in the borough of Queens in New York City (4, 5). [A previous project in the same soil deposit involving the use of the mandrel method proved unsatisfactory because of excessive settlements caused by remolding of the soil structure (4).]

After the success of the auger method used in sensitive soils in Connecticut and New York, other states adopted the use of augered sand drains. As a consequence, other nondisplacement methods, as listed below, were introduced (6, 7, 8, 9) in the United States. (1 cm = 0.39 in. Jet-bailer and Sandwick drains, jet augers, and the auger method may be protected by U.S. patents.)

Descriptive Name	Usual Diameter (cm)	Backfill
Pressed casing	Up to 45	Placed at time of casing withdrawal
Jet-bailer drains	30	Placed after hole is formed
Jet augers and jet casing	Up to 45	Placed at time of drill or casing withdrawal
Jetted mandrel	30 to 50	Placed at time of mandrel withdrawal
Rotary jet	Up to 50	Placed after hole is formed
Auger method	Up to 45	Placed during or after auger withdrawal
Sandwick drains	Up to 15	Fabric-filled wick placed in any suitable hole formed by nondisplacement techniques

The improvement in the performance of nondisplacement installations over displacement methods has been related to a reduction in smear. Smear (1) is defined as the ratio of the diameter of the remolded zone immediately adjacent to the cavity periphery to the diameter of the cavity itself. Inasmuch as the formation of the remolded zone can only be produced by lateral soil displacement (5), the simple rubbing of a cavity-forming tool over the periphery of cavities formed by nondisplacement techniques will not result in smear when the rate of tool advance is controlled to ensure full cavity excavation. Any differences in performance that may be observed between various displacement techniques as well as between various nondisplacement installation methods must be related to disturbance effects associated with field as well as operating conditions. As such, various techniques may be substantially superior in one type of soil than in another (10) for reasons that are not definable by purely theoretical considerations.

SAND DRAIN DESIGN

The principal purpose of a sand drain installation is to accelerate the primary consolidation of compressible subsoils during the construction period and to limit the magnitude and rate of postconstruction settlements to acceptable values. Slope stability is improved as a result of a concurrent increase in soil strength. Most often, this involves achievement of about 85 percent of primary consolidation during construction and substantial limitations on postconstruction settlements to secondary values. Where settlements approach 100 percent of primary consolidation during construction, a surcharge load is needed. Where differential rather than total settlement is the controlling factor, surcharge loading may be avoided when the thickness of the compressible subsoil does not vary sharply and finished grade requirements are not critical.

The theory of consolidation is well known (11). Where slope stability can be developed, the feasibility of using sand drain stabilization depends on the magnitude and rate of residual primary and secondary consolidation falling within limits acceptable for the proposed construction. The magnitude of secondary consolidation is established by the relationship:

$$H_{sec} = Lc_{sec} \log(t/t_c) \quad (1)$$

where

H_{sec} = secondary settlement at time interval t,
L = thickness of compressible stratum,
c_{sec} = coefficient of secondary consolidation,
t_c = time interval to reach 85 percent of primary consolidation,
t = time interval (must be greater than t_c).

The rate of secondary settlement (Δh_{sec}) will be essentially equal to the rate of primary settlement at the time of substantial completion of primary consolidation and is approximately expressed as

$$\Delta h_{sec} = 0.435L(c_{sec}/t_c) \quad (2)$$

If the foregoing values as determined from Equations 1 and 2 meet design requirements, then sand drain stabilization can be considered for the project. Stability and settlement analyses are performed to determine the need for subsoil strength increase or berm stabilization to ensure safe completion of the proposed construction, and to estimate the total values of settlement incurred under the design loading. Consideration of soil strength increase with consolidation related to nondisturbance installation techniques can be handled by correlating strength with moisture content or by an evaluation of effective stresses as consolidation occurs (11). In general, for normally consolidated soils, analyses are based on average values of test data obtained from undisturbed samples. For precompressed soil the values used would distinguish between characteristics above and below the preconsolidation loading.

The basic equations involved in the design of sand drain installations, as concerns the determination of the rate at which primary consolidation can be expected to occur, are as follows for consolidation related to vertical drainage,

$$t_p = [T_v(L/f_v)^2]/c_v \quad (3)$$

where

t_p = time interval during primary consolidation,
T_v = time factor for specific degree of consolidation,
f_v = vertical drainage factor [1 (single drainage) or 2 (double drainage)], and
c_v^c = coefficient of vertical consolidation.

For consolidation related only to radial drainage,

$$t_h = [T_h(f_h S)^2]/c_h = (T_h D_e^2)/c_h \quad (4)$$

where

T_h = time factor for horizontal consolidation,
f_h = radial drainage grid factor [1.13 (square grid) or 1.07 triangular grid)],
S = spacing of sand drains in grid pattern,
c_h = coefficient of horizontal consolidation, and
D_e = diameter of sand drain influence.

Time factor curves for vertical and radial drainage are presented in Figure 1. Approximate values for the indicated ranges of consolidation can be obtained by using Equations 5 and 6 (approximately):

$$T_v \overset{\times}{=} 0.8\, u_v^2 \text{ and } 0 \leq u_v \leq 0.5 \quad (5)$$

where u_v = vertical degree of consolidation.

$$T_h \overset{\times}{=} 0.8\, u_h^{2.5} \log_{10}(n/2) \text{ and } \begin{matrix} 0.5 \leq n \leq 20 \\ 0.7 \leq u_h \leq 0.9 \end{matrix} \quad (6)$$

where

u_h = horizontal degree of consolidation and
n = ratio of D_e to d_w.

In the foregoing equations, as in later expressions, no distinction is made between free strain and equal strain settlement, as the difference is negligible as compared to many other uncertainties in design (2).

Where vertical consolidation is found to exceed 5 percent ($u_v \geq 0.05$) for the assumed construction period, the vertical consolidation is often considered in determining total consolidation. Where the total percentile magnitude of desired consolidation is established and the corresponding value of vertical consolidation is known, the settlement contribution required from the sand drain installation can be found by

$$U_h = 100\% - (100 - U_c)/(1 - U_v/100) \quad (7)$$

where

U_h = percent of consolidation, horizontal;
U_c = percent of consolidation of construction; and
U_v = percent of consolidation, vertical.

An alternative expression relating the terms is

$$u_h = 1 - (1 - u_c)/(1 - u_v) \quad (8)$$

Where u_c = degree of consolidation of construction. The geometry of the san drain pattern to attain the desired consolidation can be developed in the following manner:

1. By experience, assume a value for D_e, with d_w as 45 cm (1.5 ft) and develop a trial value of n. (The value of d_w can be increased or decreased at will based on theoretical considerations; however, the initial design should be based on a specified value of d_w.)

Figure 1. Time factor versus percent consolidation.

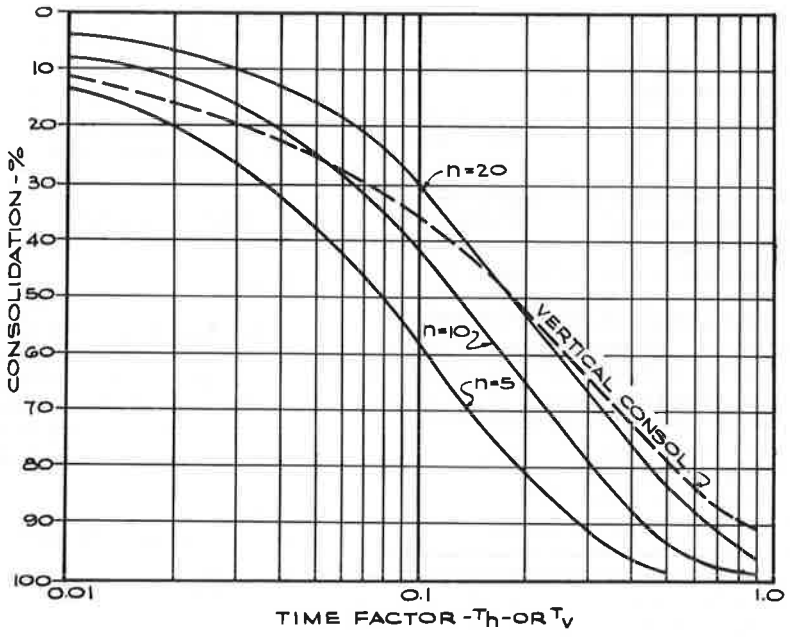

Figure 2. Time-settlement (typical).

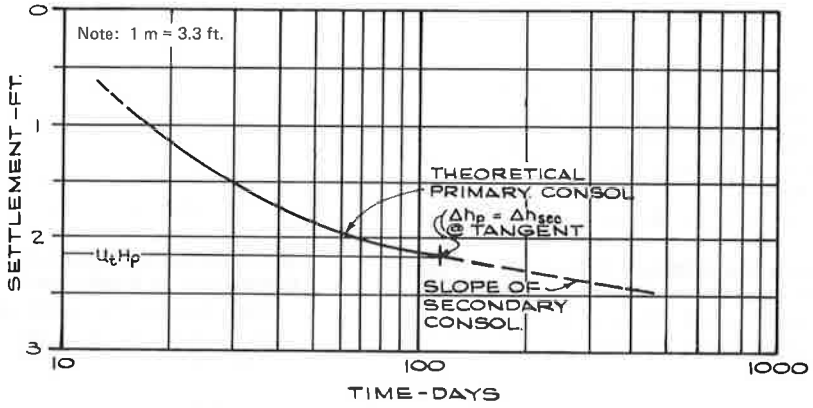

2. With the values of t_h (= t_c), D_e, and c_h, enter Equation 4 to find the required value of T_h.

3. Use Figure 1 or Equation 6 with T_h and n to find the degree of consolidation involved ($U_h = 100u_h$).

4. If U_h is other than the desired value, alter the assumption for D_e and repeat the foregoing steps until U_h meets design requirements.

Secondary Consolidation

Although surcharge has been used to reduce the rate of secondary settlement, postconstruction settlements cannot be less or slower than values related to secondary consolidation. As such, the optimum sand drain design will be one that develops a rate of primary consolidation equal to that of secondary at the time of completion of construction. Inasmuch as the occurrence of secondary consolidation relates only to the thickness of the compressible stratum and is presumed to start toward the end of primary consolidation, it is evident from the expression for secondary consolidation shown in Equation 1 that the graph of consolidation versus time will be a straight line on a semilogarithmic scale.

By superimposition of the secondary consolidation curve on the primary consolidation curve so that the two are tangent, the optimum end point for primary consolidation (u_c) can be established (Figure 2). (This model was designed for U.S. customary units only; therefore values in Figure 2 are not given in SI units.) Inasmuch as U_v at t_c is fixed, u_h can be established by means of Equation 7. Returning to Equation 4 using any desired value of d_w, the value of D_e can be established by trial and error.

Once a workable set of values is established for D_e and n, Equation 9 can be used to approximate an equivalent set of values should it be desired to alter either D_e or n.

$$(D_e/E_w^{1/2})\,[\mathrm{Log}_{10}(n/2)]^{1/2} = M \qquad (9)$$

where

E_w = efficiency of sand drain,
t_f = field or final time,
t_d = design or theoretical time,
u_f = field or final degree of consolidation at t_f,
u_d = design or theoretical degree of consolidation, at t_d,
M = sand drain grid equivalence factor, and

$$t_f = t_d \begin{cases} E_w = T_{hf}/T_{hd}, \text{ or} \\ E_w \approx (u_f/u_d)^{2.5} \\ \text{when } 0.7 \le u_h \le 0.9. \end{cases}$$

The value M is a constant for any set of field conditions. The foregoing relationship also permits applying the sand

drain efficiency (E_w) to each sand drain installation method contemplated. A theoretical set of efficiency curves for the mandrel method is shown in Figure 3. Where d_w is a constant, use $n = n_o/E_w^{1/2}$ in Equation 9.

Sand Drain and Sand Blanket Material

Equivalent sand drain designs can be developed for a given set of soil conditions and time parameters by varying the sand drain diameter (d_w) and its diameter of influence (D_e) in accordance with Equation 3. It can be shown mathematically that equivalent designs based on a large percentile change in d_w will reflect only as a small change in D_e^2 and the capacity of the sand drain to carry water varies with d_w^2, then for equivalent designs a smaller-sized drain diameter will necessitate the use of higher permeability sand backfill material to avoid introducing excessive head losses within the sand drain itself. The effect of such head losses reflects as backpressure, which affects sand drain performance as described by Barron (2).

Where hydrostatic backpressure is permitted, the backfill permeability may be approximated by Equation 10:

$$k_w = \Delta h n^2 (L+B)/2(P_t - P_o - P_b) \quad (10)$$

Figure 3. Grid efficiency versus permeability ratio for mandrel method.

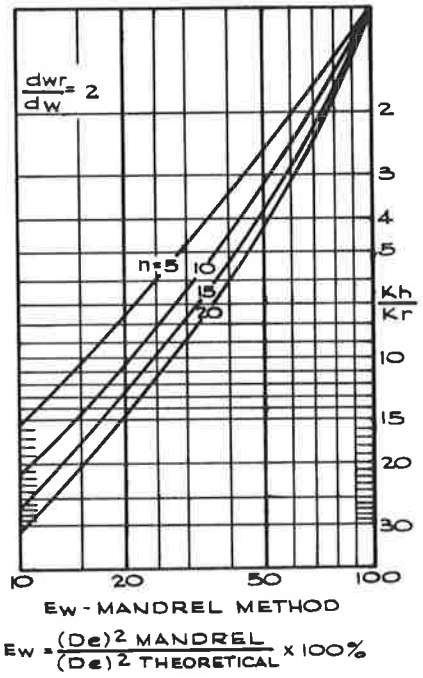

where

k_w = permeability of sand drain backfill;
Δh = settlement rate;
B = sand blanket thickness;
P_t = total load expressed as hydrostatic head;
P_o = initial ground level above natural water table, expressed as hydrostatic head; and
P_b = sand blanket or lateral drainage channel load or hydrostatic backpressure.

Thus, the larger the sand drain diameter for equal settlement rates (Equation 9), the lower the permissible permeability of the backfill material, which would reflect as a cost differential for the installation.

Similarly (as shown in Figure 4) an approximation can be derived for the permeability of the sand blanket material, as follows:

$$k_b = \Delta h W^2/[2B(B + P_b)] \quad (11)$$

If, instead of using a uniform sand blanket, French drains (height, B) are used to interconnect the sand drains, an expression similar to that above can be developed:

$$k_b = \Delta h W^2 S/[2A_b(B + P_b)] \quad (12)$$

where

k_b = sand blanket permeability,
W = half width of embankment (stabilized), and
A_b = sand blanket cross-section area.

As in the case of the sand drain backfill, the sand blanket permeability presumes an acceptable hydrostatic backpressure of P_b. The consideration of sand blanket permeability is important inasmuch as coarse sand material is often scarce and, therefore, can be costly to obtain. Equations 11 and 12 permit an economic evaluation of the best means to provide a drainage blanket for the sand drain installation. A substantial factor of safety (such as 10 or more) should be applied to K_b where feasible.

Surcharge

The use of surcharge in conjunction with the design of sand drain installations may be desirable if:

1. Postconstruction total settlements without surcharge exceed maximum tolerable limits for the type of construction involved;
2. The cost of surcharge material (including placement and removal) is less than the cost of using a closer

Figure 4. Instrumentation configuration (typical for test sections).

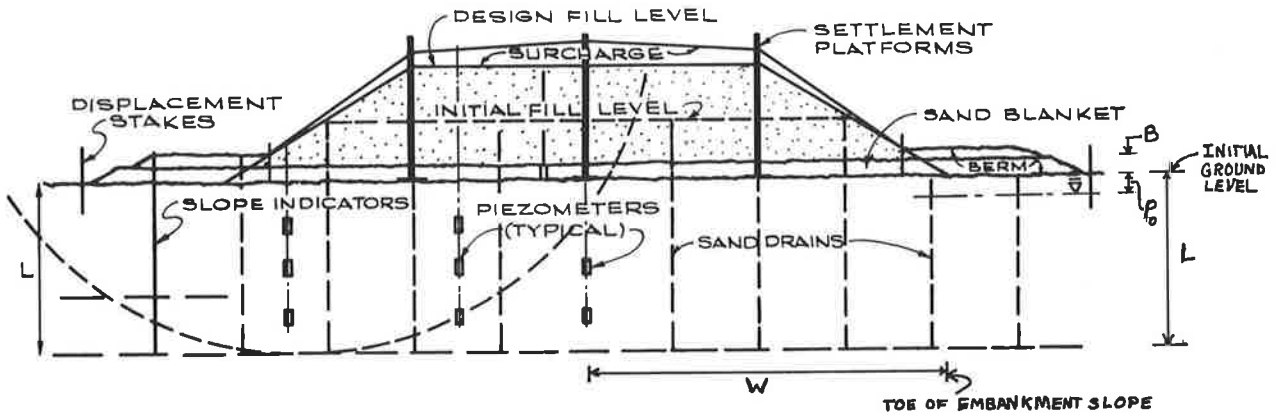

spaced sand drain grid to accomplish substantially the same end result; and

3. The addition of surcharge does not result in embankment instability.

Determination of the surcharge required to achieve a desired degree of primary consolidation (u_t) based on attaining an effective value (u_e) by sand drain stabilization can be accomplished by Equation 13:

$$\log_{10}(P_f + P_{sur})/P_p = [a_v(P_p - P_0)(u_t - u_e) + u_t C_c \log_{10}(P_f/P_p)]\, u_e C_c \quad (13)$$

where

P_f = field or design load,
P_{sur} = required surcharge load,
P_p = preconsolidation load of subsoil,
a_v = coefficient of compressibility,
u_t = degree of consolidation required for load P_f,
u_e = degree of consolidation to be achieved with surcharge added, and
C_c = compression index.

Effects of Installation Methods

It has often been demonstrated that subsoil disturbance will have an adverse effect on the performance of sand drain installations by virtue of changes effected in subsoil characteristics of sensitive soils (12, 13). The principal changes in performance of installations involving disturbance to sensitive soils are expected to relate to the disturbance ratio (R_z) as defined in Equation 14 (14).

$$R_z = (c_{vu} - c_{vz})/(c_{vu} - c_{vr}) = (q_u - q_z)/(q_u - q_r) \quad (14)$$

where

R_z = disturbance ratio,
c_{vu} = undisturbed vertical coefficient of consolidation,
c_{vz} = disturbed vertical coefficient of consolidation,
c_{vr} = remolded vertical coefficient of consolidation,
q_u = undisturbed compression strength,
q_z = disturbed compression strength, and
q_r = remolded compression strength

and exhibits the following effects:

1. The rate of occurrence of primary consolidation is decreased.
2. The rate of occurrence of secondary consolidation is increased.
3. The magnitude of primary settlement is increased.
4. In situ shear strength characteristics are decreased (at least during the early stages of stabilization).

Other adverse effects include an increase in pore pressure not related to construction loading; destruction of the continuity of varves and partings; thus impeding horizontal drainage; and lateral displacements, which may result in the shearing of previously installed drains. These effects must be compensated for by the selection of conservative soil characteristics, as well as by high factors of safety, in the development of designs involving displacement methods applied in sensitive soils. Conversely, the use of disturbed soils characteristics might be costly in designing installations involving nondisplacement techniques as the field results could exceed the expectations of the engineer. It is necessary, therefore, that more accurate determination of subsoil design characteristics be made where nondisplacement installation methods are to be employed in order to take full advantage of the potential efficiency of such methods.

To permit a more accurate means of designing for nondisplacement sand drain installations, in situ soil characteristics must be developed. It is equally important to determine the efficiency of each method based on its performance in the field (Equation 9) so that in situ characteristics may be used in design. On major projects, prototype performance may be determined in advance of design by means of test sections. In addition to being an aid to design, such field tests would also permit development of efficiency data for methods of sand drain installation used. Where test sections cannot be implemented, selected areas of the construction can be staged and closely monitored as a means for verifying the design and obtaining data for evaluation of sand drain performance.

EVALUATION OF SAND DRAIN INSTALLATIONS

In order to evaluate each of the various methods of installation (particularly if a comparative test section is not utilized), it is important to develop a reproducible body of soil characteristics based on the use of laboratory test data. Samples are often at least partially disturbed as a result of normal soil sampling and handling methods as well as in laboratory test preparation and work; therefore, it would seem appropriate to use only maximum test results for design purposes. Conversely, if a reproducible basis for comparison is to be developed, perhaps all results should be compared to the most conservative design, involving the use of average values of remolded soil data and parameters.

In order to advance the present state of knowledge, it would be desirable to compare performance in the field with designs established on paper for maximum values from test results (after discarding inconsistent values), as well as paper designs based on remolded test values, with settlement estimates based on initial void ratios (e_o) derived from in situ moisture contents. So that there be no misunderstanding concerning the paper designs, these need not be the designs on which the installations would actually be constructed. The engineer would continue to prepare construction plans and specifications in accordance with current knowledge and experience. However, inasmuch as the selection of design values from test data is almost entirely subjective, the success of field installations would not result in any improvement in the working knowledge concerning various methods of installation. Inasmuch as average values of remolded test data are more likely to be reproducible for any soil type, and the maximum range of test values might also be reproducible, the subjective aspects involved in the paper designs would be largely eliminated. By using these limiting values and minimizing the use of subjectively derived data, a degree of uniformity in the classification of field performance will ultimately be developed.

Comparisons of field results to remolded design values are best reported as specific improvement factors, but field results and field-derived values are best compared to maximum laboratory values as efficiency factors. On this basis, the following factors are suggested for describing field performance relative to design performance (I = improvement factor, E = efficiency factor, v = vertical, h = horizontal, sec = secondary, p = primary, t = total, s = strength, and w = sand drain).

Relevant Item	Improvement	Efficiency
Vertical consolidation	I_v	E_v
Horizontal consolidation	I_h	E_h

Relevant Item	Improvement	Efficiency
Secondary consolidation	I_{sec}	E_{sec}
Settlement factor, primary	I_p	E_p
Settlement factor, total (20 years by extrapolated data)	I_t	E_t
Shear strength or cohesion	I_s	E_s
Sand drain grid	I_w	E_w

The consolidation factors refer to ratios of field values to laboratory values using coefficients of primary and secondary consolidation. The settlement factor (primary) is a ratio of design estimates to field settlements under each loading condition (including surcharge loading where used). Strength and sand drain grid factors are based on tests of undisturbed samples from borings obtained after stabilization to values obtained from design boring data as well as from field data.

The most difficult element to establish in the laboratory is the value of the horizontal coefficient of consolidation (c_h) for use in determining the horizontal consolidation factors. In isotropic silty or clayey soils, it is recommended that c_h be taken arbitrarily as ten times the laboratory c_v (undisturbed) value for the efficiency factor, and as being equal to c_v for the improvement factor. In silty and clayey varved soils, the c_h value should be taken as ten times the c_v (undisturbed) value of the more permeable of the varves involved. Where substantially continuous sand partings and varves are involved, then c_h for use in determining the consolidation efficiency factor should be taken as equal to c_v derived from the permeability of the sand.

SAND DRAIN INSTALLATIONS

To ensure uniformity in construction of sand drain installations, development of a set of specifications applicable to nondisplacement methods is required. The following key points are suggested to be covered for all nondisplacement techniques. These recommendations are based on experience involving sand drain installations at the Maine and East St. Louis test section sites.

1. No alternate raising and lowering or free fall of the cavity-forming tool is permitted. A maximum 30-cm (12-in) free fall of the jetting tool is permitted if it is shown that the jetting tool forms a cavity at least 30 cm ahead of the tool.
2. The vertical alignment of the cavity-forming tool shall be maintained to a plumbness and axial linearity within a maximum deviation of 1 percent at all times during the sand drain cavity formation and held to within 7.5 cm (0.25 ft) of plan location.
3. The maximum rate of tool advance shall be limited to one pitch length per revolution for augers but is to be maintained at a lower rate to ensure excavation of the subsoil. Thus consideration is given to the physical volume of the auger. Reverse auger rotation is not permitted.
4. The maximum rate of advances of the jetting tool shall be 3 m/min (10 ft/min), and the actual rate increased or decreased as required in the field to ensure nondisplacement cavity excavation (zero pore-pressure increase).
5. Fluid pressures used in excavating or backfilling the sand drain cavity shall not exceed twice the existing hydrostatic pressure in the subsoil at the level of the bottom of the cutting tool as the apparatus is progressed through the compressible soil; however, fluid pressure of 275.8 kPa (40 lb/in^2) is permissible at all depths in the compressible soil during backfill. Higher pressures may be allowed where it is ascertained that jetting-induced excess hydrostatic pressure dissipates within 24 h.
6. Effluent from jetting installations must be disposed of in a manner that will not affect environmental conditions adversely.
7. At the discretion of the engineer, where jetting is performed in the vicinity of waterways, a casing may be desirable for use with the jetting apparatus, and the contractor shall do all that is necessary to ensure return of all jetting water and effluent to the top of the casing. Such return water shall be accumulated or disposed of off the site as required by the engineer to ensure against the inadvertent pollution of the adjacent waterway.
8. In all methods used, rigid cavity support shall be provided at all times for the portion of the sand drain that passes through the sand blanket and any soft or granular subsoil stratum encountered to prevent yielding or collapse of the formed cavity. The sand drain shall be backfilled simultaneously with the removal of cavity support in a manner to ensure columnar continuity by applying 206.8 kPa (30 lb/in^2) (min) air pressure to the sand during backfill. Such air pressure should not exceed twice the in situ hydrostatic head at the depth of backfill placement.
9. Where sand drain cavities are not rigidly supported, measure each for size and depth. For rigidly supported cavities, control the rate of support removal to reflect the rate of backfill. Check the volume of backfill used, as needed for proper control.
10. Develop backfill permeability requirements for the range of sand drain sizes permitted.

CONSTRUCTION SEQUENCE FOR SAND DRAIN SECTIONS

The following procedure is proposed for construction of sand drain installations. Although this is most appropriately applicable to test sections where extensive monitoring can be implemented without impeding project completion, the procedure can be tailored to meet the varying control requirements for specific construction projects that utilize sand drain stabilization.

1. Install construction control devices as early as possible in the construction (preferably in advance of any fill placement). Such devices include settlement platforms and piezometers; deep settlement points, displacement stakes, and slope indicators are used as appropriate. Settlement platforms should be located at points of change in the loading shape as well as at the center of the construction. Piezometers should be placed to permit development of longitudinal as well as vertical pore-pressure profiles (Figure 4). Add displacement stakes and slope indicators where lateral movements (creep and potential slope stability problems) are anticipated.
2. In test sections and where economically feasible in construction, place sand blanket and fill material to highest possible level (or to the top of berm level, where contemplated) but no higher than 50 percent of the design load for full width of the embankment. Displacement stakes are best located outside the toes of slope, but the slope indicators are best located so as to pass through the anticipated critical failure plane (Figure 4). Install piezometers within 60 cm (2 ft) of the first few sand drains as a means of establishing a maximum rate of cavity-forming-tool advance consistent with complete dissipation of induced pore pressure within 24 h.
3. In test sections, and where feasible in actual construction, allow the fill to remain in place as long as possible without delay to the construction schedules, to permit development of settlement data for use in establishing c_v.

Figure 5. Strength ratio versus consolidation ratio.

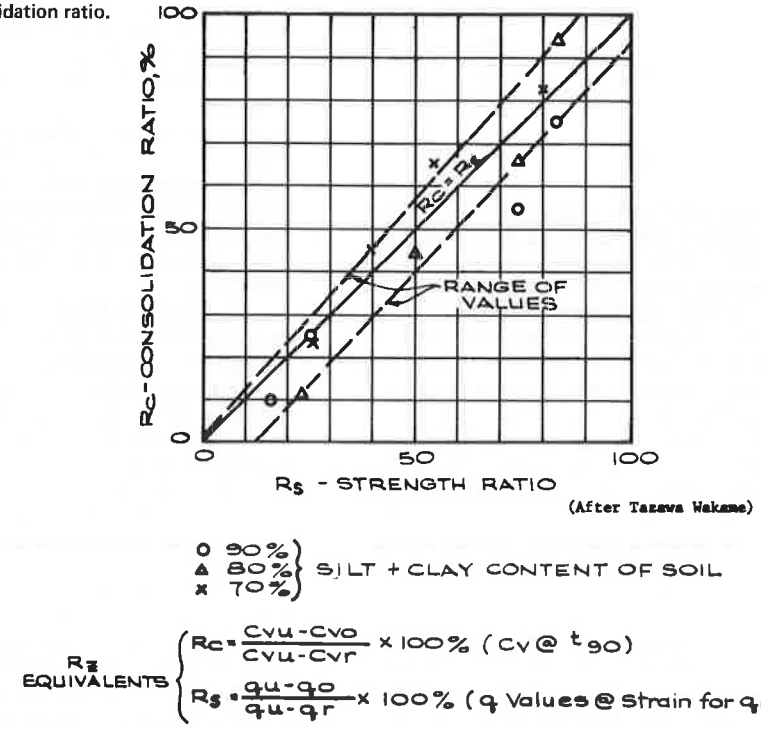

4. Install sand drains as required. For test sections, install drains in more than one grid pattern if feasible.

5. Additional piezometers are to be installed after sand drain work is completed. For test sections, piezometers are also to be placed within typical drains as well as within the sand blanket.

6. Bring fill up to final design level plus surcharge at a uniform rate of filling and allow to remain in place for as long as possible (for test sections until at least 85 percent consolidation is achieved).

7. After review of field data, establish the amount of surcharge to be removed so that the degree of consolidation (u_t in Equation 13) is substantially 1.0.

8. Where feasible, maintain at least a portion of the instrumentation in place for a sufficient time to develop the secondary consolidation characteristic of the subsoil.

9. Take borings and undisturbed samples for testing to redefine soil characteristics developed for the design as well as to evaluate disturbance (Figure 5 and Equation 14).

10. Test sections should include a control area without stabilization, using berms as needed for stability. Sand drains should be installed by displacement as well as by nondisplacement methods at equivalent spacings in accordance with Equation 9.

EVALUATION OF FIELD DATA

The rate of occurrence and value of total primary settlement may be determined in the field by using settlement platform and instrumentation data. Incremental settlements at intermediate levels within strata may be determined by means of earth anchor devices installed at specific depths through bore holes. Piezometer data permit an estimation of the degree of consolidation at any time during construction. By employing the suggested construction sequence, the evaluation of the sand drain installations can be accomplished in the following manner:

1. If fill is left in place prior to installing sand drains, sufficient data are developed to permit interim evaluation of c_v. A final evaluation of c_v is made after the value for any control area is established by using total primary settlement from field data after sand drain installation and substantial completion (85 percent) of primary settlement.

2. The value of t_o applicable to installation of sand drains for the initial fill level is closely approximated by the actual date that sand drains are installed.

3. Theories developed to evaluate consolidation of sand drain installations under uniform rates of fill can be checked by using data obtained for loads placed after sand drain installation (15) and consolidation factors.

4. The coefficient of consolidation can be checked for the final loading condition by approximating a new t_o taken at the midpoint of the loading cycle, which will permit evaluation of consolidation factors and sand drain efficiency.

5. By removing the surcharge portion of the fill, a check can be made of the coefficient of secondary consolidation and settlement factors since in situ fill produces a loading that is consistent with achievement in the field of 100 percent of primary settlement.

6. Piezometer data in the drains and in the sand blanket will indicate differences in backpressure, which will provide needed information on the effects of sand drain backfill and sand blanket permeability.

7. The evaluation of effective stresses as well as testing of undisturbed samples from final borings will permit a determination of the strength or cohesion factors. Moisture-content profile changes determined from final borings can be used to check observed settlement data and to compute settlement factors.

COMPARISON OF INSTALLATION METHODS

The results of the test sections as well as other instrumented construction projects can be evaluated on a quantitative basis, which can ultimately be used to reflect cost differences relative to each of the methods of

sand drain installation available. Improvement and efficiency factors determined for each installation over the predicted paper design performance will permit tying field performance to reproducible laboratory test values. In this manner, it will be possible to determine variations in quantities relative to size and spacing of sand drains and fill requirements due to differences in primary and secondary settlements, surcharge, and berms. It will also be possible to evaluate the need for specific sand blanket and sand drain backfill materials.

When a test section is involved, it will become possible to compare directly the various methods of installation utilized. Such comparisons may be made in a manner similar to that for the Maine test section (6, 7, 8), based on ratios of performance to design values. The term settlement ratio (R_y) is the ratio of field settlement (H_f) to theoretical settlement (H_d). Effectiveness ratio (R_e) is the relationship between the backfigured value of c_h for each method to that of the base method selected. These results for the Maine test section are presented in Tables 1 and 2. The mandrel method was the base method for Table 1 (9).

The following can be used to establish true costs of sand drain installations:

1. If the use of 45-cm (1.5-ft) diameter sand drains in a 3-m (10-ft) triangular pattern of mandrel sand drains for the back cove site is assumed, an equivalent set of data for 30-cm (1-ft) diameter drains as well as corresponding values of influence area [fS^2 ($=n^2A_w$)] may be established for the jetting and auger methods, as shown in Table 3.
2. Using the settlement ratio (such as in Table 3) and corresponding values of influence area, a fill quantity increase can be established for each method and drain size, which will reflect as a unit cost increment (F_c) per foot of sand drain installed:

$$F_c = F_f\, Hn^2 A_w (Ry - 1)/L_w \qquad (15)$$

where

F_c = unit cost increment,
F_f = field or final unit cost,
H = settlement,
n = ratio of D_e to d_w,
A_w = sand drain cross-section area,
R_y = settlement ratio, and
L_w = average length of sand drain.

3. The volume of fill used in berms (and surcharge) (B_v) for equivalent stability and consolidation, as well as any credit (where applicable) for reduction in fill (f_vA_w) due to ground heave (displacement methods) or the reuse of spoil developed in excavating sand drain cavities by augering (Figure 6) are factors in establishing a supplemental cost increment (or credit) (ΔF_c) per foot of sand drain installed:

$$\Delta F_c = F_f(B_v/\Sigma L_w) - f_v A_w \qquad (16)$$

where

ΔF_c = supplement cost increment,
B_v = total volume of berm and surchange, and
Σ = number of sand drains for total project.

4. To compare the costs of various methods and alternative designs, the unit price (F_w) actually bid for each method of installation is increased by F_c and ΔF_c and the total divided by the applicable effectiveness ratio (R_e) to obtain the effective unit cost (F_e) per foot of sand drain installed.

$$F_e = (F_w + F_c + \Delta F_c)/R_e \qquad (17)$$

where

F_e = effective unit cost,
F_w = sand drain unit cost, and
R_e = effectiveness ratio.

A typical computation format for determining the pattern of sand drains applicable to each method considered is presented in Table 3. Also included in Table 3 is the incremental fill quantity reflecting induced soil consolidation characteristics altered by disturbance effects of each method.

In developing true comparisons, certain misconceptions must be avoided. Because of the tendency to employ specifications developed by others, certain methods have become standardized as to size. As an illustration, the jetting method has been specified as permitting the use of 30-cm (1-ft) and 45-cm (1.5-ft) sand drains; for the auger method only 45-cm diameter drains are usually specified. The larger diameter drains are often required in an effort to make certain of sand drain continuity where a degree of lateral yield or creep may need to be accommodated. Where lateral creep is not anticipated, and where the stratification overlying the soft soil requiring treatment is 10 m (30 ft) or more of stiff (desiccated or preloaded) clay, the sand drain diameter should be fixed for bidding purposes, with the construction contractor permitted the option to vary the diameter used within a specified range and theoretical spacing based on the efficiency of the installation method. Whereas jetted drains can be penetrated to great depths with relatively small changes in equipment size, the size of the auger and mandrel equipment generally increase in power and weight substantially in direct proportion to the drain length. It is noted that it takes approximately one-half the weight and power to install a 30-cm drain by the auger method as compared to a 45-cm diameter drain. Whereas there may be approximately 20 percent more drains required for a 30-cm diameter, the saving in equipment and sand backfill may more than compensate for the extra number of drains to be installed. The same would undoubtedly be true for the mandrel method.

The designer is also cautioned that there may be circumstances when specific sand drain installation methods are not appropriate. Jetted drains should be avoided where adjacent structures are in place and migration of water used in jetting may affect its foundation adversely, as in the case of piers and bulkheads. In urban areas where noise codes are in effect, the use of driven sand drains may be prohibitive in cost if special equipment is required to limit noise. Care must also be taken to ensure cavity support during backfill of each sand drain cavity. Although limits are suggested in drain sizes for specific methods of installation, such limits only reflect common usage; there is no reason to assume that equipment does not exist or cannot be made to install sand drains of greater or smaller size in each instance. However, it is desirable to establish a realistic range limit on drain sizes, e.g., 10-cm (4-in) minimum for sand drains installed in supported cavities, 30-cm (1-ft) minimum for those installed in unsupported cavities, and a maximum 60-cm (2-ft) diameter allowed. Sand drain spacing should be limited to 7.6 m (25 ft), while jetted and driven drains should not be spaced closer than 2.4 m (8 ft) to avoid any adverse effects on previously completed drains.

CONCLUSIONS AND RECOMMENDATIONS

1. Available theory of sand drain design is adequate to approximate field performance provided that information is available to permit a determination of the effects of the available methods of sand drain installation on subsoil characteristics.

2. In view of the subjective aspects involved in the selection of laboratory test data for use in design, a reproducible standard should be developed to serve as a basis for evaluation of field performance of sand drain installations. Such values selected without subjectivity would be used to produce paper designs without any factor of safety being applied or the need to be conservative

Table 1. Effectiveness ratio.

Soil Type	Drain Spacing (m)	Effectiveness Ratio Values[a]		
		Mandrel Method	Jetting Method	Auger Method
Silty clay	3	1.0	1.6	2.0
Silty clay	4.3	1.0	2.1	2.5
Organic clay	4.3	1.0	1.2	1.2

Notes: 1 m = 3.3 ft.
The greater the effectiveness, the greater the efficiency of the method of installation. The increase in efficiency with with sand drain spacing is predictable, Figure 3.

[a] Use as minimum value $R_{e2} : R_{e1} \sim I_{w2} : I_{w1} = E_{w2} : E_{w1}$.

Table 2. Settlement ratio.

Soil Type	Drain Spacing (m)	Settlement Ratio Values[a]		
		Mandrel Method	Jetting Method	Auger Method
Silty clay	3	1.56	1.54	0.91
Silty clay	4.3	1.23	2.03	1.14
Organic clay	4.3	1.33	1.18	1.15

Notes: 1 m = 3.3 ft.
The lower the settlement ratio, the less the disturbance developed by the method of installation. For a given diameter of sand drain and method, R_y should decrease with an increase in drain spacing.

[a] Use as minimum value $R_y = 1/E_t > 1.0$, $R_{y2} : R_{y1} \sim E_{t1} : E_{t2}$.

Table 3. Settlement volume increment.

Sand Drain Installation	d_w = 45 cm			d_w = 30 cm			Comments
	Auger Method	Jetted Casing Method	Mandrel Method	Auger Method	Jetted Casing Method	Mandrel Method	
Effectiveness ratio, R_e (S = 3.0 m)	2.0	1.6	1.0	1.63	1.31	0.82	$R_{e2} = R_{e1}\,(d_{w2}/d_{w1})^{0.5}$
Drain spacing when equal E_w, S, m	4.3	3.8	3.0	3.88	3.44	2.72	$S_2 = S_1(R_{e2}/R_{e1})^{0.5}$
Corrected effectiveness ratio, R_e	2.5	1.84	1.0	2.04	1.50	0.82	Interpolated-Table 1
Corrected sand drain spacing, S	4.74	4.07	3.0	4.29	3.68	2.72	Using corrected R_e
Influence area, $f_w S^2$, m^2	20.22	14.91	8.1	16.56	12.19	6.66	f_w = 0.9, triangular grid
Settlement ratio, R_y	0.91[a]	1.54	1.56	0.91[a]	1.54	1.56	From Table 2, Use 1.0[a]
Settlement factor, f_y, m^3/m	0	8.05	4.54	0	6.58	3.73	Added fill/settlement/ sand drain installed

Notes: 1 m = 3.3 ft.
R_e values use the mandrel method performance as the base.

[a] R_y is defined as field settlement/theoretical settlement. Use R_y = 1 as minimum. The volume of fill required to compensate for settlement per sand drain installed is $H(f_y + 1)$. The settlement volume increment related to the method of sand drain installation, expressed per sand drain installed is Hf_y.

Figure 6. Volumetric effects of soil heave and spoil reuse.

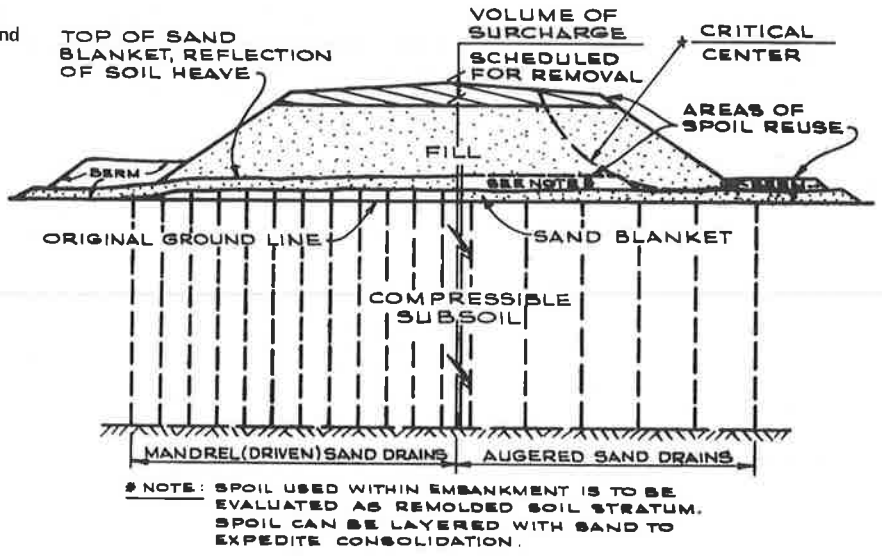

as concerns field performance.

3. Fully instrumented sand drain test sections should be planned under state and federal research funds to permit accumulation of comparable field data, at least for the available nondisplacement methods of installation, so as to ultimately provide a basis for developing equal designs. In so doing, the state of the art will be advanced and the degree of conservatism now exercised in current sand drain design practice can be reduced, for substantial savings in construction cost.

4. A uniform set of key specification requirements should be established for auger and jetting methods of sand drain installations, as an important first step toward ensuring reproducibility of field results. With uniformity in construction, including environmental safeguards, it will be possible to develop means of establishing meaningful efficiency and improvement characteristics for available methods of sand drain installation. Of importance in such specifications are controls on: cavity verticality, rates of tool advance and withdrawal, fluid pressure in forming and backfilling cavities, and pore pressure increase during sand drain installation.

5. Evaluation of the performance of sand drain installations is not limited to the determination of the rate of occurrence of settlement and environmental effects of each method but must also include an economic evaluation.

6. The design of sand drain installations may involve drain diameters ranging from 7.5 to 65 cm (0.25 to 2 ft) depending on the methods of installation considered. Where more than one method is specified as acceptable, alternative designs (size and spacing of drains) for each method must reflect performance efficiency by taking into account the permeability of the available backfill material. Where lateral yielding or creep is a problem, the larger diameter drains are preferable.

ACKNOWLEDGMENTS

This is to acknowledge the contribution of L. Moore and R. Forsyth for their encouragement in the preparation of this paper, as well as the many committee members who have taken the time and extended their effort in guiding its final preparation. Also, the comments and assistance of S. J. Johnson of the U.S. Army Engineer Waterways Experiment Station have been invaluable, as were the efforts of E. Goerler and the drafting by C. Mattson of De Leuw, Cather and Company. Sand drain design has traditionally been a controversial topic and publication of this paper is intended to stimulate further research on this subject. It is noted that I hold patents on various aspects and methods of sand drain installation.

REFERENCES

1. Study of Deep Soil Stabilization by Vertical Sand Drains. Moran, Proctor, Mueser, and Rutledge; Bureau of Yards and Docks, U.S. Navy Rept. NOy 88812, 1958.
2. R. A. Barron. Consolidation of Fine-Grained Soils by Drain Wells. ASCE Trans., Vol. 113, 1948, pp. 718-742.
3. R. E. Landau. Post Hole Digger Comes of Age in Sand Drain Work. Contractors and Engineers Monthly, April 1958.
4. L. Moore. Appraisal of Sand Drain Projects Designed and Constructed by the New York State Department of Transportation. 1968.
5. R. E. Landau. Method of Installation as a Factor in Sand Drain Stabilization Design. HRB, Highway Research Record 133, 1966, pp. 75-97.
6. E. Margason and I. Arango. Sand Drain Performance on a San Francisco Bay Mud Site. Proc., ASCE, Specialty Conference on Performance of Earth and Earth Supported Structures, Purdue Univ., June 11-14, 1972.
7. C. Ladd, J. Rixner, and D. Gifford. Performance of Embankments With Sand Drains on Sensitive Clay. Proc., ASCE, Specialty Conference on Performance of Earth and Earth Supported Structures, Purdue Univ., June 11-14, 1972.
8. D. Rafaeli. Design of the South Island for the Second Hampton Roads Crossing. Proc., ASCE, Specialty Conference on Performance of Earth and Earth Supported Structures, Purdue Univ., June 11-14, 1972.
9. H. Aldrich and E. Johnson. Embankment Test Sections to Evaluate Field Performance of Vertical Sand Drains for Interstate 295 in Portland, Maine. HRB, Highway Research Record 405, 1972, pp. 60-74.
10. R. Olson, D. Daniel, and T. Liu. Finite Difference Analyses for Sand Drain Problems. Proc., ASCE, Specialty Conference on Analysis and Design in Geotechnical Engineering, Univ. of Texas, Austin, June 1974, pp. 100-101.
11. Design Manual Soil Mechanics, Foundations, and Earth Structures. Department of the Navy, U.S. Department of Defense, NAVFAC DM-7, March 1971.
12. W. G. Weber. Experimental Sand Drain Fill at Napa River. HRB, Highway Research Record 133, 1966, pp. 23-44.
13. S. J. Johnson. Precompression for Improving Foundation Soils. Proc., ASCE, Soil Mechanics and Foundations Division, Jan. 1970.
14. M. Tazawa and Y. Wakame. Changes in Coefficient of Consolidation of Disturbed Cohesive Soils. Journal of Taisei Corporation, Dec. 1976.
15. R. L. Schiffman. Consolidation of Soil Under Time-Dependent Loading and Varying Permeability. Proc., HRB, Vol. 37, 1958, pp. 584-617.

Discussion

R. D. Holtz, School of Civil Engineering, Purdue University, West Lafayette, Indiana

The primary objective of this discussion will be to request additional information and clarification of points that I find unclear. Furthermore, the validity and importance of many worthwhile ideas are often obscured by what unfortunately appears to be an attempt by Landau to promote a particular drain installation system in which he has a strong commercial interest. Therefore, a second objective will be to present additional sources of information and alternative viewpoints on some of the more controversial aspects of the paper. For easy reference, the discussion will follow the main headings of the paper.

BACKGROUND

In the excellent, comprehensive paper on sand drains, Johnson (16, pp. 156-157) discusses the controversy regarding the relative merits of various drain installation techniques. He points out that

> Any installation method must cause some disturbing effects, just as disturbance results when obtaining even the best undisturbed soil samples. It is obvious, therefore, that primary interest must be focused upon assessing the severity of these effects on results obtained, rather than upon the question of whether disturbance does or does not exist.

The first drains presented are all installed with a mandrel. The drains in the second in-text table may be installed with less displacement than conventional large-diameter, closed-end mandrel sand drains, but there will still be some soil displacement, remolding, smear, or distortion of thin sand layers (16, Table 2). Perhaps these methods should be termed minimum displacement drains. Even though the Kjellman paper drains are mandrel driven, their size and spacing may actually cause less disturbance in certain soil conditions than the other methods.

The first two in-text tables should also include some recent European and Japanese developments. The Geodrain and Alidrain, both invented by O. Wager of the Swedish Geotechnical Institute, are improvements of the Kjellman paper drains. They are also band-shaped, about 100 mm wide by 4 mm thick, and they have a plastic core surrounded by a paper or nonwoven fabric filter (17). They can be pushed, vibrated, or jetted into the soil by a mandrel slightly larger than the drain itself (18, 19). Japanese engineers have developed a similar band-shaped drain. A 100-mm wide corrugated plastic core is covered by a fabric filter (20). Another recent European development is the AV-Colbond drain. It is composed entirely of a nonwoven polyester fabric 300 mm wide by 4 mm thick (21, 22). A hollow lance with the strip of fabric attached is jetted into the ground to the desired depth. The fabric acts as both a filter and a conduit for the water. From several field tests, the drain seems to be as effective as ordinary sand drains (19, 21, 22). Moran (1) and Richart (23, p. 723) have shown that even small-diameter drains can be effective in dissipating excess pore-water pressure. Finally, Johnson (16, pp. 160-161) gives an excellent summary of the major considerations involved in the selection of sand drain installation procedures.

SAND DRAIN DESIGN

The author suggests that the feasibility of using sand drains depends on the magnitude and rates of residual primary and secondary consolidation. It would be helpful if he would tell us how to obtain these rates, especially c_{sec}. Does he recommend laboratory test or field observations? Laboratory tests sometimes overestimate rates of secondary compression (24, p. 458). A distinctly better design approach would be to follow Moran (1) or Johnson (16). I am not sure about the practicality of the suggestion that strength increase with consolidation can be correlated with water contents. The wide range (scatter) of natural water contents observed in most deposits of soft clay would make such correlations difficult to conduct in practice.

Some minor points: The c_{sec} in Equations 1 and 2 is not the same as C_α defined in the literature (1, 13, 16); rather it is $c_\alpha/1 + e$, where e is some reference void ratio, usually the end of primary e_p. There seems to be a typographical error in Equation 2. Figure 1 is essentially as presented by Moran and Barron (1, 2). Equations 7 and 8 may be more familiar as

$$U = U_h + U_v - U_h U_v = 1 - (1 - U_h)(1 - U_v) \qquad (7a \text{ and } 8a)$$

as developed by Carrillo (25) and others. Under Item 3, U_h does not equal 100 u_h (26, p. 233).

Of course the real design problem is to determine the soil properties necessary to compute U_h. The four-step design procedure proposed by Landau is apparently only an outline of the procedure given by NAVFAC Manual DM-7, Chapter 6 (11). The designer is also advised to consider carefully some of the recent developments in deep drainage mentioned previously.

Secondary Consolidation

Several important points in this section are not immediately obvious. Why is the optimum sand drain design the one in which the rate of primary consolidation is equal to the rate of secondary at the end of construction? Landau states that "secondary compression relates only to the thickness of the compressible stratum." This is an oversimplification; many other factors also affect secondary compression, such as time, consolidation pressure, precompression, duration of the previous load increment, remolding, and rate of increase of effective stress (27). How is the superposition of the two curves, primary and secondary, so that their slopes are the same (Figure 2) different from the common Casagrande construction for determining t_{100} (26, p. 241)?

For the design of sand drains wherein some consideration of secondary compression rates is to be made, it is probably easier to use the procedures suggested in the literature (1, 11, 13), especially if a surcharge is to be utilized in conjunction with deep drainage.

The design equation (Equation 9) proposed by Landau is not easy to understand. Perhaps Landau could give the derivation or at least a reference to the derivation of this equation. Figure 3 is also not very clear. How were the theoretical efficiency curves determined? Should the definition of E_w given in Figure 3 be inverted to be consistent with the definitions given in Equation 9? Even if, as stated, the value of M is a constant for a given set of field conditions, it would be helpful to know how to obtain these factors for typical design situations. How is $n = n_e/E_w^{1/2}$ obtained when d_w is a constant? Is not d_w always a constant for a particular installation? A numerical example showing the reader how to use Equation 9 and Figure 3 would help considerably in following Landau's suggested design procedure.

Sand Drain and Sand Blanket Material

Landau's contention that backpressure in the drain itself is important is apparently not shared by others. For example, Moran (1, p. 35) and Richart (23, p. 721) state that for practical values of n and reasonable geometries, the resistance of the drain wells should be insignificant. The dissipation of excess hydrostatic pressure in the clay is not really a function of the coefficient of permeability of the drain (k_w), but rather it is a function of the ratio of the permeabilities of the two materials. This is the classic case of impeded drainage from the theory of consolidation. Bishop and Gibson (28) show that as long as the ratio of the permeabilities is at least 100, the drain could be considered for practical purposes to be infinitely permeable. Perhaps Landau can present some data to show why he thinks the resistance of the drains is significant.

After Equation 10, Landau states: "Thus, the larger the sand drain diameter for equal settlement rates (Equation 9), the lower the permissible permeability of

the backfill material, which would reflect as a cost differential for the installation." It should be recognized that cost differential (presumably a lower cost in this case) may not be immediately realized, since the larger the drain diameter, the larger volume of sand required, which might offset any savings from using poorer quality backfill materials. Where on Figure 4 is it shown how the approximation of Equation 11 is developed? Equations 10 through 12 seem to be related to Darcy's law—it would be helpful if Landau would give the source, or better, the derivation of these equations.

Landau states that Equations 11 and 12, "permit an economic evaluation of the best means to provide a drainage blanket...." Without being facetious, it might occur to the design engineer that the best means to provide a drainage blanket probably would be with conventional construction and hauling equipment, and no way to evaluate these costs is indicated in Equations 11 and 12. Finally, would Landau please explain how to apply a factor of safety to a coefficient of permeability?

Surcharge

One of the important possible objectives for using a surcharge is to reduce secondary compressions, as was suggested by Landau. Thus, it is indeed strange that procedures for surcharge design to consider secondary compression are not mentioned in this section.

In regard to Equation 13: The coefficient of compressibility a_v ($= -de/d\sigma'$) cannot be equal to zero for a normally consolidated clay. Since the derivation and source of Equation 13 is not immediately apparent, the procedure given by Johnson (13, pp. 122-133) or Moran (1, pp. 79-85) should be followed for the details of precompression design.

Effects of Installation Methods

Not all of the effects indicated by Landau as resulting from disturbance due to installation of displacement sand drains occur in all soils. For example, Johnson (13, Figure 7, and 16, p. 157) indicates that the rate of secondary compression decreases rather than increases, as stated by Landau (effect 2). In some cases, the magnitude of primary settlement may increase with increasing disturbance, but the amount of the effect will depend on the relative stress increase due to the fill or surcharge load. In a well-documented field test series in Sweden, Holtz and Broms (24, p. 462) found no significant increase in primary settlement due to driving of closed-end mandrel drains.

I would suggest that accurate determination of in situ soil properties and subsurface drainage characteristics is required for all deep drainage methods and not just for nondisplacement techniques.

Evaluation of Sand Drain Installations

I strongly disagree with the suggested design evaluation procedure. The comparison of designs utilizing soil properties backcalculated from field observations with designs based on soil properties determined on (a) completely remolded soil samples and (b) maximum values of soil properties determined on (presumably) relatively good undisturbed samples seems highly dubious.

It is difficult to see how soil properties determined on completely remolded samples have any relation to soil properties in situ. Are all pertinent soil properties comparable when tests are conducted on such samples? Presumably these tests would be carried out at natural water contents. Anyone who has tried to remold even a soft clay to determine its sensitivity knows that the procedure is not that simple. Not only are some soils difficult to remold thoroughly at field water contents, but the remolded properties of some highly sensitive soils (e.g., Leda clay) depend strongly on how much energy or effort is applied to remold them. Once such soils are thoroughly remolded, however, they may have the consistency of a viscous liquid. Consequently, such a procedure for all pertinent soil properties tests seems at best impractical.

Appropos the suggestion that, because of sample disturbance, maximum rather than average values of soil properties determined on undisturbed samples be used, one might ask if all pertinent soil properties are reduced because of mechanical disturbance? How would the natural variability in soil properties from point to point within the same site be considered in the procedure?

A much more straightforward evaluation procedure has been suggested by, among others, Moran (1) and Taylor (26). This is to compare field observations with predictions from existing theory (2, 23) using soil properties obtained on the best possible undisturbed samples and utilizing the highest quality laboratory testing techniques. Grid factors mentioned in this section were defined in an earlier paper by Landau (5).

In the last paragraph of this section, Landau makes the rather astounding suggestion that for isotropic silty or clayey soils the c_h be taken arbitrarily as 10 times the undisturbed laboratory c_v for comparison of the efficiencies of various installation methods. Even for varved clays, a factor of 10 may be too large. Careful laboratory and field investigations of a varved clay by Chan and Kenney (29, 30) found the ratio k_h/k_v to be less than 5. Hansbo (31) found c_h/c_v to be between 3 and 5. Thus, the suggestion that c_h/c_v be taken as 10 seems arbitrary and without foundation, even for obviously varved clays.

SAND DRAIN INSTALLATIONS

It is in this section that Landau's commercial interest in the hollow-stem auger technique is evident. Some of the points suggested will either preclude competitive nondisplacement techniques or require expensive (and probably unnecessary) alterations in equipment and procedures. I would prefer that the specifications be more general and include all the minimum displacements methods listed in the second in-text table as well as the newer band-shaped drains described earlier. Perhaps Landau would consider altering his suggested points to make them more generally applicable and, therefore, more useful to the profession. The following comments are offered to assist him in the task.

1. By not allowing the alternate raising and lowering of the cavity-forming tool, Landau effectively precludes one of his strongest competitors, the Dutch Jet-Bailer method. Other jetting techniques may also utilize an up-and-down action of the jetting tool. The important item here is that the tool should be operated in such a manner as to minimize displacement and disturbance of the soil. It would also seem that different techniques might be applicable to different soil types and geologic conditions.
2. The vertical alignment of the formed drain is probably less critical to its function than either the continuity or the disturbance factor. It is interesting to note that in 1972, Landau proposed vertical alignment limitations of 0.55 percent (9, p. 72); Aldrich and Johnson (9, p. 74) pointed out that such a specification was excessively strict and difficult to verify in practice. Apparently, Landau has followed their suggestion and relaxed his plumbness criterion somewhat. It seems that

this specification is relatively unimportant and furthermore is difficult to verify in practice, especially after the drain is installed.

3. This item is applicable to augers only.

4. Landau's suggestion to adjust the rate of advance of the jetting tool as required in the field is better than specifying an exact maximum. Some jetting specifications have permitted tool advance rates twice as fast as he recommends [up to 0.102 km/s (20 ft/min)] without apparent excessive disturbance. Field tests or past experience could be used to determine the appropriate rate.

One hopes that Landau does not really mean to equate nondisplacement with zero pore-pressure increase. (a) An increase in excess pore pressure results from an increase in total stress and does not necessarily mean soil disturbance has occurred. (b) If a pore-pressure increase is indicative of disturbance, then the auger method apparently caused some disturbance to the clays in the Maine test section he later refers to. Aldrich and Johnson (9, p. 72) report excess pore pressures up to 2.13 m (7 ft) of water head as a result of installation of drains by the hollow-stem auger method. It should also be mentioned that this excess pore pressure was the least of the three methods tested (32, p. 46).

One wonders if it is reasonable to apply specific requirements under the rubric jetting to all the jetting installation techniques in the second text table.

5. Where does Landau recommend that limiting jetting pressures be measured? What is the purpose of limiting the pressure (however determined) to twice the existing hydrostatic pressure in the soil at that depth? A better approach would be to utilize jetting pressures that are adequate to do the job. Actual pressures would be determined by experience or by preliminary field trials. They must be somewhat soil and site dependent (i.e., not all pressures will work satisfactorily for all sites). If jetting-induced pore pressures dissipate within 24 h the soil should be rather permeable. Is deep drainage really required at such sites?

6. This item should also include a statement that spoil from all auger methods must be disposed of properly.

7. This is covered by item 6 if protection of the environment is the objective.

8. Why is it necessary that a rigid cavity support be provided when penetrating the granular working platform or sand blanket under the fill? It would be better to simply require that the cavity be maintained or at least the drain should have continuity with the drainage blanket. As long as the cavity is filled with water, there should be little problem with collapse of the hole. Also is it really necessary to backfill the hole simultaneously with the removal of the cavity support? As long as the hole stays open until the hole is completely filled, that should be sufficient. Careful inspection during backfilling operations would ensure that collapse or excessive squeeze has not occurred. In fact, an added advantage accrues with some jetting methods in that the hole can be inspected for depth, diameter, and plumbness prior to backfilling. Finally, why is the recommended 206.84 kPa (30 lb/in^2) (minimum) air pressure limited to twice the in situ hydrostatic pressure? How is one assured that arching in the pipe or hollow stem and, therefore, a void in the sand drain has not occurred?

9. Landau might want to point out that sometimes sand bulks and there might be some difficulty in knowing the volume of the sand backfilled, i.e., volumetric measurements must be at the same relative densities.

CONSTRUCTION SEQUENCE FOR SAND DRAIN SECTIONS

The procedure suggested in item 2 would rarely, if ever, be followed in actual practice for several reasons. Potential stability problems at very soft sites would dictate that sand drain installations be carried out from low working platforms of free-draining granular materials (this platform would later serve as the drainage blanket). The advantage is that there would be less distance to drive, push, auger, or jet the drains, and drain lengths would thereby be minimized.

Installation of piezometers within 60 cm (2 ft) of the first few sand drains is not so easily accomplished. As pointed out by Hansbo (31, p. 90) and from personal experience, it is difficult to know the exact location of the tip after installation, especially if the piezometers are slowly pushed into the ground as is common in very soft deposits. Anyway, why not attempt to install the piezometer tip halfway between two drains? What is the significance of the 24-h dissipation time? Is there some valid reason for recommending 85 percent instead of the more common 90 percent for nearly complete consolidation?

Under item 9, Landau recommends use of Equation 14 and Figure 5 for the evaluations of disturbance (presumably for comparison of different spacings and installation techniques). Can the range of values indicated on Figure 5 be extrapolated to other sites and soil conditions? What values of the two disturbance parameters should be allowable in practice? Finally, is strength loss due to drain installation really one of the properties we want to use to compare different methods? As mentioned before, it is doubtful that such an approach is practical in many sedimentary deposits due to the natural variation of undrained strength with depth and across the site.

EVALUATION OF FIELD DATA

Backcalculation of soil properties, especially consolidation properties, from field measurements of settlement and pore pressures is not always so easy (33). For example, in the previous section the problem of knowing the exact location of the piezometer tip was mentioned. Calculations of c_v from pore-pressure dissipation data require a precise knowledge of the distance from the piezometer tip to the drainage surface of the sand drain. Another problem in evaluating field data occurs in slightly overconsolidated soils if the stress increase due to the fill does not substantially exceed the preconsolidation stress. Leaving the fill in place prior to installation of the drains may be a worthwhile suggestion, but it is probably only practical for test sections. Then one has the problem of c_h, which is required in the design calculations. What will be the relation between the c_v (as backcalculated from field observations) and the c_h?

The suggestion in item 4 seems unnecessarily complicated. It would be simpler to use the piezometer observations to check for dissipation of excess pore-water pressures. Under item 5, perhaps Landau can recommend a practical method for estimating the completion of primary in advance of complete dissipation of excess pore-water pressure. Does he recommend extrapolation of the surface settlement-time curves, or would he utilize the compressibilities from conventional laboratory consolidation tests?

While the suggestion in item 7 to use changes in water contents to check settlements is attractive, I have not found it to be particularly successful (24, pp. 460-462), even in relatively (by U.S. standards) homogeneous clays.

COMPARISON OF INSTALLATION METHODS

It is a pity the results and observations of the East St. Louis test section, so often referred to by Landau, have never been published. Thus he has unfortunately only one case history to illustrate his suggested procedure for comparing methods of installation. Tables 1 and 2 appear to be identical to those presented by him previously in his discussion of Aldrich and Johnson (9). A detailed critique of these tables and Landau's procedures has already been effectively done by Aldrich and Johnson in their closure (9, pp. 72-74).

The suggestion that spoil from augered sand drains can be utilized in the embankment fill itself (Figure 6) is somewhat doubtful, due to the generally poor quality soils to be sand drained. They are often silty and organic, have high water contents, and are difficult to compact properly. Such materials should only be used in the berms.

To Landau's comments on developing true comparisons must be added differences in site conditions, geology, availability and cost of backfill materials, depth of stratum to be drained, labor (including local union regulations), weather, and a myriad of other factors that must be considered for any cost comparison to be meaningful. Finally, I believe that within a few years some of the newer European and Japanese drainage techniques described earlier will make much of the controversy about sand drain installation techniques irrelevant.

COMMENTS ON DRIVEN SAND DRAINS

As noted by Johnson (16), depending on choice of c_v and magnitude of additional load, mandrel-driven sand drains have been satisfactory at a large number of sites. Disadvantages of increased settlement and decreased c_v due to smear and disturbance may be negligible and of little practical importance (16, p. 160). A hypothesis will now be offered as to why this has often been the case.

In 1972, Holtz and Holm (34) excavated more than 2 m around some sand drains at the Skå-Edeby test field in Sweden and examined carefully the surrounding soft clays for evidence of disturbance and remolding. We were astonished to find vertical cracks in this very soft clay ($s_u < 10$ kPa, $S_t \sim 15$) filled with sand as far as 200 mm away from the drain face. In other words, the operating diameter of the sand drain was not 180 mm as originally installed, but up to 380 mm in places. Drain spacing at this site (test area no. 1) was 0.9 m (i.e., the actual $n \sim 2.4$, or about half the design n of 5). Thus the time for consolidation would have been about four times faster than calculated if no allowance was made for disturbance (c_h versus c_v). The cracks probably resulted from hydraulic fracturing. Recent theoretical work and field observations during pile driving by Massarsch and Broms (35) and Massarsch (36) show that fractures in soft clays will tend to form in the vertical direction, which verifies the field observations by Holtz and Holm (34). Thus, hydraulic fracturing with the associated formation of sand-filled vertical cracks may be another plausible explanation why closed-end mandrel-driven sand drains, with all their disturbance and smear, still have worked reasonably well at so many sites.

ACKNOWLEDGMENTS

I wish to acknowledge helpful discussions with several members of the committee, particularly R. A. Forsyth, L. H. Moore, and C. C. Ladd. I am also grateful for the contributions of O. Wager, B. H. Fellenius, and M. J. Warren.

REFERENCES

16. S. J. Johnson. Foundation Precompression With Vertical Sand Drains. Journal of Soil Mechanics and Foundation Div., Proc., ASCE, Vol. 96, No. SM1, 1970, pp. 145-175.
17. R. D. Holtz and P. Boman. A New Technique for Reduction of Excess Pore Pressures During Pile Driving. Canadian Geotechnical Journal, Vol. 11, No. 3, 1974, pp. 423-430.
18. S. Hansbo and B. A. Torstensson. Geodrain and Other Vertical Drain Behavior. In Proc., 9th International Conference on Soil Mechanics and Foundation Engineering, Tokyo, Vol. 1, 1977, pp. 533-540.
19. W. F. J. De Jager and R. J. Termaat. Test Areas With Several Vertical Drainage Systems on State Highway No. 19 at Schipluiden, NL. Proc., International Conference on the Use of Fabrics in Geotechnics, Paris, Vol. 2, 1977, pp. 257-263.
20. Drain and Pump Network Consolidates Landfill Island. Engineering News-Record, Nov. 14, 1974, p. 14.
21. L. W. A. Van Den Elzen, P. Risseeuw, and M. G. Beyer. The AV-Colbond Vertical Drainage System. Ground Engineering, Vol. 10, No. 2, 1977, pp. 28-31.
22. P. Risseeuw and L. W. A. Van Den Elzen. Construction on Compressible Saturated Subsoils With the Use of Non-Woven Strips as Vertical Drains. Proc., International Conference on the Use of Fabrics in Geotechnics, Paris, Vol. 2, 1977, pp. 265-271.
23. F. E. Richart, Jr. Review of the Theories for Sand Drains. Trans., ASCE, Vol. 124, 1959, pp. 709-736 and discussions.
24. R. D. Holtz and B. B. Broms. Long-Term Loading Tests at Skå-Edeby, Sweden. Proc., ASCE Specialty Conference on the Performance of Earth and Earth-Supported Structures, Purdue Univ., Vol. 1, Pt. 1, 1972, pp. 435-464.
25. N. Carillo. Simple Two and Three Dimensional Cases in the Theory of Consolidation of Soils. Journal of Mathematical Physics, Vol. 21, 1942, p. 1.
26. D. W. Taylor. Fundamentals of Soil Mechanics. Wiley, New York, 1948.
27. G. Mesri. Coefficient of Secondary Compression. Journal of the Soil Mechanics and Foundations Division, Proc., ASCE, Vol. 99, No. SM1, 1973, pp. 123-137.
28. A. W. Bishop and R. E. Gibson. The Influence of the Provisions for Boundary Drainage on Strength and Consolidation Characteristics of Soils Measured in the Triaxial Apparatus. In Laboratory Shear Testing of Soils, ASTM, STP 361, 1963, pp. 435-451.
29. H. T. Chan and T. C. Kenney. Laboratory Investigations of Permeability Ratio of New Liskeard Varved Soil. Canadian Geotechnical Journal, Vol. 11, No. 3, 1973, pp. 453-472.
30. T. C. Kenney and H. T. Chan. Field Investigation of Permeability Ratio of New Liskeard Varved Soil. Canadian Geotechnical Journal, Vol. 10, No. 3, 1973, pp. 473-488.
31. S. Hansbo. Consolidation of Clay, With Special Reference to Influence of Vertical Sand Drains. Proc., Swedish Geotechnical Institute, No. 18, 1960.

32. S. J. Poulos. Densification After Placement (Drains): Report to Session III. Proc., ASCE Specialty Conference on Placement and Improvement of Soil to Support Structures, Cambridge, MA, 1968, pp. 43-52.
33. Soil Properties From In Situ Measurements: A Symposium. HRB, Highway Research Record 243, 1968.
34. R. D. Holtz and B. G. Holm. Excavation and Sampling Around Some Sand Drains at Skå-Edeby, Sweden. In, Lectures of the 6th Scandinavian Geotechnical Meeting, Trondheim, Norway, Aug. 1972, Norwegian Geotechnical Institute, pp. 79-85.
35. K. R. Massarsch and B. B. Broms. Fracturing of Soil Caused by Pile Driving in Clay. Proc., 9th International Conference on Soil Mechanics and Foundation Engineering, Tokyo, Vol. 1, 1977, pp. 197-200.
36. K. R. Massarsch. New Aspects of Soil Fracturing in Clay. Journal of the Geotechnical Engineering Division, Proc., ASCE, in preparation.

Publication of this paper sponsored by Committee on Embankments and Earth Slopes.

Analysis of Settlement Data From Sand-Drained Areas

Richard P. Long and Peter J. Carey, Department of Civil Engineering, University of Connecticut, Storrs

Rate of field consolidation is usually calculated from changes with time of piezometer readings. Presented here is a technique for analysis of field settlement observations to determine the field rate of consolidation and total settlement for sand-drained areas. This technique is developed from equal strain consolidation theory. The approach is demonstrated and verified using field data from three construction sites. For each site, the settlement data were analyzed for rate of consolidation and total settlement. The coefficient of consolidation values extracted from the settlement data are compared to those calculated from changes in pore pressures. Total settlement indicated by the analysis is compared to the maximum settlement observed at each platform. Piezometers are important for controlling construction. However, by use of this technique the complete analysis of field data can be achieved independent of piezometer readings.

Analysis of field data for rate and amount of settlement provides a check on design parameters and assumptions. A review of field data from previous projects in similar soil deposits can be a valuable guide to the most economic design. This is particularly important when considering vertical sand drains, since the expense of drain installation must be offset by faster consolidation.

Vertical sand drains have been used for nearly 50 years to shorten the time to achieve settlements in clay layers (1). There is, however, some question about sand drain effectiveness in sensitive clays when displacement methods are used to form the drains (2, 3, 4, 5, 6, 7). A judgment on the effectiveness of sand drains usually requires analysis of field data for rate and amount of settlement and the comparison of these field values to the parameters predicted from laboratory tests. The analysis of field data also provides information on soil disturbance due to the method of drain installation, since disturbance tends to decrease the rate of consolidation and increase the amount of settlement.

Field data often include information on rate of filling, piezometer readings, and settlement platform observations. Field values of rate of consolidation are normally computed from the change with time of the excess pore pressures as indicated by piezometers. The amount of ultimate consolidation settlement the fill will experience is usually computed from the change in piezometer readings and settlement platform observations. Steps in the analysis using piezometer readings have been outlined by Johnson (1) and Moran and others (8).

Settlement platforms are less expensive to install and easier to maintain than piezometers. The determination of rate of consolidation from settlement data alone has been considered difficult or impossible (1). Presented here, however, is a simple technique for using settlement data only to analyze for rate of consolidation and total settlement. The technique is based on equal strain consolidation theory for vertical sand drains and is as easily applied as the conventional analysis of pore pressures. The values of rate, as indicated by the coefficient of consolidation, analyzed by this settlement method are compared to values determined from piezometer readings. Computed total settlements are compared to the maximum observed settlement. This technique allows more extensive analysis of field data from sand-drained areas.

THEORETICAL BASIS

Consolidation in a sand-drained area can be envisaged as dissipation of excess pore pressures in the vertical and radial directions with reasonably well-defined boundary conditions. The average consolidation reflects the dissipation in both directions and can be written (9)

$$1 - U_c = (1 - U_R)(1 - U_v) \quad (1)$$

where

U_c = average consolidation of the clay layer,
U_R = average consolidation if only radial flow to the sand drains occurs, and
U_v = average consolidation if only vertical drainage occurs.

The expression for average consolidation due to radial drainage, assuming equal strain, is (10)

$$U_R = 1 - \exp[-2T_R/F(n)] \quad (2)$$

$$F(n) = \{[n^2/(n^2 - 1)] \ln(n) - (3n^2 - 1)/4n^2\} \quad (3)$$

where

$n = r_e/r_w$,
r_e = effective radius of the sand drain,
r_w = radius of the sand well,
$T_R = C_R t/r_e^2$ (dimensionless time factor),
C_R = coefficient of consolidation in the radial direction, and
t = time.

The relation for vertical consolidation, which can be found in most textbooks on soil mechanics is (9, 11, 12)

$$U_v = 1 - \sum_{m=0}^{m=\infty} 2/M^2 \exp(-M^2 T_v) \quad (4)$$

$$M = (2m + 1)\pi/2 \quad (5)$$

where

T_v = time factor = $C_v t/H^2$,
C_v = coefficient of consolidation in the vertical direction, and
H = maximum drainage path.

An example is presented to illustrate the expected field behavior. Using Equations 2 and 4, the progress of average consolidation under combined vertical and radial flow can be computed. A family of curves was computed using a value of n = 20 and a different value of the ratio T_R/T_v for each curve. The ratio of the time factors includes the ratios of the coefficients of consolidation as well as the squares of the respective drainage paths. The results of these computations are shown in Figure 1. The shape of the curves for combined consolidation is similar to the shape of the consolidation curve for radial drainage alone in that the logarithms of $(1-U_c)$ plots as a straight line at times greater than $T_R = 0.1$. The effect of vertical drainage is to steepen the slope. The curves shown in Figure 1 indicate that at higher values of the time factor, the slopes of a field settlement-time curve can be described with the aid of the equation:

$$1 - U_c = \exp[-2T_{Rc}/F(n)] \quad (6)$$

where $T_{Rc} = C_{Rc} t/r_e^2$, and C_{Rc} = combined coefficient of consolidation.

The combined coefficient of consolidation (C_{Rc}) is greater than the coefficient in the radial direction (C_R) because of the influence of vertical drainage.

Figure 1. $(1 - U_c)$ versus T_R for combined radial and vertical flow.

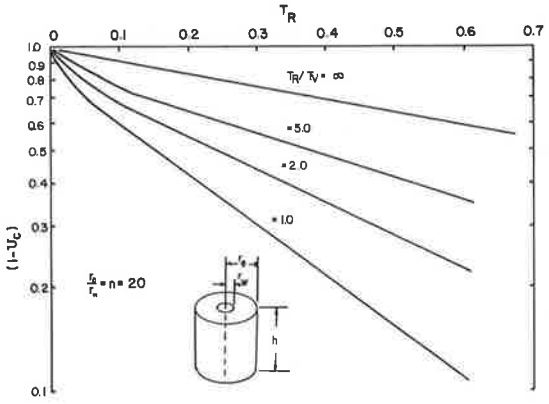

TECHNIQUE FOR FIELD DATA

When filling is complete and consolidation is proceeding, the observed settlements can be described by the equation (9, 13)

$$\rho = \rho_r + U_c \rho_{cf} \quad (7)$$

where

ρ = observed settlement at the time of interest,
ρ_r = rapid settlements accompanying fill placement, and
ρ_{cf} = final consolidation settlement.

Substituting the value of U_c from Equation 6 into Equation 7 yields

$$\rho = \rho_t - \exp[-2C_{Rc}t/F(n)r_e^2]\, \rho_{cf} \quad (8)$$

where $\rho_t = \rho_r + \rho_{cf}$.

Differentiating Equation 8 with respect to time

$$d\rho/dt = \exp[-2C_{Rc}t/F(n)r_e^2]\, [2C_{Rc}\rho_{cf}/F(n)r_e^2] \quad (9)$$

$$\log d\rho/dt = \log[2C_{Rc}\rho_{cf}/F(n)r_e^2] - [0.868C_{Rc}/F(n)r_e^2]\, t \quad (10)$$

Equation 10 indicates that if the slopes of the time settlement curve are determined at three or more times after filling and the logarithm of each slope is plotted against the time at which the slope is determined, the plot forms a straight line whose slope is proportional to the combined coefficient of consolidation (C_{Rc}). The final consolidation settlement does not affect the slope but appears in Equation 10 as an intercept.

In general, a reliable estimate of the total settlement ($\rho_t = \rho_r + \rho_{cf}$) can be obtained by an additional manipulation of Equation 8.

$$\ln(\rho_t - \rho)/\rho_{cf} = -2C_{Rc}t/F(n)r_e^2 \quad (11)$$

Applying Equation 11 at two different times and subtracting

$$\ln(\rho_t - \rho_2)/(\rho_t - \rho_1) = -[2C_{Rc}/F(n)r_e^2]\, (t_2 - t_1) \quad (12)$$

where ρ_1 = observed settlement at time t_1 and ρ_2 = observed settlement at time t_2.

Equation 12 contains only one unknown, ρ_t, since C_{Rc} is now known from Equation 10.

Verification

The applicability of this technique for field data was verified by comparing the coefficients of consolidation determined by Equation 10 to those determined by analyzing pore pressures. The total settlements computed from Equation 12 for data over a limited period were compared to the maximum observed settlements. The technique presented here can be applied to any sand-drained area where settlement data are available.

The data for each settlement platform were plotted against time and a smooth curve drawn through the points as shown in Figure 2. Although the tangent of the settlement-time curve at various points is required, the normal to the curve can be more accurately located by eye by use of a front-surface mirror. The mirror is placed on the curve at time of interest and rotated until the curve and its reflected image appear symmetrical in the vicinity of the mirror. A pencil line is then drawn along the mirror, which is now perpendicular to the curve. Using a mirror allows the person doing the anal-

Figure 2. Settlement versus time from field data.

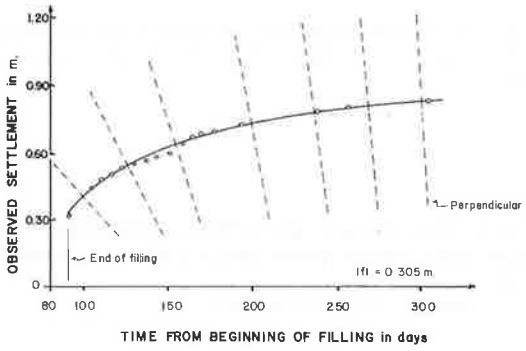

Figure 3. Log $d\rho/dt$ against time.

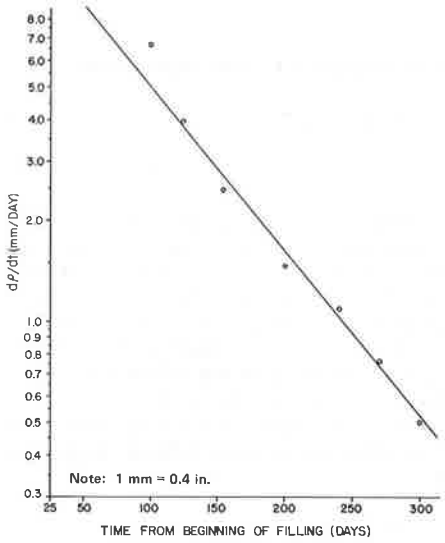

ysis to concentrate on the curve in the vicinity of each selected time. A front-surface mirror eliminates refraction. Figure 2 shows the perpendiculars determined with a mirror. The slopes of the perpendiculars were then converted to the tangents with

$$(\Delta y/\Delta x)_{tangent} = -1/[(\Delta y/\Delta x)_{normal}\,(\text{x scale/y scale})^2] \qquad (13)$$

A typical semilog plot of the tangents ($d\rho/dt$) against time is shown in Figure 3. As can be seen from Figure 3, the points fall close to a straight line for times between 125 and 300 d. The slope of this straight line was used in Equations 10 and 12 to determine C_{R_0} and ρ_t.

Also note from Figure 3 that the plotted slope of the settlement-time curve at 110 d is above the line formed by the slopes at greater times. This behavior was observed in several plots. The predicted effect of vertical drainage is to steepen the consolidation-time curve as shown in Figure 1. This effect is greater at times less than $T_R = 0.1$.

This technique was applied to field data from three highway construction sites.

Site Descriptions

Site 1: Southern Tier Expressway

This site is located in Jamestown, New York. Details of the site were recorded by Leathers (14). The profile

Figure 4. Plan and center line profile, Southern Tier Expressway, ramp KJ, site 1.

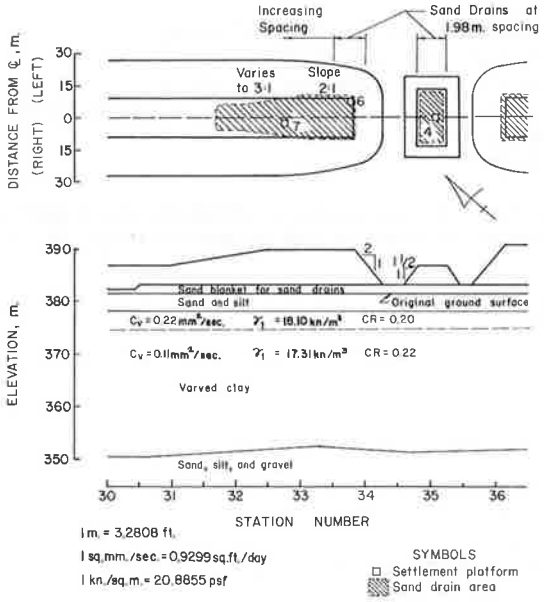

Figure 5. Soil and fill profile for the high fill at east approach to Putnam Bridge, site 2.

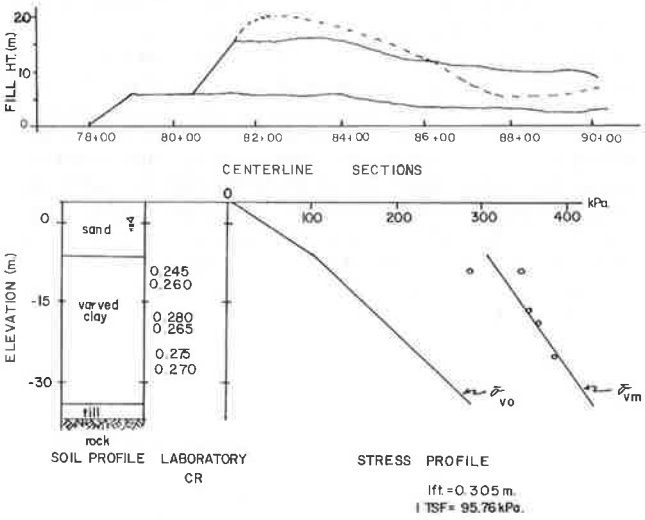

shown in Figure 4 gives the basic soils and properties at the site. The major deposit is a layer of varved clay about 27.4 m (90 ft) thick, which is covered by sand and silt and underlain by sand, silt, and gravel. Sand drains were installed by jetting. Minimum sand drain spacing was 2.0 m (6.5 ft), increasing toward the northwest under the higher embankment as shown in Figure 4. The drain spacing at settlement platforms 4 and 6 was assumed as 2.0 m. The drain spacing at settlement platform 7 was about 5.5 m (18 ft). The diameter of the sand drains was 0.3 m (12 in).

Site 2: East Approach to the Putnam Bridge

The Putnam Bridge spans the Connecticut River a few kilometers south of Hartford, between Wethersfield and Glastonbury, Connecticut. The east approach required a high fill that was stabilized by berms. Sand drains 0.45 m (18 in) in diameter were installed with a continuous flight

auger (6). Spacing of the sand drains near the functioning piezometers was 3.05 m (10 ft). The fill and soil profiles are shown in Figure 5. The varved clay is about 27.4 m (90 ft) thick. A layer of sand covers the varved clay and a stratum of till separates the clay from bedrock.

Site 3: I-95, Portsmouth, New Hampshire

This site is located in New Hampshire at the intersection of the New Hampshire and Spaulding turnpikes. Details of the soils and construction have been published elsewhere (15, 16). A typical profile shows a shallow layer of organic materials, a 1.5-m (5-ft) clay crust, and then 6- to 11-m (20- to 35-ft) soft, somewhat sensitive, marine clay underlain by a sandy glacial till over bedrock. The marine clay had a liquidity index between 1.5 to 2.0. The sand drain spacing varied between 2.7 and 4.9 m (9 and 16 ft), depending on location along the highway. Most of the sand drains are beneath the high part of the fill. The drain diameter is 0.30 m (12 in). The Dutch jet-bailer method of jetting was used to install the sand drains (16).

RESULTS

Southern Tier Expressway and Putnam Bridge

The results from these two projects are reported in Table 1. The method outlined by Johnson (1) was used in compute C_{Rc} from the piezometer readings. Values of ρ_t were computed from Equation 12.

The values of C_{Rc} for the Southern Tier Expressway from settlement data are about the same as those computed from piezometer readings for platforms 6 and 7 and are slightly low for platform 4. At both of these sites the drain spacing is small compared to the vertical thickness of the clay deposit. The influence of vertical drainage is small and C_{Rc} will be close to C_R.

The values of ρ_t from the settlement data are approximately equal to the maximum observed settlements. The maximum observed settlements may contain some secondary compression settlements.

Only two piezometer groups at the east approach to the Putnam Bridge functioned long enough to determine a value of C_{Rc}. However, as can be seen from Table 1, the values of C_{Rc} as analyzed from the settlement data alone are about the same as values determined from the piezometer readings. The values of ρ_t are slightly larger than the maximum observed settlements, indicating that the consolidation was not complete, which was supported by the piezometer readings.

I-95, Portsmouth, New Hampshire

The consolidation at this site was influenced most by vertical drainage. The thickness of the clay layer was about 12.2 m (40 ft). Since laboratory data were available for C_v, the values of C_R were separated from C_{Rc}.

The separation of C_R from C_{Rc} requires that either the value of C_v or the ratio C_R/C_v be known. Since the combined behavior is similar to the radial behavior, Equation 1 can be written

$$\exp\{-[2/F(n)]\,(T_{Rc} - T_R)\} = 1 - U_v \qquad (14)$$

where the subscripts indicate the coefficient of consolidation used to compute the time factors. To use Equation 14, substitute the approximate expressions for U_v (11) and take the natural logarithms of both sides, which yields

$$\text{if } T_v \leq 0.28 \quad \{-[2/F(n)]\,(T_{Rc} - T_R)\} = \ln[1 - (4T_v/\pi)^{1/2}] \qquad (15a)$$

$$\text{if } T_v \geq 0.28 \quad [-2/F(n)](T_{Rc} - T_R) = \ln(8/\pi^2) - \pi^2 T_v/4 \qquad (15b)$$

When computing the time factors for use in Equation 15, an adjustment must be made for construction time. This is normally done, in accordance with the method of Taylor, by halving the construction time (11).

Equation 15 is convenient to use when C_v is known. When there is more confidence in the ratio C_R/C_v, Equation 15 can be rewritten

$$t = r_e^2 T_R/C_R = H^2 T_v/C_v \qquad (16a)$$

Therefore,

$$T_v = (C_v/C_R)(r_e^2/H^2)T_R \qquad (16b)$$

Equations 15a and 15b then become:

$$-[2/F(n)]\,(T_{Rc} - T_R) = \ln\left[1 - \{[(4/\pi)(C_v/C_R)(r_e^2/H^2)]\,T_R\}^{1/2}\right] \qquad (17a)$$

$$-[2/F(n)]\,(T_{Rc} - T_R) = +\ln(8/\pi^2) - (\pi^2/4) \times \{[(C_v/C_R)(r_e^2/H^2)]\,T_R\} \qquad (17b)$$

Equation 17 must be solved by trial and error. A few trials are usually sufficient to obtain the proper value of T_R. The best estimate of C_R by either Equation 15 or 17 is obtained by first computing T_R for a series of times, then determining C_R on an increment of time basis from

$$\Delta T_R = (C_R \Delta t)/r_e^2 \qquad (18)$$

The results of analysis from I-95 are shown in Table 2. Values of C_{Rc} and ρ_t were found as explained for Table 1. The value of C_R was estimated at 0.13 mm^2/s (0.12 ft^2/d) from laboratory data. Having appropriate values of C_R, H, C_{Rc}, and r_e, values of the time factors T_v and T_{Rc} can be calculated for any time. These time factors were then used in Equations 15 and 18 to determine C_R. As can be seen from Table 2, the values of C_R by both methods are comparable and the values of ρ_t are slightly larger in most cases than the maximum observed settlements.

COMMENTS AND CONCLUSIONS

Information on pore pressure behavior during construction is invaluable. Piezometers tend to have a limited functional life in areas experiencing large settlements. On routine projects piezometers are most needed to monitor pore pressures generated during filling. After pore pressures have peaked, malfunctioning piezometers are seldom replaced. Settlement platforms perform their functions for longer periods of time, making settlement data more readily available. This technique fills a need to be able to analyze settlement data when no piezometer readings are available.

The technique is relatively simple to apply. In addition to standard engineering office supplies, the technique requires a mirror, preferably a front-surface mirror. The analysis of data from each settlement platform requires about 1 h. Field settlement data alone can be analyzed to yield valid rate of consolidation and total settlement values.

Table 1. Summary of C_{Rc} results, sites 1 and 2.

Project Name	Settlement Platform No.	Sand Drain Spacing (m)	C_{Rc}[a] (piezometer) (mm^2/s)	C_{Rc} (settlement data) (mm^2/s)	ρ (m)	Maximum Observed Settlement (m)
Southern tier expressway	4	2.0	0.27-0.71	0.13	0.21	0.22
	6	2.0	0.12-0.26	0.15	0.42	0.45
	7	5.5	0.70-1.69	1.02	0.48	0.51
East approach Putnam Bridge	1	3.0		0.12	0.41	0.39
	2	3.0	0.15	0.18	0.88	0.84
	3	3.0		0.14	1.48	1.28
	4	3.0		0.29	1.19	1.08
	7	3.0		0.09	0.47	0.43
	11	3.0	0.16	-	-	1.55

Note: 1 mm^2/s = 0.93 ft^2/d; 1 m = 3.3 ft.

[a] As reported by Leathers (14) and Long and Healy (17).

Table 2. Summary of C_R results, site 3.

Project Name	Settlement Platform No.	Sand Drain Spacing (m)	C_{Rc}[a] (piezometer) (mm^2/s)	C_{Rc} (settlement data) (mm^2/s)	ρ_t (m)	Maximum Observed Settlement (m)
I-95 Interchange	C-1	2.7	0.27-0.48	0.38	1.37	1.34
	C-2	2.7	0.22-0.35	0.37	1.01	1.01
	C-3	3.8	0.09-0.48	0.15	1.28	1.01
	C-4	2.7	0.15-0.37	0.37	1.34	1.31
	C-5	3.8	0.16-0.59	0.10	0.98	0.61
	C-7	2.7	0.10-0.27	0.27	1.25	1.19
	C-8	4.9	0.32-1.08	0.92	0.73	0.82

Notes: 1 mm^2/s = 0.93 ft^2/d; 1 m = 3.3 ft.

[a] As reported by Gifford (15) and Ladd, Rixner, and Gifford (16).

ACKNOWLEDGMENT

Long began this study while on sabbatical leave at Massachusetts Institute of Technology in 1975 and he wishes to thank C. C. Ladd for his discussion and suggestions. Part of the analysis (Putnam Bridge) was accomplished under a project sponsored by the Joint Highway Research Advisory Council of the University of Connecticut and the Connecticut Department of Transportation.

REFERENCES

1. S. J. Johnson. Foundation Precompression With Vertical Sand Drains. Journal of the Soil Mechanics and Foundation Div., Proc., ASCE, Vol. 96, No. SM1, Jan. 1970, pp. 145-175.
2. L. Casagrande and S. Poulos. On the Effectiveness of Sand Drains. Canadian Geotechnical Journal, 6, 1969, pp. 287-326.
3. W. S. Housel. Checking-Up on Vertical Sand Drains. HRB, Bulletin 90, 1954, pp. 1-20.
4. L. H. Moore and T. Grosert. An Appraisal of Sand Drain Projects Designed and Constructed by the New York State Department of Transportation. New York State Department of Transportation, Physical Research Rept. 68-1, Feb. 1968.
5. H. P. Aldrich and E. G. Johnson. Embankment Test Sections to Evaluate Field Performance of Vertical Sand Drains for Interstate 295 in Portland, Maine. HRB, Highway Research Record 405, 1972, pp. 60-74.
6. R. E. London. Method of Installation as a Factor in Sand Drain Stabilization Design. HRB, Highway Research Record 133, 1966, pp. 75-97.
7. R. E. Olson, D. E. Daniel, and T. K. Liu. Finite Differences for Sand Drain Problems. Proc., Conf. on Analysis and Design in Geotechnical Engineering, Austin, TX, June 1974, pp. 85-110.
8. Study of Deep Soil Stabilization by Vertical Sand Drains. Moran, Proctor, Mueser, and Rutledge; and Bureau of Yards and Docks, U.S. Navy, Rept. NOy 88812, 1958.
9. T. W. Lambe and R. V. Whitman. Soil Mechanics. Wiley, New York, 1969.
10. R. A. Barron. Consolidation of Fine-Grained Soils by Drain Wells. ASCE Trans., Vol. 113, 1948, pp. 718-742.
11. R. F. Scott. Principles of Soil Mechanics. Addison-Wesley, Reading, MA, 1963.
12. D. W. Taylor. Fundamentals of Soil Mechanics. Wiley, New York, 1948.
13. R. P. Long and K. A. Healy. Analyzing Field Data for Undrained Shear Settlements. Department of Civil Engineering, Univ. of Connecticut, Storrs, Rept. CE 74-88, Dec. 1974.
14. F. D. Leathers. Behavior of Embankments on New York Varved Clay. Master's thesis, MIT, Cambridge, MA, Aug. 1974.
15. D. G. Gifford. The Performance of Jetted Sand Drains in a Sensitive Clay. Master's thesis, MIT, Cambridge, MA, Jan. 1971.
16. C. C. Ladd, J. J. Rixner, and D. C. Gifford. Performance of Embankments With Sand Drains on Sensitive Clay. ASCE Soil Mechanics and Foundations Div. Specialty Conference on Performance of Earth and Earth-Supported Structures, Purdue Univ., Lafayette, IN, June 1972.
17. R. P. Long and K. A. Healy. Field Consolidation of Varved Clay: Rept. 3. Department of Civil Engineering, Univ. of Connecticut, Storrs, JHR 72-55, Aug. 1972.

Publication of this paper sponsored by Committee on Embankments and Earth Slopes.

Abridgment

Settlement Rate Experience for the Use of Sand Drains in a Tidal Marsh Deposit

A. A. Seymour-Jones, Howard Needles Tammen and Bergendoff, New York

Tidal marsh deposits are found over a wide range of coastal areas in the world. Technical publications have noted the results of the use of surcharge and sand drain treatment to stabilize tidal marsh deposits. This paper supplements existing information on settlement rates in tidal marsh deposits and compares it with previously published data.

The use of surcharge treatment and conventional displacement sand drains was utilized to construct two approach roadway embankments over a tidal marsh deposit adjoining a bridge over the Maurice River at Mauricetown, New Jersey. The tidal marsh deposit generally ranges from 7.6 to 15.2 m (25 to 50 ft) in depth and consists of organic silty clay having a Unified Soil Classification System classification of OH. This soil exhibits a relatively wide variation in natural moisture content and compressibility.

The approach embankment heights for the Maurice River project ranged from 1.5 to 4.6 m (5 to 15 ft). The design height of embankment with surcharge ranged from 3.0 to 9.1 m (10 to 30 ft), twice the embankment height. The relatively large surcharge was used to eliminate most of the relatively large anticipated secondary settlement, which is typical of organic soils as well as of the primary settlement. The intent of this design was to obtain 90 percent consolidation of the underlying organic silty clay due to the weight of the embankment and surcharge during a 14-month surcharge period. To obtain this objective, displacement sand drains were used where the depth of tidal marsh deposit exceeded 7.6 m (25 ft) or where the height of embankment with surcharge exceeded 7.3 m (24 ft). The need for sand drains and the required sand drain spacing were based on the rapid decrease in the coefficient of consolidation with the increase of the average consolidation pressure, as illustrated by the design curve in Figure 1.

The different sand drain spacing used was due to the variation in the coefficient of consolidation associated with the consolidation pressures resulting from the different fill heights and depths of tidal marsh deposit. Sand drain spacings of 3.7, 4.3, and 4.9 m (12, 14, and 16 ft) center to center on a square pattern were used as well as surcharge treatment without sand drains.

Settlement platform data were used to evaluate the field coefficient of consolidation by use of the square root of time versus settlement plot relation. Consolidation by both vertical and horizontal flow, assuming equal permeability in both directions, was used to determine the field coefficient of consolidation.

The calculated values of the coefficient of consolidation of the field data versus the average consolidation pressure are shown in Figure 1 along with the original design curve. It shows much better correlation than the laboratory data had. The field data range from 25 percent below to 50 percent above the design curve.

The effect of the sand drain spacing on the coefficient of consolidation based on the field measurements was evaluated. A plot of the coefficient of consolidation versus sand drain spacing was developed and is shown in Figure 2. Points 1 to 4 are for this project. Points 5, 6, and 7 are based on data from the files of my firm for the other projects that involved the use of surcharge and sand drains in tidal marsh soils.

Published data by others involving the use of surcharge and sand drains in tidal marsh soils were also added and are denoted by points 8 through 29. It should be noted that five of the points (4, 7, 10, 11, and 27) are for surcharge treatment without the use of sand drains. Four other points are for nondisplacement sand drains—points 14 and 24 are for augered sand drains and points 25 and 26 are for jetted sand drains.

The data in Figure 2 exhibit an appreciable variation, but indicate that the coefficient of consolidation decreases with decreasing sand drain spacing. This could be due to the increased disturbance effects caused by a closer sand drain spacing. Figure 1 shows that the consolidation pressure magnitude also affects the coefficient of consolidation, i.e., the higher the consolidation pressure, the lower the coefficient of consolidation.

To evaluate the relative effects of sand drain spacing and consolidation pressure, selected data for points on Figure 2 were replotted showing the coefficient of consolidation versus total consolidation pressure in Figure 3. Points 15, 16, and 17 show a decrease in the coefficient of consolidation with a decrease in sand drain spacing for the same total consolidation pressure as do the points 22 and 23. A comparison of points 22 and 23 with points 24 and 25, which are for the same total consolidation pressure, indicate the potential benefits to be derived from using nondisplacement sand drains. The data indicate that disturbance effects resulting in a lower coefficient of consolidation do occur with decreased sand

Figure 1. Coefficient of consolidation field data.

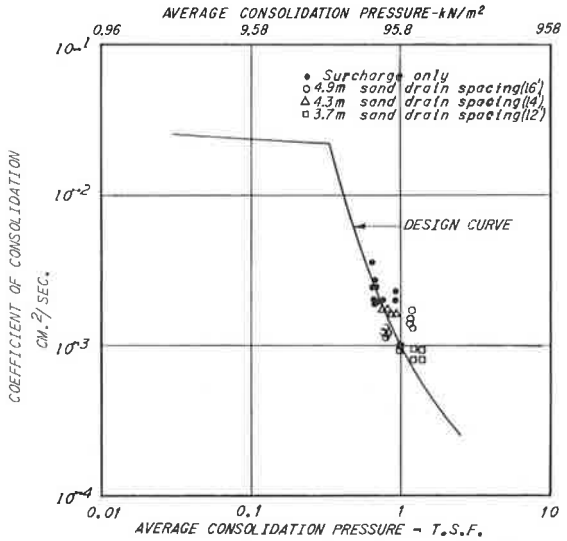

Note: 1 m = 3.3 ft, 1 cm²/s = 3.9 ft²/h, 1 kPa = 0.01 ton/ft².

Figure 2. Relationship between coefficient of consolidation field data and sand drain spacing.

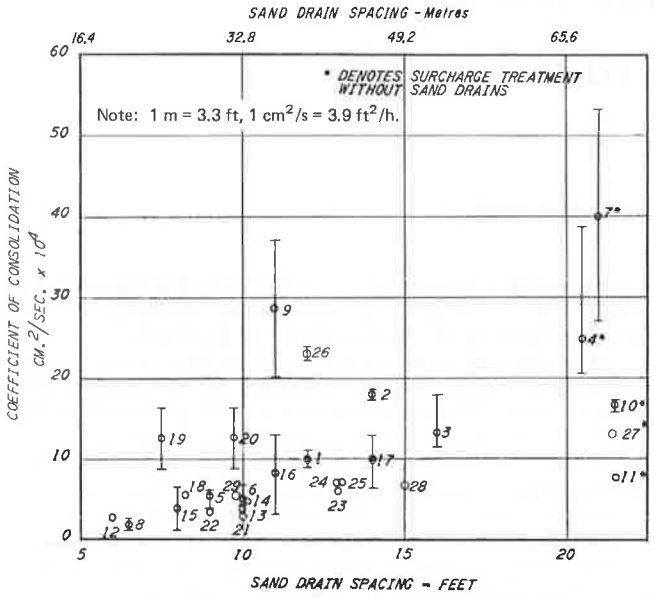

Figure 3. Relationship between coefficient of consolidation field data and total consolidation pressure.

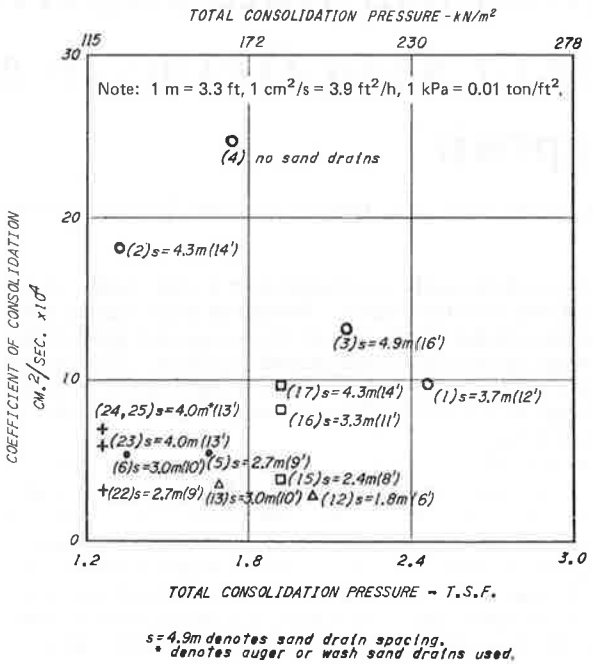

s = 4.9m denotes sand drain spacing.
* denotes auger or wash sand drains used.

drain spacing and nondisplacement sand drains produce a lesser magnitude of disturbance than displacement sand drains.

The relatively high coefficient of consolidation for point 4 with respect to points 1, 2, and 3 is probably due to the omission of sand drains for point 4 and the resulting absence of the disturbance effect due to sand drain installation.

Figures 2 and 3 show that in at least some cases the spacing used with conventional displacement sand drains does materially affect the field coefficient of consolidation and thus the field settlement rate. It is possible that for some of the other data the use of closer sand drain spacings resulted from design considerations such as lower laboratory coefficients of consolidation.

This study led to the following conclusions:

1. A review of field settlement platform data showed that the range in the settlement rate was much narrower than that indicated by the laboratory test data.
2. The field settlement data corroborated that, for the design of displacement sand drains in tidal marsh deposits, the average coefficient of consolidation from conventional laboratory consolidation samples should be used and that any increase in horizontal over vertical permeability should be neglected.
3. The plot of coefficient of consolidation versus sand drain spacing shows a significant trend for a large number of different tidal marsh deposits. For some of these data a closer spacing of conventional displacement sand drains showed a resulting reduction in the coefficient of consolidation as measured from field data and appears to be due to disturbance effects. These data also show that the total consolidation pressure has a marked effect on the field-measured coefficient of consolidation, as would be expected from the laboratory consolidation test data.

Publication of this paper sponsored by Committee on Embankments and Earth Slopes.

The Iowa K-Test

R. L. Handy, A. J. Lutenegger, and J. M. Hoover, Department of Civil Engineering, Iowa State University, Ames

A simple and rapid laboratory test that uses standard 9.44 cm^3 (0.03 ft^3) compacted soil specimens for strength comparisons is presented and discussed. The test gives discrete evaluations of undrained c, ϕ, and other strength parameters from single soil specimens. The specimens are subjected to vertical compression while confined in a split steel mold, which acts as a spring, so that spreading of the mold provides a measure of lateral stress. Thus, K, or the ratio of soil horizontal to vertical stress, may be continuously monitored and used to obtain strength parameters and moduli as the test progresses. In addition, a direct measure of soil-to-steel friction as a function of normal stress is obtained. The K-test simulates an undrained, rapid field-loading situation and appears particularly applicable for transportation facilities. This paper presents representative results on several soils, discusses errors in the assumptions, and describes some potential uses of the test for design and control purposes.

Lateral stress induced from an applied vertical pressure on soil has been of fundamental concern since the classical work of Coulomb on retaining structures (1). Rankine (2) suggested that a ratio of lateral to vertical stress is a discrete property of granular soils, the lateral stress being reduced by the soil's internal resistance to sliding—termed the active state. Rankine (3) later suggested that the value of the ratio (K) is not only important for design of retaining structures but also for simple, direct analyses of bearing capacity.

HISTORY OF SELECTED K-TESTS

One of the earliest attempts at direct measurement of the active state ratio was made by Goodrich (4). His apparatus consisted of a cast-iron cylinder that had a circular hole near the bottom, into which a plug was carefully fitted. Soil pressure on the plug activated a buzzer, and the force required to push the plug back, breaking the electrical circuit, was measured.

Tschebotarioff (5) described a lateral earth pressure meter consisting of a thick-walled cylinder, one-half of which consists of 12 horizontal half-circular ball-bearing mounted rings, each ring connected to a dynamometer with SR-4 strain gauges. Values of $K_0 = \sigma_h/\sigma_v$ are computed for each ring, assuming constant σ_v throughout depth of specimen. Since some lateral movement occurs, the measured value of K_0 may not be a correct representation.

A simpler apparatus developed by Sowers (6) used SR-4 gauges applied directly to the walls of a horizontally slotted thin-walled mold. Since little specimen movement was allowed, the test was considered advantageous for K_0 estimation. Other means for measurement of K_0 were devised by Terzaghi (7) and Obercian (8).

A widely used method to obtain a measure of K is the Hveem stabilometer (ASTM D2844-69) wherein lateral stress in a cylindrical specimen is measured as fluid pressure in a liquid-filled cell (9). Stabilometer R values may be modified to account for variable resistance of a soil to lateral deformation (10).

Housel (11) proposed a more conventional triaxial stabilometer test and pressure transmission factor, the latter being a function of changes in lateral and vertical stresses. In this test, lateral deformation is considerable. Recognizing this fault, Wedzinski (12) measured induced lateral pressures in silts in a closed-system water-filled triaxial cell where magnitude of pressure was observed by means of movement of a closed air bubble in a side-mounted capillary tube.

INDIRECT EVALUATIONS OF K FROM TRIAXIAL DATA

For design purposes, K is commonly evaluated by triaxial tests at several preset values of lateral stress (σ_3) or by direct shear tests at several preset values of normal stress (σ_n); derived values are internal friction angle (ϕ) and cohesion (c). For cohesionless soils, K is found from the Rankine formula,

$$K_{(c=0)} = (1 - \sin\phi)/(1 + \sin\phi) \quad (1)$$

Conventional shear tests are not realistic for several reasons, one being that the lateral stress σ_h (or the normal stress σ_n in direct shear) is held constant, whereas in field loading these stresses gradually increase as a consequence of increasing vertical load. Nevertheless, stress-strain relations evolved from triaxial tests are widely interpreted as accurately representing field behavior and are used in sophisticated computer-based techniques. Yet in tests conducted with the lateral stress held at a single value, vertical stress climbs to a peak and then declines, whereas in tests where σ_h floats upward, vertical stress likewise climbs and there may be no peak strength but simply a continuing dependence of vertical stress on lateral restraint. Field failure occurs when sufficient lateral restraint cannot be mobilized or when vertical deformation is excessive for a given load.

IOWA CONTINUOUS K-TEST

The present K-testing concept began when a commercial split Proctor mold was left unlocked, a compacted soil specimen was placed inside, and it was squeezed between steel end plates while mold expansion was monitored with a dial gauge. The mold was calibrated using a tangential force, and later air pressure in a rubber membrane. Figure 1 shows the results from testing three different soils with this primitive apparatus. The higher the lateral stress ratio, the lower the stability. The silt test sprang the mold.

c and ϕ

The data of Figure 1 show that K was not constant but varied as a function of σ_1. This may be accounted for by converting K values to equivalent c and ϕ, more commonly used in design. From a Mohr circle, a c-ϕ soil at failure produces (5)

$$K = \sigma_3/\sigma_1 = \tan^2(45° - \phi/2) - (2c/\sigma_1)\tan(45° - \phi/2) \quad (2)$$

If c = 0, the second term is 0, and Equation 2 is identical to Equation 1. If $\phi = 0$, Equation 2 becomes

$$K_{(\phi=0)} = 1 - 2c/\sigma_1 \quad (3)$$

Thus, for a c-soil, K increases as σ_1 increases. This behavior is shown by the clay and early stages of the silt in Figure 1. Thus, as a generalization, a constant K with respect to σ_1 should signify a granular or ϕ-soil, and a K that increases with σ_1 should signify a c-soil.

Most soils have both internal friction and cohesion. Since any two points in a K-test represent two Mohr circles, if failure is in progress these will define a tangential failure envelope such as AA' (Figure 2). Linear extrapolation to the abscissa gives

$$\phi = \sin^{-1}[(\sigma_1 - \sigma_3)/(\sigma_1 + \sigma_3 - 2\sigma_i)] \quad (4)$$

For any two Mohr circles that describe a failure condition, Equation 4 may be written for each circle. Solving for σ_i gives

$$\sigma_i = (\sigma_{1_1}\sigma_{3_2} - \sigma_{1_2}\sigma_{3_1})/(\sigma_{1_1} - \sigma_{1_2} - \sigma_{3_1} + \sigma_{3_2}) \quad (5)$$

Thus, the numerical procedure to reduce any pair of K-test data points is as follows: σ_i is obtained by Equation 5, ϕ by Equation 4, and c from

$$c = -\sigma_i \tan\phi \quad (6)$$

The above procedure applied to the data of Figure 1 gives relationships such as shown in Figure 3 for the clay. In this case, ϕ starts high and decreases to 0 as the load is applied, the soil compresses, and pore pressures develop. Simultaneously, c increases. Error in c also increases to the right due to the longer lever arm (AA' in Figure 2) as Mohr circles shift to the right.

The erratic, zig-zag nature of the plot suggests experimental error, but it also may reflect a test periodicity, such as stick-slip. That is, gradual develop-

Figure 1. Lateral stress ratios from several soils compacted with standard effort and optimum moisture content, tested in a split Proctor mold.

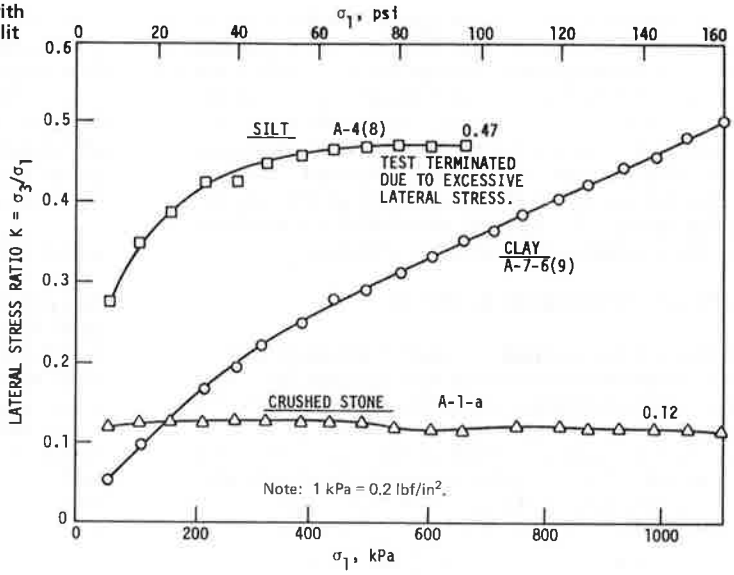

Figure 2. Mohr envelope from two K-test points.

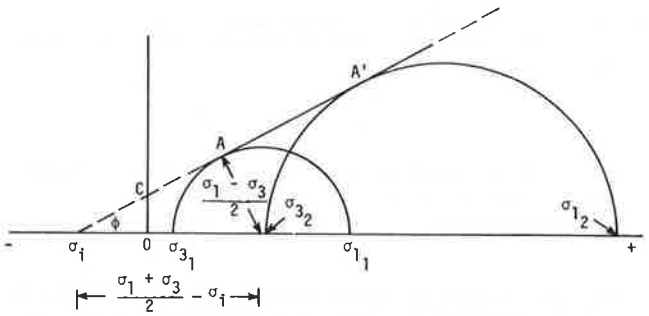

Figure 3. Increase in c and decrease in ϕ for a clay under increasing load in the K-test.

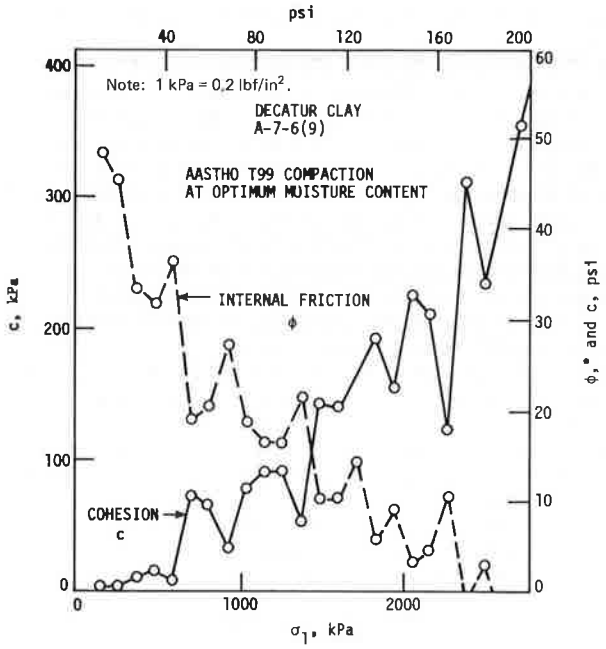

ment of cohesion may be periodically interrupted by a sudden, temporarily disruptive slip. Evidence for this is that the curves are not random ups and downs, since the highs of c (and lows of ϕ) usually last for two or three points, whereas the lows of c (and highs of ϕ) are single points.

Similar treatment of the data for crushed stone gave a consistent ϕ around 51°, with c hovering about 0. The loess behaved first as a weak granular material, with ϕ about 20° and c around 14 kPa (2 lb/in^2), then showed effects from pore pressure: ϕ dropped and c increased with increasing σ_1.

In summary, the trends of c and ϕ are about as expected, although actual indicated values may be incorrect.

Mold Redesign

A special K-test mold was made with the wall thicker at the back (Figure 4) in the zone of maximum bending moment. The opposite side is slotted, with an internal Teflon strip acting as a seal. The interior of the mold is polished and chromium plated to resist abrasion. A 0.0025-mm (0.0001-in) dial gauge is mounted externally to monitor expansion. With uniform internal pressure the change in mold radius is not uniform but gives two radial bulges about 90° to one another and 45° from the mold slot. The mold is slightly larger than the specimen diameter, thus avoiding an initial passive condition from soil being forced into the mold (i.e., the horizontal confining stress initially must not exceed the vertical stress, or an initial passive stress state must be overcome before obtaining active state K data).

Several procedures that involve air pressure were used to calibrate the K-test molds. More successful, however, has been an artificial soft thermoplastic soil specimen with K nominally equal to 1.0. In this way, horizontal stress is assumed to equal the applied vertical stress, and a horizontal stress versus mold opening calibration is prepared. Calibrations are linear, enabling data reduction by linear equations.

Stress Path Interpretation of K-Test Data

Graphs such as Figure 3, while of interest for showing how strength may develop in a soil under increasing load, are of little direct use in design where mean values of c and ϕ are needed across the anticipated range of field loading. It may be more convenient to plot a p-q dia-

gram, as in Figure 5, and fit a line by least squares regression, converting slope and intercept to ϕ and c (13). This also has the advantage of plotting several tests on a single graph.

Tests of Dry Sand

Results from 20 K-tests on dry standard Ottawa sand with initial void ratios varying from 0.55 to 0.74 were analyzed by the stress path method (14). Stress path plots were exceptionally linear, and all regression coefficients exceeded 0.999. The friction angle ϕ varied from 30° to 41° and was inversely related to the initial void ratio, $\phi = 64.5° - 44.2\ (e_0)$; r = 0.68.

Taylor and Leps (15) report essentially the same trend for Ottawa sand but with ϕ lower by 5° to 10°, depending on the normal stress. Though cohesion values should be 0, c from the K-tests averaged 17.6 ± 15.4 kPa (2.6 ± 2.2 lb/in^2), the ± value indicating standard deviation, and showed no relation to e_0. An important source of this error is boundary stress between soil and mold and between soil and end-loading platens. Such friction must be quite high in the case of the sand, which tended to score the mold, and is discussed later.

In summary, K-tests of Ottawa sand showed excellent linearity and precision in the determination of c and ϕ by the stress path method. Furthermore, the trend of ϕ in relation to void ratio is as it should be; however, on the average, ϕ appeared to be overestimated by about 5°, and c by about 20 kPa (3 lb/in^2).

Figure 4. Constant-E model Iowa K-test mold for Proctor or equivalent-size specimens.

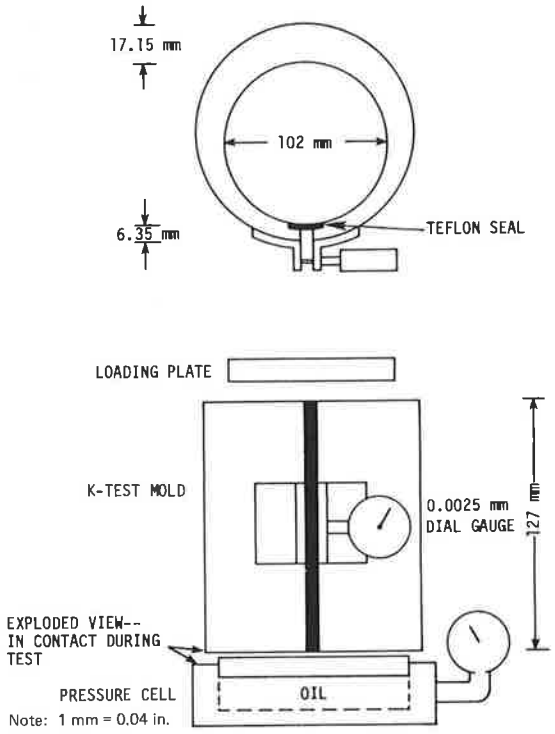

Glacial Till

Figure 6 shows the results of 25 K-tests on a glacial till-derived Shelby series soil molded by AASHTO T-99 compaction. Since c and ϕ of cohesive soils vary during the test, the use of a linear stress path is an averaging approximation, the degree of departure from a line causing a decrease in correlation coefficient (r), which varied from 0.86 to 0.999. The ϕ and r values are lower for wetter samples, indicating development of positive pore pressures.

Figure 6 shows the expected trends—the higher the moisture content, the lower are ϕ and c. Extrapolation to predict the moisture content at which ϕ and c are 0 gives 29 and 32 percent, respectively. The plastic limit of this soil is 32 percent. From these data, it appears that pore pressure is a most important variable, particularly when comparing results of K-tests with more conventional laboratory tests. This does not mean that the uncorrected total stress parameters ϕ and c cannot be useful for design purposes. On the contrary, where anticipated loading rate and conditions inhibit or prohibit drainage, ϕ and c may be more useful than effective stress parameters ϕ' and c' because field pore pressures are not very predictable. As will be shown, the influence of pore-water pressure in the K-test may be di-

Figure 5. Stress paths from typical K-tests.

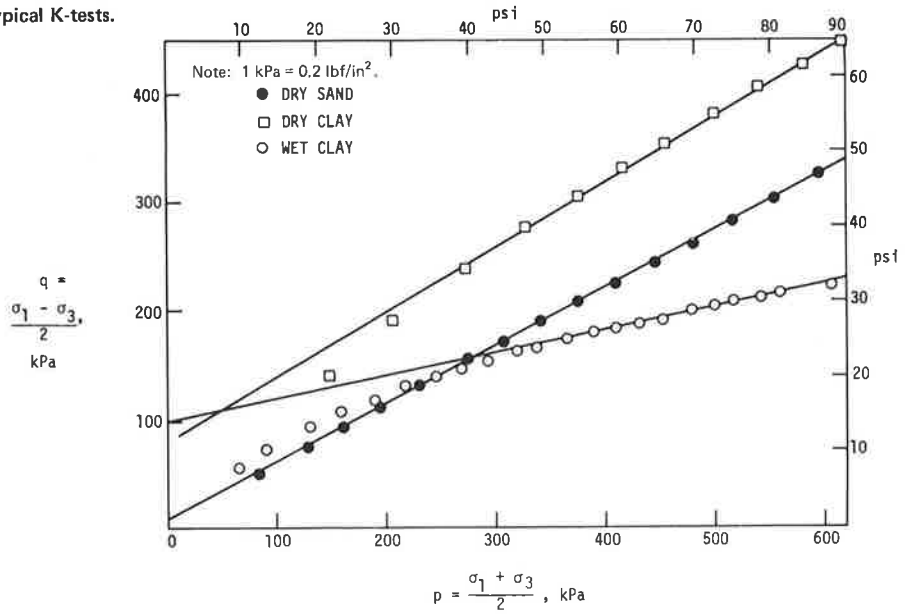

rectly monitored through a measured reduction in side friction.

E and ν

An estimate of the vertical deformation modulus E_z, useful in pavement design and required for finite element modeling, may be directly obtained from K-test stress-strain plots (Figure 7). E_z is not a true elastic modulus since the soil is in failure but should be a fairly accurate reflection of field behavior. The stress-strain relation is much more linear than in triaxial tests where lateral stress is constant and may explain the success of elastic theory for predicting soil stresses in the field under load. The E_z for Ottawa sand increased during the test, which is indicative of compaction.

Another measure required for characterization of stress under load for application of elastic theory or the finite element method is Poisson's ratio (ν). For a homogeneous, isotropic, elastic material it can be shown that

$$\nu = (\epsilon_r \sigma_z - \epsilon_z \sigma_r)/[2\epsilon_r \sigma_r - \epsilon_z(\sigma_r + \sigma_z)] \quad (7)$$

where ϵ_r and ϵ_z are radial and vertical unit strains, and σ_r and σ_z are corresponding stresses. Since these values of stress and strain are measured in the K-test, a direct evaluation of Poisson's ratio may be obtained.

Figure 6. K-test ϕ (top) and c (middle), and γ_d (bottom) versus compaction moisture content for a glacial till soil.

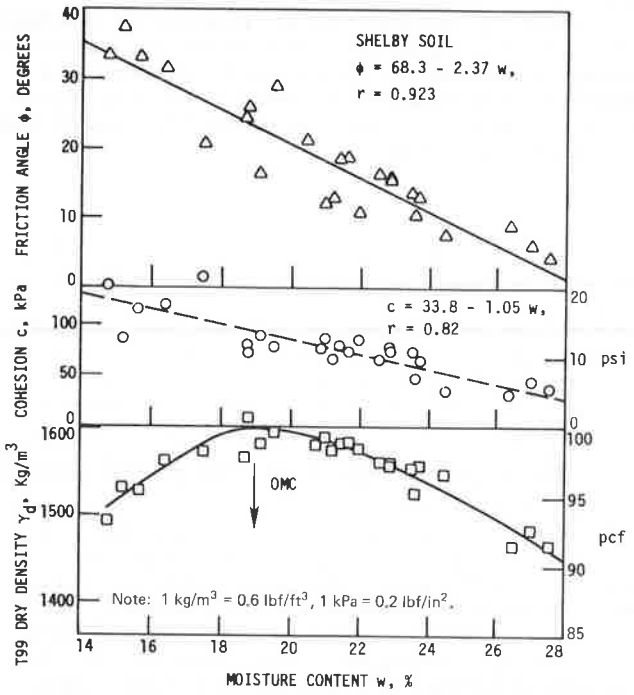

Figure 7. Typical stress versus strain diagram from K-test.

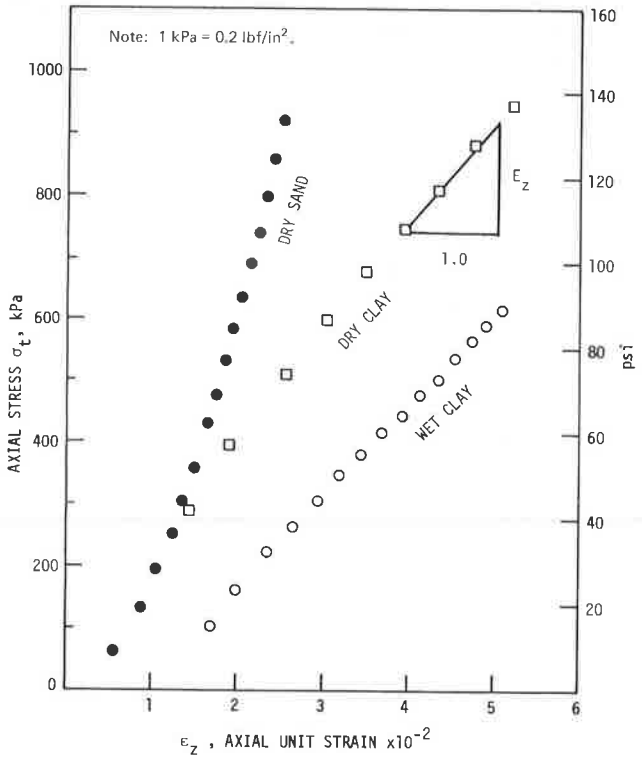

Side Friction Experiments

A major criticism of the K-test is the influence of friction between the soil and its confining steel mold and end platens. Platen friction is also a problem in triaxial tests where its effects are standardized by adapting a standard height-diameter ratio, normally 2.0. In the K-test, this ratio is closer to 1:1, and there is the additional friction from the mold.

Two approaches to the side friction problem are to minimize it and to measure it. Measurement offers some unique advantages:

1. Soil-to-steel friction is directly obtained as a function of normal stress, giving soil-to-steel sliding friction parameters (c_s and ϕ_s) that are potentially useful in design of pile, earth movers, and farm implements.
2. If the measured soil-to-steel friction parameters are assumed to apply to end platens of similar material and finish, the average boundary stresses will be known, and there exists a potential for a complete solution of stresses within the specimen. This would appear to offer a substantial advance over present triaxial testing.
3. Pore pressure effects may be evaluated directly from the influence on side friction, rather than through pressure transducers.

Side friction was measured by supporting the K-test mold on a pressure cell, such that the soil specimen would move downward and push on the base cell piston (14). In this way, all side friction was mobilized upward. Summing vertical forces on the soil gives

$$F_t = F_b + F_s \quad (8)$$

where

F_t = the top load on the soil,
F_b = the bottom load, and
F_s = the side friction.

Substituting stresses times respective end and side areas and solving,

$$\tau_s = (A_e/A_s)(\sigma_t - \sigma_b) \quad (9)$$

$$\tau_s = (R/2H)(\sigma_t - \sigma_b) \quad (10)$$

Table 1. K-test soil and soil-to-steel friction data for Shelby soil.

Moisture Content, W (%)	Soil Parameters		Soil-to-Steel Parameters		Effective Stress Soil Parameters	
	ϕ (degrees)	c (kPa)	ϕ_s (degrees)	c_s (kPa)	ϕ' (degrees)	c' (kPa)
12.4	39.1	132	28.0	18	39.1	132
15.2	37.4	87	27.0	5	38.0	85
15.3	34.8	119	25.5	18	35.4	128
16.5	31.6	121	23.2	10	33.3	130
17.3	30.5	119	18.2	21	36.6	118
18.8	25.9	71	15.4	3	35.6	66
19.5	23.8	43	13.1	17	39.8	80
20.1	22.6	17	11.5	23	36.2	74
21.7	18.6	74	7.7	12	38.5	57
22.6	16.1	66	6.1	10	38.2	50
22.9	17.3	76	5.7	26	44.2	43

Notes: 1 kPa = 0.145 lbf/in^2.
Parameters are uncorrected for side friction.
Regressions for total stress are ϕ = 70.9 - 2.39w, r = 0.988; ϕ_s = 61.6 - 2.45w, r = 0.981; c = 199 - 5.5w, r = 0.775; c_s = 4.9 + 0.55w, r = 0.269; and ϕ_s = 1.03 - 11.3, r = 0.992.
Regressions for effective stress are ϕ' = 31.2 + 0.35w, r = 0.417; and c' = 250 - 9.0w, r = 0.877.

where

τ_s = the average side frictional stress,
A_e and A_s = end and side areas of the cylindrical soil specimen, respectively,
R and H = its radius and height, and
σ_t and σ_b = the nominal vertical stresses on its top and bottom.

Typical plots of K-test side friction versus normal stress obtained from the mold expansion give linear relationships. Slope of the plot is the soil-to-steel friction angle (ϕ_s) and the intercept is soil-to-steel adhesion (c_s). In every case, it was found that the slope $\phi_s < \phi$, and the intercept $c_s < c$. However, neither ϕ_s/ϕ nor c_s/c describes any specified ratio, as often assumed for pile design.

A summary of soil and side friction parameters is given in Table 1. Regressions of total stress data in Table 1 indicate that for the Shelby soil $\phi_s = \phi - 11.3°$. A series of tests on compacted friable loess gave a similar result: $\phi_s = \phi - 12.8°$. Part of the approximate 12° difference between ϕ_s and ϕ may be an overestimation of ϕ by the K-test, whereas the vertical and horizontal forces to calculate ϕ_s are directly measured, and there should be no analogous error in its determination.

The adhesion c_s (Table 1) is low and erratic but tends to increase with increasing moisture content. Since the tests were performed immediately after compaction, there was little time for soil-steel adhesion to develop.

An unusual feature of the K-test is the evaluation of pore pressure from the effect on side friction rather than measurement under dynamic loading. The equation for side friction on an effective stress basis (indicated by ′) is

$$\tau_s' = c_s' = (\sigma_h - u) \tan \phi_s' \quad (11)$$

where

τ_s' = shearing stress,
c_s' = adhesion,
ϕ_s' = soil-to-steel friction angle,
σ_h = total horizontal stress obtained from mold expansion, and
u = pore water pressure.

Solving,

$$u = \sigma_h \left\{1 - [\tan \phi_s / \tan \phi_s' + (c_s' - c_s)/\tan \phi_s']\right\} \quad (12)$$

Since c_s is small and probably not affected by pore pressure (i.e., $c_s' = c_s$) the equation may be simplified to

$$u = \sigma_h (1 - \tan \phi_s / \tan \phi_s') \quad (13)$$

As previously discussed, ϕ and ϕ_s for a wet soil change as the test progresses due to development of pore water pressure. Side friction should be particularly sensitive to pore water pressure because there is no dilatancy. The soil is pressed against an impermeable steel face; therefore, pore pressure developed at the face should be essentially the same as that within the specimen.

In the initial stages of a side friction test, the slope is ϕ_s' if u = 0. This is shown by the first six points of the wet clay sample (Figure 5). Pore pressure then determined from Equation 13 gives effective stress data (Table 1).

Regressions of the effective stress parameters (Table 1) show a higher dependence of c′ on moisture content than the total stress parameter c, and a higher correlation coefficient. As should be expected, ϕ' changes relatively little with moisture content, and appears to increase with increasing w. However, the standard error indicates about a 70 percent possibility that the relation is due to chance. Wetting has been observed to substantially increase ϕ' of nonclay minerals while reducing that of clays (13).

Actual Stress Distribution

A previously cited advantage of the K-test is the direct determination of side friction as a function of measured normal stress. If the end platens are of the same material and finish as the mold, radial end friction should also be characterized. If all soil-to-steel friction is fully mobilized, vertical stresses at the top and bottom (σ_t and σ_b) should plot on the soil-to-steel side-friction envelope rather than on the abscissa of $\tau = 0$. The indicated horizontal shearing stresses at the platens (τ_t and τ_b) must decrease to 0 and reverse directions near the platen centers, so τ_t and τ_b are positive extremes. Downward within the soil specimen, τ also must decrease to 0 and then reverse. The mean stress on horizontal planes within the specimen, therefore, must be within the shaded trapezoid of Figure 8.

Approximations to a Mean Failure Envelope

The precise topography of stress distribution within the K-test specimen is not known but should be within the capability of finite element modeling once boundary conditions and soil behavior are fully defined. However, the test purpose is to define soil behavior, so a stress distribution must be assumed. If desired, the approximation may be tested on the basis of derived behavior.

The first approximation used in this paper assumes $\sigma_t = \sigma_1$ and $\sigma_h = \sigma_3$, a very simple procedure adapted for routine tests and not requiring bottom pressure readings. This is shown by the solid-line uncorrected failure circles (Figure 8).

A second approximation that should be closer to reality can be based on assumed validity of the soil-to-steel failure envelope, which is directly measured (Figure 8). The top and bottom normal stresses (σ_t and σ_b) also directly measured, must plot on or slightly below this envelope. The horizontal shearing stress τ is a maximum at the upper platen but must decrease to 0 and reverse both across and downward within the soil specimens; hence the upper σ_1 limb of the Mohr circle must pass somewhere through the shaded area of Figure 8,

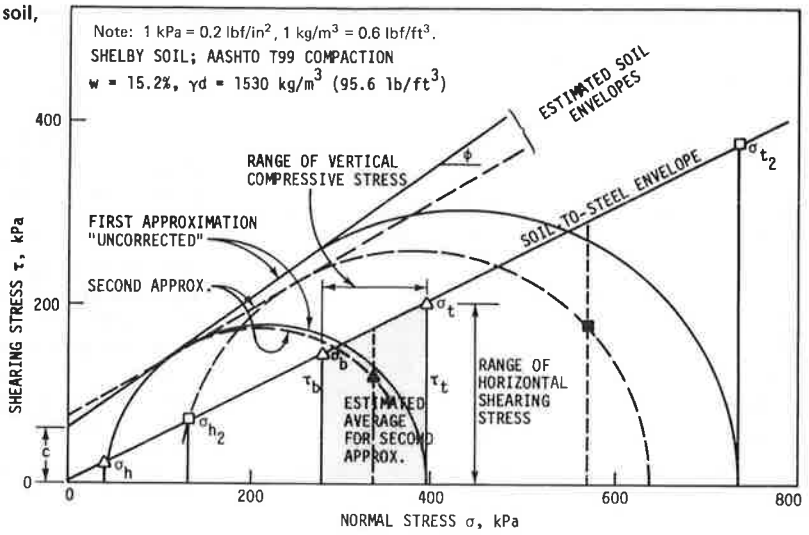

Figure 8. Two data points from a test on Shelby soil, showing two methods to obtain ϕ and c.

rather than simply through its lower right corner. The lower σ_3 limb likewise should plot through σ_h plotted on the soil-to-steel envelope, and since the measured σ_h is an average, its indicated τ also represents an average.

The problem is to ascertain a realistic average stress condition for the upper limb. On the basis of the assumption that σ_b and σ_t may be averaged, and the mean τ is 60 percent of that at the specimen boundaries, the solid points and corresponding dashed second approximation circles were drawn. The resulting failure envelopes give

Approximation	ϕ	c
First	35.6°	103 kPa
Second	30.5°	131 kPa

That the second approximation is better than the first is shown by the lower ϕ and slightly higher c, consistent with observations that uncorrected K-test values are too high, and, with exception of the Ottawa sand, c values are too low compared to other data. The analysis also shows why the initial assumption that $\sigma_t = \sigma_1$ gives fairly reasonable results since the Mohr circle passing through (σ_t, 0) is a good preliminary estimate.

Height-to-Diameter Ratio

Stress distribution within a K-test specimen should depend on the height-to-diameter ratio (H/D) and on whether the mold is supported, since support causes all side friction to act one way. Support and a large H/D will increase the roll of side friction relative to end friction. Preliminary investigations with a 25.4-mm (1-in) diameter K-test mold indicate that an H/D ratio close to 1.0, with the mold supported, minimized ϕ and c for the sand and appeared reasonable.

Circumferential Friction

Circumferential friction of soil on steel acts on the inner mold surface, opposing opening of the mold and reducing the measured σ_h. A calculation of this effect shows that it is minor and may be ignored. Secondly, since only the vertical component of side friction is measured in the test, total side friction is not axisymmetric and is underestimated. Extent of this error depends on the direction of movement: The maximum amount of circumferential slip occurs adjacent to the mold split, about 1.3 mm (0.050 in), whereas the maximum amount of vertical deflection typically is about 6.4 mm (0.25 in). As an extreme, the correct $\tau = \tau_s$ sec/tan (1.3/6.4) = 1.02 τ_s, a 2 percent error, which is minor and may be ignored.

SOME POTENTIAL USES OF THE K-TEST

The K-test modulus of deformation (E_z) would appear to have an excellent potential for rigid pavement design or for comparison with, and fill-in between, relatively expensive plate bearing tests. It should be emphasized that the K-test requires about 15 min and utilizes specimens already available from Proctor compaction tests.

The speed and ease with which K-tests provide c and ϕ values mean extremely rapid calculation of bearing capacity pertinent to flexible pavement design, at a cost well below that of comparable California bearing ratio (CBR) tests. It will be noted that a laboratory CBR uses a rigid steel mold, whereas structural deterioration of flexible pavements often begins at the edges where lateral confining stress is low and is not correctly modeled in CBR.

K-test specimens may be vacuum or capillary saturated prior to test; however, molding at slightly above optimum moisture content may achieve the same result in less time.

Earthwork Control

Present methods for compaction control are of necessity indirect; although strength is the desired criterion, strength tests have been too inaccurate (as with the Proctor penetrometer) or too time consuming and expensive. We therefore rely on density, moisture content, and soil identification, all three needing arduous attention if failures are to be avoided. K-tests of cores could provide a much more rapid accept-reject criterion—if the soil is too clayey, this will adversely affect K-test results. Since only a simple unconfined compression tester is needed, Shelby tube specimens may be extruded, immediately tested in the field, and results compared with laboratory controls. In addition, calculation of bearing capacity may give a rapid determination of weight requirements for field compactions.

Earthwork Specifications

The choice between 90 and 95 percent T-99 or T-180 density is usually a matter of engineering skill and judgment based on anticipated loads and performance records of particular soils. By means of K-tests on specimens molded at variable compactive efforts, the advantage and amount of additional field compactive effort may be quickly and directly ascertained; also the K-test is sensitive to overcompaction, as indicated by a drop in c and increase in ϕ.

Pile

Use of the K-test to evaluate side friction data directly, and thus predict skin friction on pile, needs no further elaboration. Tests conducted show that the method of using fractionally reduced soil ϕ and c values may be in error, normally but not necessarily conservative.

The above suggested uses may seem somewhat overstated or even flamboyant at first encounter. The K-test can be fast, cheap, and readily computerized. Since the known errors are biased rather than random, corrections appear possible. Meanwhile, an arbitrary reduction in ϕ and c may be made or their overestimation covered in a factor of safety. A major advantage of a cheap and rapid test is to evaluate variability of soils, which has been a major problem in soil testing. Similar comparisons seldom are possible by triaxial testing because of the prohibitive cost; an abbreviated version; however, is the stage-triaxial test, which is increasing in use, particularly by consulting firms. The latter is a stepwise analogue of the K-test, requiring judgment of where failure is about to occur in order to increase confining stress; in the K-test, this is automatic.

CONCLUSIONS

1. A soil test to measure the Rankine active stress ratio K has been devised to utilize standard Proctor-size compacted specimens, a load frame, and a split steel K-test mold. The test has been used extensively for comparative evaluations of undrained soil strength parameters.
2. The Iowa K-test requires about 15 min to perform and provides a continuous record of uncorrected soil cohesion (c), internal friction (ϕ), and deformation moduli (E_z and ν), as the test progresses.
3. Supplemental use of a base pressure cell allows simultaneous direct measurement of soil-to-steel friction as a function of normal stress and, hence, of the soil-to-steel friction parameters (c_s and ϕ_s).
4. Errors in the uncorrected soil c and ϕ data are discussed, and a preliminary method for correction is presented. An accurate correction will require a much more extensive analysis of stress distribution; however, preliminary analyses and comparative tests indicate that the uncorrected data are not so seriously in error that they would not be covered by usual factors of safety. Since many tests can be performed in a reasonable time span, a probabilistic approach to design and construction control becomes feasible.

ACKNOWLEDGMENTS

The first Iowa K-test was conducted October 11, 1974, by R. L. Handy and J. M. Hoover, and was observed by Darwin E. Fox. Since that time, thousands of tests have been conducted in conjunction with Federal Highway Administration project, Chemical Compaction Aids for Fine-Grained Soils, in order to assess effects of chemical additives, moisture content, and compaction energy on strength parameters. Developmental research on the K-test has been sponsored by the Iowa State University Engineering Research Institute and the Iowa State University Research Foundation.

REFERENCES

1. C. A. Coulomb. Essai sur une application de règles de maximis et minimis à quelques problèmes de statique relatifs à l'architecture. Mémoires de la Mathématique et de Physique, Vol. 7, Année 1773, De L'Imprimerie Royale, Paris, 1776.
2. W. J. M. Rankine. On the Stability of Loose Earth. Philosophical Transactions, Royal Society of London, Vol. 147, 1857.
3. W. J. M. Rankine. A Manual of Applied Mechanics. Charles Griffin and Co., London, 1885, pp. 219-220.
4. E. P. Goodrich. Lateral Earth Pressures and Related Phenomena. ASCE Transactions, 1904, pp. 272-290.
5. G. P. Tschebotarioff. Foundations, Retaining and Earth Structures. McGraw-Hill, New York, 1951.
6. G. F. Sowers, A. D. Robb, C. H. Mullis, and A. J. Glenn. The Residual Lateral Pressures Produced by Compacting Soils. International Conference on Soil Mechanics and Foundations, England, 1957.
7. K. Terzaghi. Old Earth Pressure Theories and New Test Results. ENR, Sept. 30, 1920, p. 633.
8. V. Obercian. Determination of Lateral Pressures Associated With Consolidation of Granular Soils. HRB, Highway Research Record 284, 1969, pp. 13-25.
9. F. N. Hveem and R. M. Carmany. The Factors Underlying the Rational Design of Pavements. Proc., HRB, Vol. 28, 1948, pp. 101-136.
10. Procedures for Testing Soils. 4th ed., ASTM, 1964, pp. 458-464.
11. W. S. Housel. Suggested Method of Test for the Internal Stability of Granular Soils and Stabilized Mixtures (stabilometer test). ASTM Procedures for Testing Soils, 1950, pp. 315-319.
12. W. Wedzinski and J. Najder. A Contribution to Laboratory Investigations on the Coefficient of Lateral Pressure of Silt. (Transl. from Polish), Office of Tech. Serv., U.S. Department of Commerce, ca. 1967.
13. M. G. Spangler and R. L. Handy. Soil Engineering, 3d ed. Intext Educational Publishers, New York, 1973.
14. A. J. Lutenegger. The Iowa Continuous K-Test: A Laboratory Test for Measuring Lateral Stresses in Soils Induced by Vertical Applied Loads. Iowa State Univ. Research Foundation, Iowa State Univ., M.S. thesis, 1977.
15. D. W. Taylor and T. M. Leps. Shearing Strength of Ottawa Standard Sand as Determined by the M.I.T. Strain-Controlled Direct Shearing Machine. Proc., Soils and Foundation Conference, U.S. Engineering Department, Boston, 1938.

Publication of this paper sponsored by Committee on Soil and Rock Properties.

Abridgment

Probability of Sliding of Soil Masses

Dimitri Athanasiou-Grivas, Rensselaer Polytechnic Institute, Troy, New York

The employment of logarithmic spiral failure surfaces in slope stability analysis was dictated by the need to bring analytical models closer to the configuration of actual failures (1). Initially, such surfaces were associated with unity safety factor and thus were used only for computations of the critical heights of slopes (2). The first attempt to adapt the log-spiral against sliding was made by Fröhlich (3). The analytical expression used was the following:

$$r = r_0 e^{-\theta t} \tag{1}$$

where

r_o = the initial radial vector,
$t(=\tan\phi)$ = the soil strength parameter, and
θ = the angle between r_o and r (Figure 1).

The factor of safety (F_s) with respect to sliding of a soil mass is equal to (3)

$$F_s = M_R/M_S \tag{2}$$

where M_R = the moment around an axis of all resisting forces acting on the sliding mass along the sliding surface, and M_S = the moment of all forces driving the soil mass towards sliding.

After moments M_R and M_S are expressed analytically, Equation 2 becomes Equation 3

$$F_s = M_R/M_S = 1 + \{(c/S)[(r_0^2 - r_H^2)/2t] - a_0\} \div [a_0 + r_H e^{\mu\theta} H^t \times t \times \sin(\mu\theta_H + \delta)] \tag{3}$$

where

r_o, r_H = radial vectors (Figure 1a),
S = the resultant of all driving forces acting on the sliding mass (Figure 1b),
a_o = the distance between the center of the spiral and S (Figure 1a),
δ = the angle between r_H and the normal to the direction of S,
θ_H = the angle between r_o and r_H,
μ = a parameter that determines the center of rotation and receives values between zero and infinity, and
$c, t(=\tan\phi)$ = the soil strength parameters.

In the above equation, all variables are treated as single-valued quantities. However, in soils, values of material parameters exhibit a considerable variation (4). The same is true (1) for the geometric factors in Equation 3 (i.e., angles θ_H and δ; distances r_o, r_H, and a_o; and quantity μ). Thus, a more reliable approach to the measure of safety of a soil slope must take into account uncertainties such as material parameters and the shape and location of the failure surface.

PROBABILITY OF SLIDING

In recent years, the use of probability theory and statistical analysis has provided an alternative to the determination of the factor of safety. In its classical formulation, sliding of a soil slope is assumed to occur when the calculated moment of all resisting forces (M_R) becomes smaller than that of the driving forces toward failure (M_S); that is, Sliding = $[M_R < M_S]$. The probability of failure in sliding is then defined as $p_f = P[M_R < M_S] = P[M_R/M_S < 1]$, where $P[\ ]$ indicates the probability that the driving forces exceed available strength. In Equation 3 the expression $M_R/M_S = F_s < 1$ is identical to $c/S[(r_o^2 - r_H^2)/2t] - a_o < 0$, i.e., the numerator of the second term of the right side of Equation 3 becomes negative. Therefore, the expression for p_f becomes

$$p_f = P\{(c/S)[(r_0^2 - r_H^2)/2t] - a_0 < 0\} \text{ or}$$
$$p_f = P[c(r_0^2 - r_H^2)/2t < Sa_0] \tag{4}$$

The quantity $(r_o^2 - r_H^2)/2t$, in Equation 4, is equal to twice the area (A) of the region OBMAO, shown in Figure 1a, or

$$(r_0^2 - r_H^2)/2t = 2A \tag{5}$$

and the quantity Sa_o gives the moment, say M_o, of the driving forces around the center of the sliding surface; i.e., $M_o = Sa_o$. In the case where the value of the factor of safety is equal to unity, or $(2c)\,A = M_o$, the moment M_o varies in proportion to the area A, the coefficient of proportionality being the double value of the c strength parameter. If this product is denoted by M, i.e., if

$$M = 2cA = c(r_0^2 - r_H^2)/2t \tag{6}$$

and the expressions for M and M_o are introduced into Equation 4,

$$P_f = P[M < M_o] \tag{7}$$

The uncertainty of the value of M reflects the uncertainties of the strength parameters c and t and, also, of the location of the center 0 of the sliding surface (the latter is determined by the geometric factors h_o and θ_o). From Equation 6 it can be seen that the value of M (random variable) ranges between zero (lower limit) and infinity (upper limit). As was the case with other random variables (1), it can be assumed that M follows a log-normal distribution. Under this assumption, the probability density function of M is (5)

$$f(M) = 1/(\sqrt{2\pi}\,\sigma_M M)\exp\{-\tfrac{1}{2}[(\ln M - \overline{M})/\sigma_M]^2\} \tag{8}$$

where $0 \le M < \infty$ and $\overline{M}$ and σ_M denote the mean value and standard deviation of M, respectively.

Combining Equations 7 and 8, the following expression for the probability p_f of sliding of the soil mass is then derived:

$$p_f = \int_0^{M_0} f(M)dM = F(M_0) \tag{9}$$

where $F(M_o)$ = the cumulative log-normal distribution evaluated at M_o.

As M is taken to be log-normally distributed, the

Figure 1. Logarithmic-spiral sliding surface and polygon of forces.

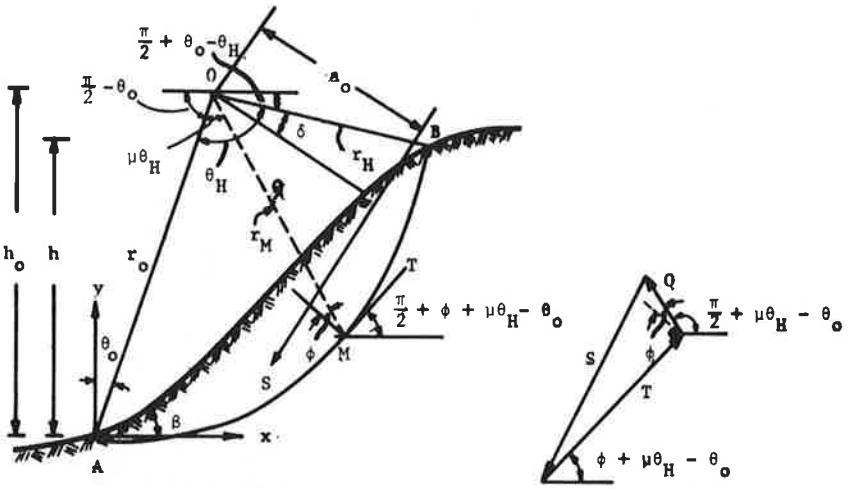

variable x, which is equal to lnM, is normally distributed. If the coefficient of variation and mean value of x are denoted by S_x and μ_x, respectively, then

$$S_x = [\ln(V_M^2 + 1)]^{1/2} \tag{10a}$$

and

$$\mu_x = \ln(\bar{M}) - S_x^2/2 \tag{10b}$$

Introducing the normalized variable z, defined as $z = (\ln M - \mu_x)/S_x$, the expression for the probability of sliding p_f becomes:

$$p_f = P[M < M_0] = P[z < z_0] = \Psi(z_0) \tag{11}$$

where z_o = the value of z evaluated at $M = M_o$, and $\Psi(\ )$ = the well-tabulated cumulative standard normal distribution.

STATISTICAL VALUES OF MOMENT (M)

Equations 10 and 11 can be solved provided that the mean value ($\bar{M}$) and standard deviation (σ_M) of M are determined. For a given surface of sliding (i.e., $\frac{1}{2}(r_o^2 - r_H^2)$ = constant = b), Equation 6 suggests that the value of moment M depends on the strength parameters c and t and the geometrical constants r_o and r_H. Equation 6 can be reduced to

$$M = b\, c/t \tag{12}$$

where $b = \frac{1}{2}(r_o^2 - r_H^2)$. If c and t are independent random variables, the mean value $\bar{M}$ and variance Var(M) of M can be found by means of a Taylor series expansion of the function M(c, t) around the point $M(\bar{c}, \bar{t})$, where $\bar{c}$ and $\bar{t}$ denote the mean values of c and t, respectively (6); i.e.,

$$\bar{M} = M(\bar{c}, \bar{t}) + \tfrac{1}{2}\{[(\partial^2 \bar{M})/\partial c^2]\ \mathrm{Var}(c) + [(\partial^2 \bar{M})/\partial t^2]\ \mathrm{Var}(t)\} \tag{13a}$$

$$\mathrm{Var}(M) = (\partial \bar{M}/\partial c)^2\ \mathrm{Var}(c) + (\partial \bar{M}/\partial t)^2\ \mathrm{Var}(t) \tag{13b}$$

where Var(c), Var(t) are the variances of c and t, respectively, and the derivatives are evaluated at the mean values of the variates.

From Equation 12 one has

$$\partial M/\partial c = b/t,\ \partial^2 M/\partial c^2 = 0,\ \partial M/\partial t = -bc/t^2,\ \partial^2 M/\partial t^2 = 2bc/t^3 \tag{14}$$

Combining Equations 13 and 14,

$$\bar{M} = b\,[\bar{c}\bar{t}^2 + \bar{c}\,\mathrm{Var}(t)]/\bar{t}^3 \tag{15a}$$

and

$$\mathrm{Var}(M) = b^2\,[\bar{t}^2\,\mathrm{Var}(c) + \bar{c}^2\,\mathrm{Var}(t)]/\bar{t}^4 \tag{15b}$$

The coefficient of variation V_M of M can be determined from Equations 15 as

$$V_M = \sigma_M/\bar{M} = \{\bar{t}/[\bar{c}\bar{t}^2 + \bar{c}\,\mathrm{Var}(t)]\}\ [t^2\,\mathrm{Var}(c) + c^2\,\mathrm{Var}(t)]^{1/2} \tag{16}$$

where V_M is independent of the constant b.

In Figure 2, the mean value of the quantity $\bar{M}/b$ is plotted versus the mean value ($\bar{t}$) of the strength parameter t for various values of $\bar{c}$. Studies of the variability of the soil strength parameters t and c have indicated (4) that their coefficients of variation V_t and V_c approach values of 15 and 70 percent, respectively. These same values for V_t and V_c have, therefore, been adopted in this paper.

EXAMPLE

The slope shown in Figure 3 has a height h = 9.75 m (32 ft) and an angle $\beta = 40°$. The mean values and coefficients of variation of the strength parameters of the soil, determined from conventional triaxial tests, are also shown in the figure. The moist unit weight of the soil is assumed to be 1762 kg/m^3 (110 lb/ft^3). The probability of failure, or the reliability of this slope, is to be determined.

Three random factors in Equation 1 reflect the uncertainty of (a) the location of the center of the rupture surface, (b) the point of initiation of the rupture surface, and (c) the value of the t-strength parameter of the soil material. A procedure necessary to generate such surfaces was presented previously (1). The assumptions involved are that the failure surface begins at the toe of the slope and the coordinates θ_o and h_o of the center of the log-spiral (Figure 1) follow a beta distribution. In Figure 3, the mean failure surface can be found through an application of the Monte Carlo simulation technique

Figure 2. Influence of the statistical values of strength parameters on the mean value of the moment (M).

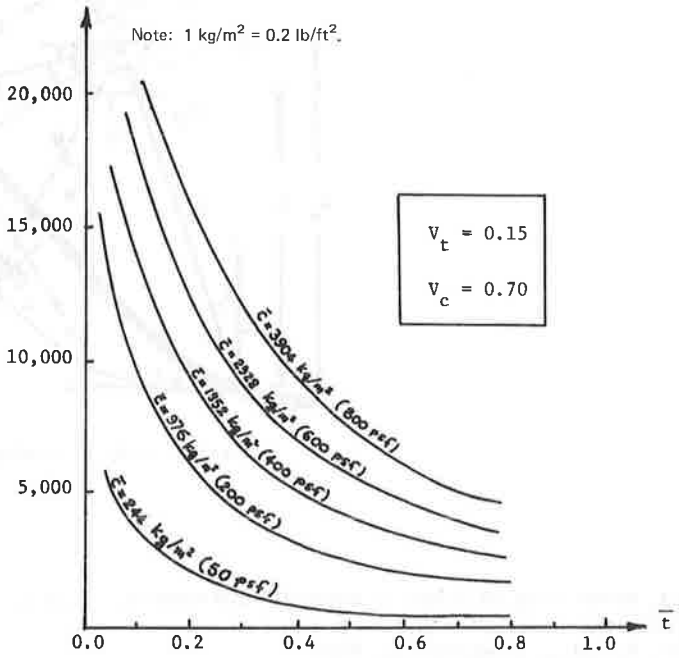

Figure 3. Slope section and soil parameters used for the case study.

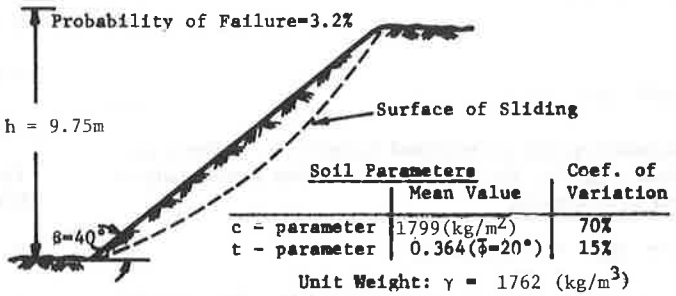

Note: 1 kg/m² = 0.2 lb/ft², 1 kg/m³ = 0.06 lb/ft³.

(1). The center of the log spiral has coordinates h_o = 22.81 m (74.83 ft) and $\theta_o = 0°$ (Figure 1). The quantities r_H and θ_H are thus equal to 17.42 m (57.14 ft) and 43°, respectively.

The driving moment (M_o) due to the weight of the sliding soil mass is equal to $M_o = Wa_o$ (3), where a_o is shown in Figure 1. Area A (determined by Equation 5) and distance a_o (measured graphically in Figure 3) are equal to 42.67 m^2/m (140 ft^2/ft) and 6.1 m (20 ft), respectively. Therefore, $M_o = \gamma \cdot A \cdot a_o$ = (1762) (42.67) (6.1) = 458 626 J/m (154 ft-tons/ft).

From Figure 2, for $\bar{t}$ = 0.364 and $\bar{c}$ = 1797.3 kg/m^2 (368.3 lb/ft^2) we find $\overline{M}/b \approx 5053$ kg/m^2 (1035 lb/ft^2), where $b = (r_o^2 - r_H^2)/2 = [(22.81)^2 - (17.42)^2]/2 = 103.15$ m^2 (1167.27 ft^2).

Therefore, $\overline{M}$ = (5053) (103.15) = 521 234 J/m (604.1 ft-tons/ft).

The coefficient of variation M (V_M) is found from Equation 16 to be equal to 70 percent.

For $\overline{M}$ = 521.234 J/m^2 (604.1 ft-tons/ft) and V_M = 70 percent, Equation 10 yields $S_x = 0.6315$ and $\mu_x = 12.96$. The probability of sliding of the slope can now be determined from Equation 11 as follows:

$$p_f = P[z < z_o] = \Psi(-1.8485) \approx 3.2\% \qquad (17)$$

DISCUSSION AND CONCLUSIONS

Statistical analysis and probability theory can be used as alternatives to conventional (deterministic) methods for evaluation of slope stability. In this paper, the reliability of a soil slope against sliding was evaluated from its probability of failure. This was defined as the probability that the resisting moment M_R was exceeded by the driving moment M_S. Sliding was assumed to occur along a log-spiral path. This assumption is consistent with results obtained through stochastic modeling of the propagation of failure surfaces (7).

As the variation of the unit weight ($\bar{\gamma}$) of the soil is relatively small, γ was assumed to be constant. Thus, moment M was expressed as a function of only two random variables: strength parameters c and t. The variability of c and t in the expression for the moment M was investigated by means of a Taylor series expansion of $M(c, t)$ around the point $M(\bar{c}, \bar{t})$. It should be noted that this method gives only approximate values for the mean and variance of M. If greater accuracy is required, a more precise procedure, possibly a simulation approach, should be employed.

In the illustrative example it was found that the probability of failure of the slope was approximately 3.2 percent or, out of 100 identical slopes, on the average, 3.2

would fail. The reliability of this slope is then said to be equal to 96.8 percent.

Based on the results of this study, it is concluded that

1. The probabilistic model developed here can be used to find a value of the probability of failure (or, the reliability) of a soil slope. This depends on the slope geometry and on the statistical values of the soil parameters.
2. The method can be applied to either deep or shallow failures. The kind of failure is reflected in the probability density functions of the coordinates of the center of the sliding surface.

REFERENCES

1. D. Athanasiou-Grivas. Reliability of Slopes of Particulate Materials. Ph.D. Thesis, Purdue Univ., Lafayette, IN, 1976.
2. L. Redulic. Ein Beitrag zur Bestimmung der Gleitsicherheit. Der Bauingenieur, No. 19/20, 1935.
3. O. K. Frölich. The Factor of Safety With Respect to Sliding of a Mass of Soil Along the Arc of a Logarithmic Spiral. Proc., 3rd International Conference on Soil Mechanics and Foundations Engineering, Switzerland, Vol. 2, 1953.
4. P. Lumb. Variability of Natural Soils. Canadian Geotechnical Journal, Vol. 3, No. 2, 1966.
5. M. E. Harr. Mechanics of Particulate Media—A Probabilistic Approach. McGraw-Hill, New York, 1977.
6. G. J. Hahn and S. S. Shapiro. Statistical Models in Engineering. Wiley, New York, 1967.
7. D. Athanasiou-Grivas and M. E. Harr. Stochastic Propagation of Rupture Surfaces Within Slopes. Proc., 2nd International Conference on Application of Statistics and Probability to Soil and Structure Engineering, Aachen, Germany, 1975.

Publication of this paper sponsored by Committee on Embankments and Earth Slopes.

Soil-Culvert Interaction Method for Design of Metal Culverts

J. M. Duncan, University of California, Berkeley

A simple and rational method for the design of metal culverts, the soil-culvert interaction method, is described and compared to currently used design procedures. The principal advantage of the soil-culvert interaction method over those previously developed is that it provides a logical procedure for determining minimum required depth of cover, by consideration of the bending moments caused by live loads. Previously, minimum depths of cover have been determined empirically, using field experience. Values of minimum cover and maximum fill height determined using the soil-culvert interaction method are compared with values from published fill-height tables. The comparisons show that the soil-culvert interaction method gives values that are in good agreement with design experience for a wide range of corrugations and culvert diameters.

A simple method for design of metal culvert structures has been developed to provide rational procedures for designing culverts with deep or shallow cover. Design for deep cover is based on consideration of ring compression forces. Design for shallow cover is based on consideration of both ring compression forces and bending moments. The method, the soil-culvert interaction (SCI) method, is applicable to circular pipes, pipe arches, and arches constructed of corrugated steel or aluminum. It may be applied to structures having stiffening ribs that are curved to conform to the shape of the culvert barrel and attached to the barrel at frequent intervals. However, it is not applicable to soil bridge structures, which use straight ribs, fin plates, and sometimes strut to stiffen the upper part of the structure. The SCI method has been found to give values of maximum and minimum cover that are in good agreement with design experience as reflected in published fill-height tables and with the observed behavior of culverts in the field.

BASIS FOR SCI METHOD

The SCI design procedure is based on the results of finite element analyses, which modeled both the culvert structure and the surrounding backfill. Detailed results of the analyses and comparisons with field measurements were described by Duncan (1). Similar analyses were performed by Allgood and Takahashi (2), Abel and others (3), and Katona and others (4). The analyses on which the SCI method is based simulated the placement of backfill around and over the structure, and subsequent application of live loads on the surface of the backfill. Nonlinear and stress-dependent stress-strain relationships for the backfill soils were employed in the analyses. The results of these analyses were used to derive coefficients for ring compression forces and bending moments for design.

STEPS IN SCI DESIGN PROCEDURE

1. Calculate the rise/span ratio (R/S). The definitions of rise and span as used in this procedure are shown in Figure 1.
2. Calculate the maximum ring compression force

$$P = K_{p1}\gamma S^2 + K_{p2}\gamma HS + K_{p3}LL \quad (1)$$

where

P = ring compression force (kN/m);
K_{p1} = ring compression coefficient or backfill, from Figure 2 (dimensionless);

Figure 1. Types of long-span metal culvert structures.

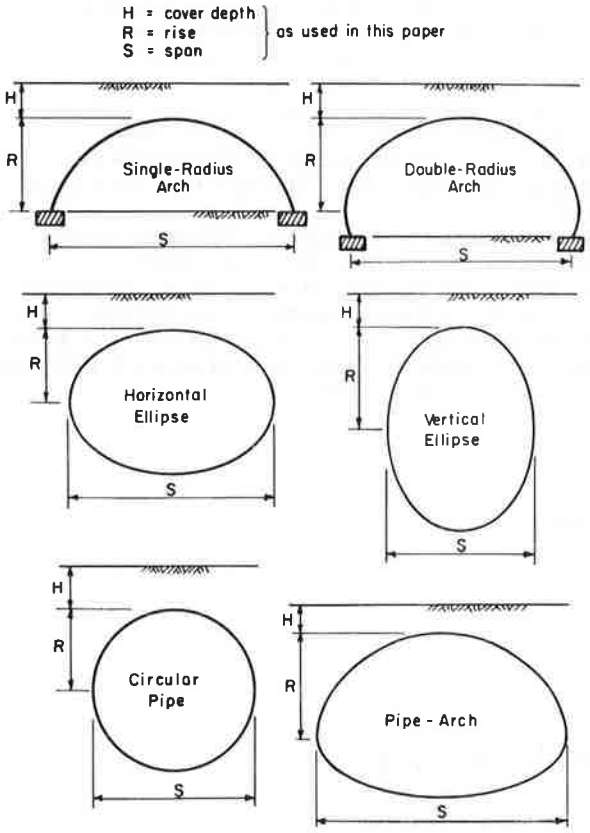

Figure 2. Axial force coefficients.

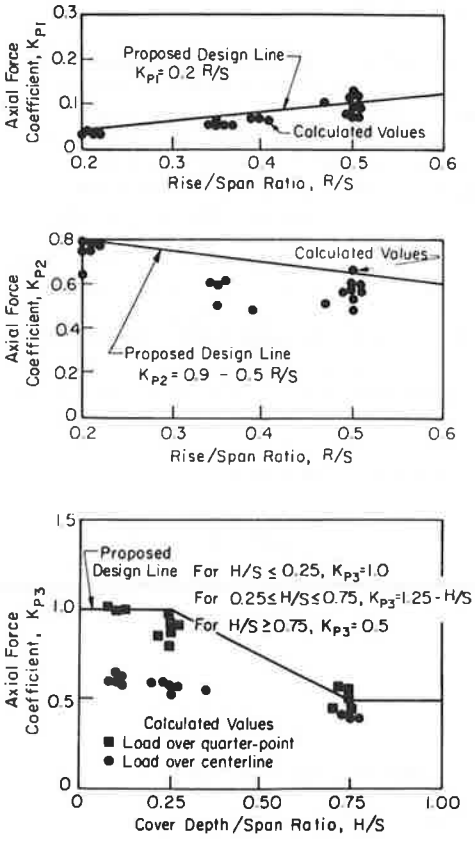

K_{p2} = ring compression coefficient for cover, from Figure 2 (dimensionless);
K_{p3} = ring compression coefficient for live load, from Figure 2 (dimensionless);
γ = unit weight of backfill (kN/m^3);
H = cover depth (m);
S = span (m); and
LL = live load (kN/m).

The table below gives values corresponding to H-20 traffic loading (1 m = 3.3 ft, 1kN/m = 74 lb/ft):

Cover Depth H (m)	Line Load LL (kN/m)	Cover Depth H (m)	Line Load LL (kN/m)
0.3	89	6.1	19
0.6	69	9.2	13
0.9	53	15.2	9
1.5	38	30.0	4
2.1	35	45.8	3
3.0	29	61.0	3
4.6	23		

Line load produces the same peak stress at depth H as do two HS-20 truck trailers that have single rear axles side by side on a two-lane road.

A section is chosen that has a seam strength sufficient to provide a factor of safety against seam compression failure that is equal to or greater than 1.50.

3. Calculate maximum bending moment at H = 0.

$$M_1 = K_{M1} R_B \gamma S^3 \quad (2)$$

where

M_1 = maximum bending moment at H = 0 (kN·m/m), which occurs at both the crown and the upper quarter-point;
K_{M1} = moment coefficient, from Figure 3 (dimensionless); and
R_B = moment reduction factor, from Figure 3 (dimensionless).

The value of the moment coefficient K_{M1} depends on the flexibility of the culvert section relative to the backfill, as defined by the flexibility number N_f:

$$N_f = (E_s S^3)/EI \quad (3)$$

where

N_f = flexibility number (dimensionless);
E_s = soil modulus, which depends on soil type, degree of compaction, and depth of overburden, from Figure 4 (kPa);
E = modulus of elasticity of metal culvert (mPa); and
I = moment of inertia of metal culvert (m^4/m).

The values of E_s shown in Figure 4 are based on the results of laboratory tests on over 100 different soils, which have been summarized by Wong and Duncan (5) and were selected to be representative of the behavior of the soils under the particular stress conditions that exist around flexible metal culverts.

The section should have sufficient moment capacity to withstand this bending moment and the corresponding axial force (calculated using Equation 1 for H = 0 and LL = 0) with a factor of safety against development of a plastic hinge (F_p) that is greater than or equal to 1.65.

The value of E_p is calculated from the following equation

$$F_p = 0.5\, P_p/p\, [\sqrt{(M/M_p)^2 (P_p/p)^2 + 4} - (M/M_p)(P_p/p)] \quad (4)$$

where

F_p = factor of safety against formation of a plastic hinge, considering both axial force and moment;
P = axial force (kN/m);
P_p = fully plastic axial force, with no moment (kN/m);
M = bending moment (kN·m/m); and
M_p = fully plastic bending moment, with no axial force (kN·m/m).

4. If the final depth of cover is greater than or equal to one-quarter of the span ($H \geq 0.25S$), bending need not be investigated for the final cover condition. If the final cover depth is less than one-quarter of the span ($H < 0.25S$), the bending moment due to both backfill and live load for the final cover condition are calculated using the following equation

$$M = M_1 - R_B K_{M2} \gamma S^2 H + R_L K_{M3} S\, LL \quad (5)$$

where

M = bending moment due to backfill and live load with cover depth H (kN·m/m);
M_1 = bending moment calculated previously for H = 0 (kN·m/m);
K_{M2} = moment coefficient, from Figure 3 (dimensionless);
R_L = moment reduction factor, from Figure 5 (dimensionless); and
K_{M3} = moment coefficient, from Figure 5 (dimensionless).

For purposes of determining K_{M2}, K_{M3}, and R_L, the value of N_f should be recalculated using a value of E_s corresponding to the final cover depth.

As for bending due to backfill loads at H = 0, the section chosen should have sufficient moment capacity to provide a factor of safety against development of a plastic hinge (F_p) greater than or equal to 1.65.

5. For arch structures, consideration must also be given to footing size, to ensure that the horizontal or vertical bearing pressures do not exceed the allowable values for the supporting soil. Similarly, for pipe arches, consideration must be given to the bearing pressures at the haunch.

MINIMUM COVER DEPTHS

Consideration of bending moments due to backfill loads and live loads in the SCI design method provides a rational means of establishing minimum cover depths

Figure 3. Coefficients for backfill moments.

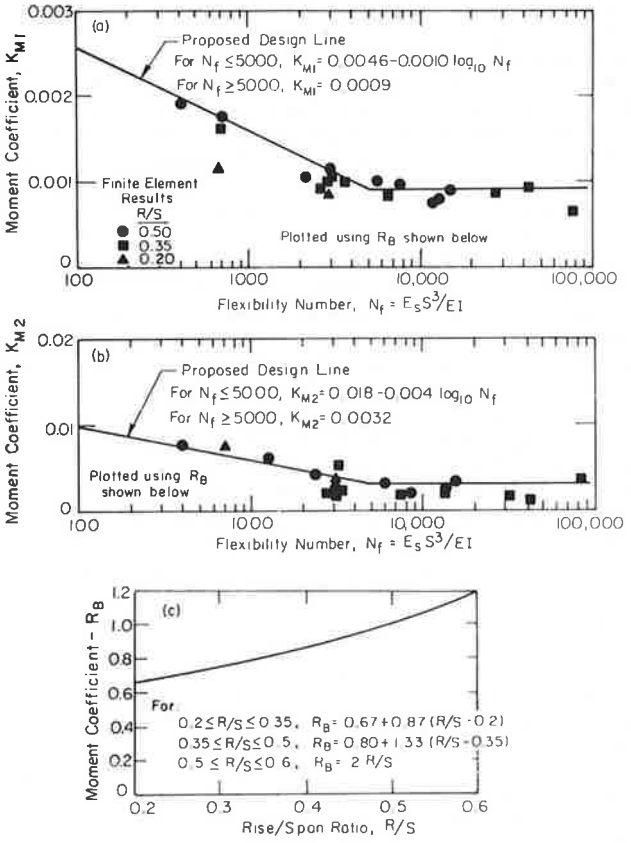

Figure 4. Approximate secant modulus values for various types of backfill.

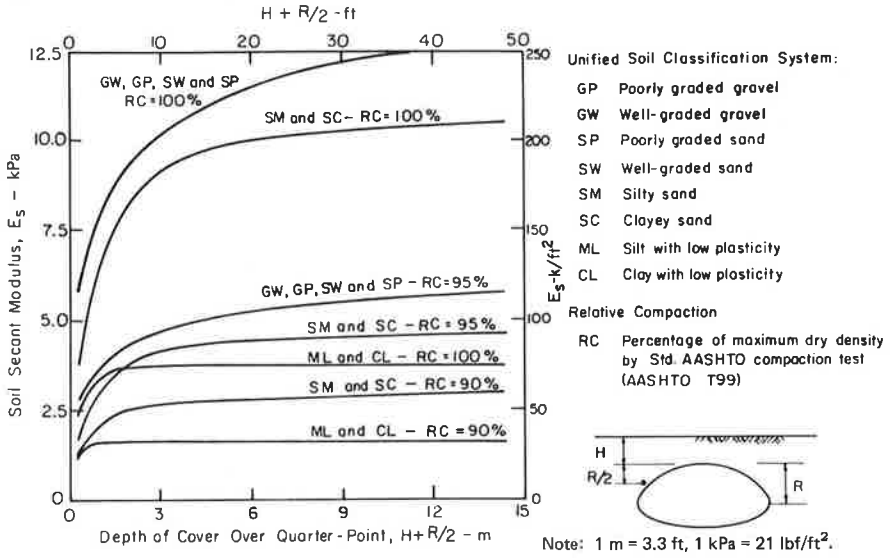

for live loads. As the depth of cover increases, the factors of safety against yield and development of a plastic hinge under live loads increase. By calculating factors of safety for a range of cover depths, it is possible to determine the minimum acceptable cover depth for a given culvert, backfill, and live load.

Minimum cover depths calculated using the SCI design method depend on a number of factors:

1. Culvert size or diameter,
2. Size of corrugation,
3. Metal thickness,
4. Yield stress of metal,
5. Backfill soil type,
6. Relative compaction of backfill, and
7. Magnitude of live load (only the HS-20 live load is considered in this paper).

Figure 5. Coefficients for live-load moments.

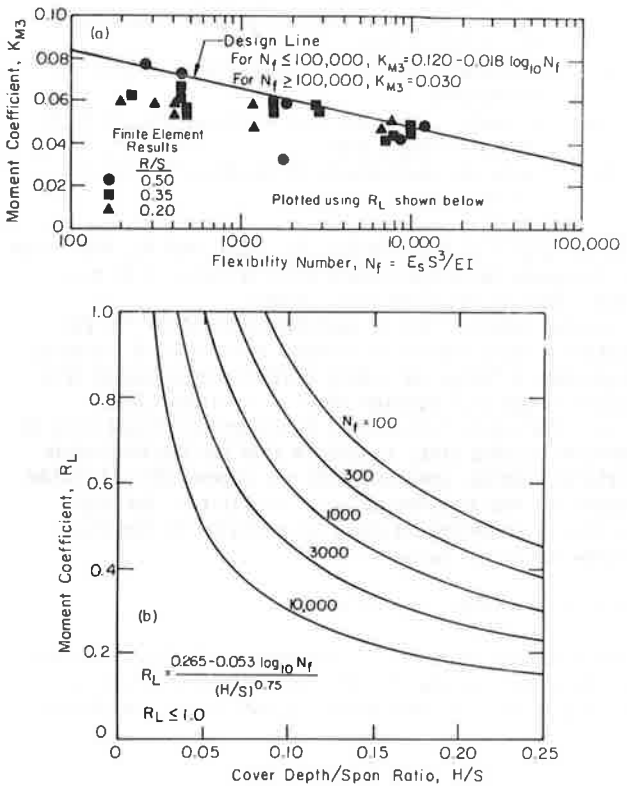

Minimum cover depths were determined for a range of culvert sizes and types so that these could be compared with minimum cover depths from published fill-height tables. These latter values are based on experience with field performance and thus provide a basis for determining if values calculated by the SCI design method are reasonable, because any method that gives values of minimum cover that differ greatly from those derived from long field experience must be considered not to be reflective of actual field behavior.

Minimum cover depths for 152 × 51-mm (6 × 2-in) corrugated steel circular pipe are shown in Table 1, together with those published by the U.S. Department of Transportation (DOT), Federal Highway Administration (FHWA), Bureau of Public Roads (BPR), American Iron and Steel Institute (AISI), and National Corrugated Steel Pipe Association (NCSPA). The criteria used in the SCI calculations were chosen to correspond closely to the conditions specified for the published fill-height tables: The value used for the yield stress of steel was 228 MPa (33 000 lb/in^2) in all cases. The unit weight of the backfill used in the SCI calculations was 19.6 KN/m^3 (125 lb/ft^3), compared to 18.8 kN/m^3 (120 lb/ft^3) specified for DOT, FHWA, BPR, AISI, and NCSPA fill-height tables. The relative compaction used in the SCI calculations was 90 percent of standard American Association of State Highway and Transportation Officials (AASHTO), as compared to 95 percent for the DOT, FHWA, and BPR tables and 85 percent for the AISI and NCSPA tables.

The values shown for the SCI method in Table 2 were calculated using the procedures outlined previously, except when the calculations indicated that a minimum cover depth less than 0.3 m (1 ft) would be acceptable. In those cases the minimum cover depth was made equal to 0.3 m, in accordance with experience and conventional practice.

It may be noted that the minimum cover depths calculated by the SCI method decrease with increasing metal thickness, except when the minimum is equal to 0.3 m. For example, for 4.5-m (15-ft) diameter pipes, the minimum cover depths calculated by the SCI method vary from 0.75 m (2.5 ft) for t = 2.77 mm (0.109 in or 12 gage) to 0.3 m for t = 7.1 mm (0.280 in or 1 gage). The other fill-height tables indicate a minimum cover depth of 0.6 m (2.0 ft) for all metal thicknesses. It is reasonable that minimum cover depth should decrease as metal thickness increases. One of the advantages of the SCI method over the use of experience alone for establishing

Table 1. Minimum cover depths for steel structural plate circular pipe HS-20 live load (152 x 51-mm corrugation).

Diameter (m)	Source	Minimum Depth of Cover (m) 2.8 mm Thick (12 gage)	4.3 mm Thick (8 gage)	5.5 mm Thick (5 gage)	7.1 mm Thick (1 gage)
1.5	SCI method	0.3	0.3	0.3	0.3
	DOT, FHWA, BPR	0.3	0.3	0.3	0.3
	AISI, NCSPA	0.3	0.3	0.3	0.3
3.0	SCI method	0.4	0.3	0.3	0.3
	DOT, FHWA, BPR	0.6	0.6	0.6	0.6
	AISI, NCSPA	0.5	0.5	0.5	0.5
4.6	SCI method	0.8	0.5	0.4	0.3
	DOT, FHWA, BPR	0.6	0.6	0.6	0.6
	AISI, NCSPA	0.6	0.6	0.6	0.6
6.1	SCI method		0.8	0.6	0.5
	DOT, FHWA, BPR			0.9	0.9
	AISI, NCSPA		0.8	0.8	0.8
7.6	SCI method				0.8
	DOT, FHWA, BPR				
	AISI, NCSPA				1.1

Notes: 1 m = 3.3 ft, 1 mm = 0.04 in.

Table 2. Minimum cover depths for corrugated steel circular pipe HS-20 live load (76 x 25-mm corrugation).

Diameter (m)	Source	Minimum Depth of Cover (m) 1.6 mm Thick (16 gage)	2.8 mm Thick (12 gage)	3.4 mm Thick (10 gage)	4.3 mm Thick (8 gage)
1.2	SCI method	0.3	0.3	0.3	0.3
	DOT, FHWA, BPR	0.3	0.3	0.3	0.3
	AISI, NCSPA	0.3	0.3	0.3	0.3
	US Steel	0.3	0.3	0.3	0.3
2.1	SCI method	0.5	0.4	0.3	0.3
	DOT, FHWA, BPR	0.3	0.3	0.3	0.3
	AISI, NCSPA	0.3	0.3	0.3	0.3
	US Steel	0.3	0.3	0.3	0.3
3.0	SCI method		0.6	0.5	0.4
	DOT, FHWA, BPR		0.6	0.6	0.6
	AISI, NCSPA		0.5	0.5	0.5
	US Steel		0.6	0.6	0.6

Notes: 1 m = 3.3 ft, 1 mm = 0.04 in.

Table 3. Minimum cover depths for corrugated steel circular pipe HS-20 live load (68 x 13-mm corrugation).

Diameter (m)	Source	Minimum Depth of Cover (m) 1.6 mm Thick (16 gage)	2.8 mm Thick (12 gage)	3.4 mm Thick (10 gage)	4.4 mm Thick (8 gage)
1.2	SCI method	0.3	0.3	0.3	0.3
	DOT, FHWA, BPR	0.3	0.3	0.3	0.3
	AISI, NCSPA	0.3	0.3	0.3	0.3
1.5	SCI method		0.3	0.3	0.3
	DOT, FHWA, BPR		0.3	0.3	0.3
	AISI, NCSPA		0.3	0.3	0.3
1.8	SCI method			0.4	0.3
	DOT, FHWA, BPR			0.3	0.3
	AISI, NCSPA			0.3	0.3
2.1	SCI method				0.4
	DOT, FHWA, BPR				0.3
	AISI, NCSPA				0.3

Notes: 1 m = 3.3 ft, 1 mm = 0.04 in.

Table 4. Minimum cover depths for corrugated aluminum circular pipe HS-20 live load (68 x 13-mm corrugation).

Diameter (m)	Source	Minimum Depth of Cover (m) 1.6 mm Thick (16 gage)	2.8 mm Thick (12 gage)	3.4 mm Thick (10 gage)	4.3 mm Thick (8 gage)
0.6	SCI method, KACS[a]	0.3	0.3	0.3	
	DOT, FHWA, BPR	0.3	0.3	0.3	0.3
1.2	SCI method, KACS[a]		0.4	0.4	0.3
	DOT, FHWA, BPR		0.3	0.3	0.3
1.8	SCI method, KACS[a]			0.5	0.4
	DOT, FHWA, BPR				0.3

Notes: 1 m = 3.3 ft, 1 mm = 0.04 in.
The values contained in the published fill-height tables (9) were established using the SCI method.
[a]KACS—Kaiser Aluminum and Chemical Sales, Inc.

minimum cover depths is that it provides a means of evaluating the benefits of increased metal thickness.

By comparing the values of minimum cover calculated using the SCI method with the values from the published fill-height tables, it may be seen that the calculated values are in good agreement with design experience. Because the values given by DOT, FHWA, BPR, AISI, and NCSPA tables are the same for all metal thicknesses in a given diameter, they are controlled by the requirements for the lightest gage, which requires the greatest depth of cover. The values of minimum cover calculated by the SCI method are in close agreement with the others for the lightest gage shown for each diameter, and smaller minimum cover depths are permitted by the SCI method for heavier gages.

Similar comparisons for 76 × 25-mm (3 × 1-in) corrugated steel pipe are shown in Table 2. In addition to values of minimum cover from the sources mentioned previously, those published by the U.S. Steel Corporation (10) are also shown in Table 2. Minimum cover depths for 68 × 13-mm (2⅔ × ½-in) corrugated steel pipe are given in Table 3, and values for 68 × 13-mm corrugated aluminum pipe are given in Table 4. In each case, the values given by the SCI method are in reasonable agreement with design experience as represented by the published fill-height tables.

MAXIMUM COVER DEPTHS

The factor of safety against seam compression failure calculated by the SCI design method provides a means of establishing maximum permissible cover depths for culverts. As shown in Table 5, similar values are used by DOT, FHWA, BPR (6), AISI (7), and NCSPA (8) design procedures, which also include criteria for buckling. However the buckling criterion is usually less critical than seam compression failure. DOT, FHWA, and BPR fill-height tables are also based on a limiting deflection equal to 5 percent of the nominal diameter, which controls the maximum fill heights in some cases.

Table 5. Criteria used in culvert design procedures.

Quantity	Value Used by Procedure Shown		
	DOT, FHWA, BPR	AISI, NCSPA	SCI Method
Yield stress for steel, MPa	228	228	228
Yield stress for aluminum, MPa	166	Not used	166
Unit weight of backfill, kN/m^3	18.8	18.8	19.6
Relative compaction, % of Std. AASHTO max. dry density	95	85	90
Vertical load on culvert	Equal to weight of overlying soil	86% of weight of overlying soil	130% of weight of overlying soil
Factor of safety on seam strength	3.33	2.0	1.5
Factor of safety on development of a plastic hinge	Not used	Not used	1.65[a]
Factor of safety on yield stress or buckling stress	2.0[b]	2.0[b]	1.1[c]
Modulus of soil reaction-E', MPa	9.7	Not used	Not used
Soil stiffness coefficient-k	0.22	Not used	Not used
Limiting deflection	5%	Not used	Not used

Notes: 1 MPa = 145 lbf/in^2, 1 kN/m^3 = 6.4 lb/ft^3.
[a] For cover depth less than one-fourth of span.
[b] For axial stress only flexural stress not considered.
[c] For combined axial and flexural stress, with elastic design.

Table 6. Maximum fill heights for steel structural plate circular pipe HS-20 live load (152 x 51-mm corrugation).

Diameter (m)	Source	Maximum Fill Height (m)[a]			
		2.8 mm Thick (12 gage)	4.3 mm Thick (8 gage)	5.5 mm Thick (5 gage)	7.1 mm Thick (1 gage)
1.5	SCI method	22	42	59	71
	DOT, FHWA, BPR	13	25	32	38
	AISI, NCSPA	25	48	62	80
3.0	SCI method	10	20	27	36
	DOT, FHWA, BPR	7	12	15[b]	16[b]
	AISI, NCSPA	12	24	31	40
4.6	SCI method	6	12	18	23
	DOT, FHWA, BPR	4	8	11	13
	AISI, NCSPA	8	16	21	27
6.1	SCI method		9	13	17
	DOT, FHWA, BPR			9	11
	AISI, NCSPA		11[c]	14[c]	18[c]
7.6	SCI method				13
	DOT, FHWA, BPR				
	AISI, NCSPA				12[c]

Notes: 1 m = 3.3 ft, 1 mm = 0.04 in.
[a] Controlled by seam strength except as noted.
[b] Controlled by deflection criterion.
[c] Controlled by buckling criterion.

Table 7. Maximum fill heights for aluminum structural plate circular pipe HS-20 live load (229 x 64-mm corrugation with steel bolts).

Diameter (m)	Source	Maximum Fill Height (m)[a]			
		2.5 mm Thick	3.8 mm Thick	5.1 mm Thick	6.4 mm Thick
2.0	SCI method, KACS[b]	8	15	21	24
	DOT, FHWA, BPR			14	17
2.7	SCI method, KACS[b]	6	10	15	18
	DOT, FHWA, BPR			10	12
3.7	SCI method, KACS[b]	4	8	10	13
	DOT, FHWA, BPR			8	9
4.6	SCI method, KACS[b]		6	8	10
	DOT, FHWA, BPR			6	7

Notes: 1 m = 3.3 ft, 1 mm = 0.04 in.
[a] All values controlled by seam strength. Values for SCI and KACS determined using backfill unit weight = 22.0 kN/m^3. Values for DOT, FHWA, BPR determined using backfill unit weight = 19.6 kN/m^3.
[b] The values contained in the published fill height tables were established using the SCI method.

Calculated values of maximum fill height for steel structural plate pipe are given in Table 6. It may be noted that the values calculated using the SCI method are somewhat smaller than those calculated using the AISI and NCSPA procedure. The differences are due to differences in the vertical loads on the culverts and the factors of safety on seam strength. In some cases the maximum fill heights calculated using the AISI and NCSPA procedure are determined by buckling considerations, and in these cases the values are closer to those calculated by the SCI procedure.

The values calculated by the SCI method are consistently larger than those determined by the DOT, FHWA, and BPR procedure. The differences are due to differences in vertical load on the culvert and the factor of safety on seam strength, and also the deflection criterion used by the DOT, FHWA, and BPR procedure.

Maximum fill heights for aluminum structural plate pipe are given in Table 7. The values published by Kaiser Aluminum and Chemical Sales, Inc. (KACS) (9) were calculated using the SCI method and, therefore, are the same as the SCI values in all cases. The values calculated using the DOT, FHWA, and BPR procedure

are smaller, for the same reasons discussed in reference to steel structural plate.

CONCLUSION

The SCI design procedure provides a rational method for determination of both minimum depths of cover and maximum fill heights. Values of minimum cover calculated using the SCI method compare well with design experience as reflected in values from published fill-height tables. The advantage of the SCI method is that it provides a rational procedure for including the effects of all the variables that affect minimum cover, namely diameter, corrugation size, metal thickness, yield stress, backfill type, degree of compaction, and magnitude of live load. The ability to account for the effects of these factors in a rational way is especially important for long-span culverts, where cover depths are often small.

Values of maximum cover calculated using the SCI method are somewhat smaller than those calculated using the AISI and NCSPA procedure. They are considerably larger than those calculated using the DOT, FHWA, and BPR procedure, especially in cases where the latter values are determined by consideration of calculated deflections.

Although all the examples of the use of the SCI method in this paper are for circular pipes, the method is also applicable to pipe-arch and arch structures. It is particularly useful for design of long-span culvert structures, for which considerations of performance under live load with shallow cover are of prime importance.

ACKNOWLEDGMENT

I am grateful to Kaiser Aluminum and Chemical Sales, Inc., for sponsoring the research studies that led to the development of the SCI method, and to Kai Wong and Gary Jaworski of the University of California, Berkeley, geotechnical research staff, who performed the finite element analyses.

REFERENCES

1. J. M. Duncan. Behavior and Design of Long-Span Metal Culvert Structures. Paper presented at the Technical Session on Soil-Structure Interaction for Shallow Foundations and Buried Structures, ASCE National Convention, San Francisco, Oct. 1977.
2. J. R. Allgood and S. K. Takahashi. Balanced Design and Finite Element Analysis of Culverts. HRB, Highway Research Record 413, 1972, pp. 45-56.
3. J. R. Abel, R. Mark, and R. Richards. Stresses Around Flexible Elliptic Pipes. Journal of the Soil Mechanics and Foundations Division, Proc., ASCE, Vol. 99, No. SM7, 1973, pp. 509-526.
4. M. G. Katona, J. B. Forrest, R. J. Odello, and J. R. Allgood. Computer Design and Analysis of Pipe Culvert. U.S. Naval Civil Engineering Laboratory, Port Hueneme, Internal Technical Rept., CA 51-040, FHWA 3-1-1170, 1974.
5. K. S. Wong and J. M. Duncan. Hyperbolic Stress-Strain Parameters for Nonlinear Analyses of Stresses and Movements in Earth Masses. University of California, Berkeley, Geotechnical Engineering Rept., TE 74-3, 1974.
6. E. W. Wolf and M. Townsend. Corrugated Metal Pipe: Structural Design Criteria and Recommended Installation Practice. U.S. Bureau of Public Roads, U.S. Government Printing Office, 1970.
7. Handbook of Steel Drainage and Highway Construction Products, 2nd Ed. American Iron and Steel Institute, New York, 1971.
8. Corrugated Steel Pipe. National Corrugated Steel Pipe Association, Chicago.
9. Aluminum Storm Sewers. Kaiser Aluminum and Chemical Sales, Inc., Oakland, CA, 1976.
10. Fill Heights for 3- by 1-in. Corrugated Steel Pipe in 'Good' Backfill. United States Steel Corp., Pittsburgh, 1967.

Publication of this paper sponsored by Committee on Subsurface Soil-Structure Interaction.

Analysis of Long-Span Culverts by the Finite Element Method

Michael G. Katona, University of Notre Dame, Notre Dame, Indiana

The long-span culvert is a synergistic unit composed of a corrugated metal liner and a compacted soil envelope that surrounds the liner. Conceptually, the system is very simple and, therefore, economically attractive as a bridge substitute. Analytically, however, the system is not simple because of the modeling difficulties associated with soil-structure interaction. Using the finite element method, this study investigates the influence of fundamental modeling assumptions on the behavior of long-span culverts. Two basic modeling assumptions are examined: large deformation theory versus small deformation theory and monolith structure versus incremented structure. In addition, the sensitivity of the following parameters are determined: compaction loads, soil stiffness, liner gage, liner shape, and special features of manufacturers. Results are shown graphically by comparing crown displacement histories between parametric families. Comparisons of maximum moment and thrust are also reported. Based on these studies, recommendations for analytical modeling techniques are summarized. The intent of this study is to provide a foundation for other studies. A systematic investigation of modeling assumptions and parameter sensitivity is a necessary step toward an analytical model for long-span culverts.

The long span is an arch or closed-shaped corrugated metal liner surrounded by compacted soil, where the horizontal span measures from 5 to 15 m (15 to 50 ft) or more. A primary use is to serve as a bridge substitute. To date, more than 600 long-span systems have been installed, and manufacturers estimate a cost savings from 30 to 75 percent over comparable conventional bridge structures. In view of the current bridge repair and replacement problem in the United States

(the Federal Highway Administration estimates that nearly 18 percent of all U.S. bridges are in disrepair or functionally obsolete), use of long-span structures will probably increase markedly. Accordingly, analytical studies of long spans are timely and can lead to improved design methods. However, in order to properly analyze long-span systems, the basic construction process must be understood.

The long span is usually constructed by bolting together curved, structural plates of corrugated metal into the shape of an arch, with the ends anchored into concrete footings. Or in some cases, elliptical or inverted pear-shaped sections are used with special beddings instead of footings. Figure 1 illustrates some basic shapes and nomenclature popularly used for long-span structures. The most important step in the construction process is placing soil (backfilling) around the corrugated metal liner. The soil must be of good structural quality and properly compacted one lift at a time, symmetrically on both sides of the liner. During this process, the lateral soil pressure moves the sides of the liner inward and the crown upward (peaking).

Figure 1. Typical long-span liner shapes and nomenclature.

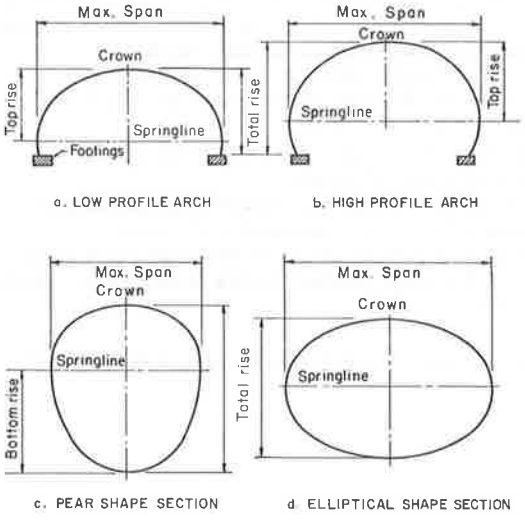

Figure 2. Special features of long spans.

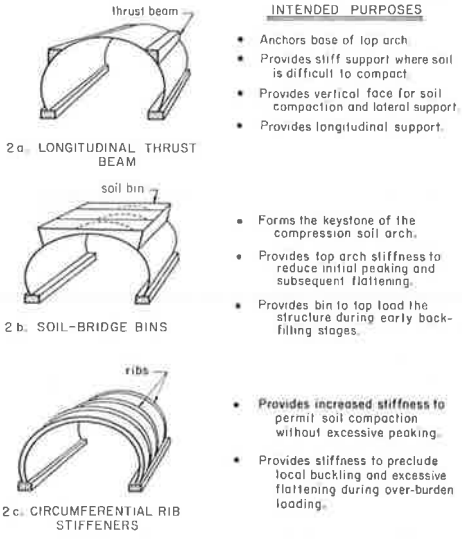

Once the backfill soil is level with the crown, subsequent soil lifts reverse this trend by pushing the crown downward and the sides outward. Outward movement mobilizes lateral soil resistance, which limits both lateral and vertical movement.

Indeed, the interaction of the soil and liner working in tandem provides the remarkable structural integrity of the long-span system. Either component, liner or soil, acting by itself would be wholly inadequate to support the loads. To promote and improve this synergistic relationship between liner and soil, several special features have been employed by various manufacturers. Some commonly used features are thrust beam, soil bin, and rib stiffeners (shown in Figure 2). Additional background information can be found in the excellent survey by Selig and others (1).

ANALYSIS-DESIGN PROBLEM

For the most part, current design methods are based on experience rather than on a viable analytical model (1). This is because a reasonable analytical model is complicated even though the long span is a conceptually simple system. Complications are due to the soil-structure interaction phenomena; that is, a long-span model must include the soil as a structural element—it cannot simply assume the soil loads on the liner. Other modeling difficulties include incremental construction (i.e., modeling the soil placement schedule during construction), various shapes, footings, and special features, as well as consideration of soil compaction, interface slippage, and other nonlinear behavior.

The finite element method (FEM) appears to be the best method for formulating and solving this complicated boundary value problem. Indeed, this is a singular point of common agreement among investigators of soil-structure interaction (1, 2, 3, 4, 5, 6, 7). In particular, recent applications of FEM to long-span systems show great promise for understanding long-span behavior (8, 9, 10). FEM is well established and has become an indispensable tool in structural research (11).

The objective is to present analytical results of a parameter study that compares various modeling assumptions of long-span culverts. The following parameters are examined using FEM:

1. Influence of large deformation theory versus small deformation theory;
2. Influence of manner of loading (i.e., monolith structure versus incremented structure with and without compaction loads);
3. Effect of fill soil stiffness (modulus);
4. Effect of liner stiffness (gage);
5. Effect of liner shape (high profile, low profile, and ellipse); and
6. Effect of special features (thrust beam, soil bin, and rib stiffeners).

The first two studies deal with the question of how to simulate the real-world behavior of long spans. The remaining studies compare the structural behavior of different idealized systems.

These objectives have a twofold purpose: (a) they provide a foundation or benchmark for other studies to compare with and build on, with the ultimate goal of achieving an accepted model; and (b) they illustrate the comparative performance between various long-span concepts.

To satisfy the objectives, a basic idealization of a typical long-span system is assumed. This basic model is used as a common reference for generating 15 different idealizations by selectively changing the system

Table 1. Parameter identification per FEM solution.

Computer[a] Designation	Liner[b] Shape	Special[c] Features	Loading[d] Method	Compaction[e] Pressure (kPa)	Fill Soil[f] Modulus (kPa)	Liner[g] Thickness Gage
A-A	HP	N	MONO	0.0	13 800	5
A-B	HP	N	MONO	0.0	13 800	5
A	HP	N	MONO	0.0	13 800	5
B	HP	N	INC	0.0	13 800	5
C (Basic)	HP	N	INC	34.5	13 800	5
D	HP	N	INC	69.0	13 800	5
E	HP	N	INC	34.5	6 900	5
F	HP	N	INC	34.5	21 600	5
G	HP	N	INC	34.5	nonlinear	5
H	HP	N	INC	34.5	13 800	10
I	HP	N	INC	34.5	13 800	1
J	LP	N	INC	34.5	13 800	5
K	EL	N	INC	34.5	13 800	5
L	HP	TB	INC	34.5	13 800	5
M	HP	SB	INC	34.5	13 800	5
N	HP	RS	INC	34.5	13 800	5

Note: 1 kPa = 0.15 lb/in^2.

[a] Run No. A-A (small deformation) and A-B are ADINA program, all others are CANDE.
[b] Liner shape: HP = high profile, LP = low profile, EL = ellipse.
[c] Special features: N = liner only, TB = thrust beams, SB = soil bins, RS = rib stiffeners.
[d] Loading method: MONO = monolith system, INC = incremented system, density = 18.9 kN/m^3 (120.96 lb/ft^3).
[e] Compaction pressure is applied to side soil lifts and removed on subsequent lift.
[f] Soil modulus is Young's modulus, Poissons ratio = 0.35 always.
[g] Liner is standard structural steel corrugation 15 x 5 cm (6 x 2 in).

parameters. Table 1 lists each idealization and the system parameters: liner shape, special features, loading method, compaction pressure, soil modulus, and liner gage. The basic idealization is designated as run C and is a high-profile arch, no special features, incremented construction with 34-kPa (5-lb/in^2) temporary compaction pressure; soil modulus is 13 800 kPa (2000 lb/in^2) and liner is 5-gage steel.

Solutions of these idealizations are obtained by the finite element program CANDE (12) except for the case of large deformations, which is solved by program ADINA (13). CANDE is a special-purpose program intended for soil-structure interaction studies and ADINA is a multipurpose program oriented to solid mechanics. Fundamental assumptions common to all solutions are plane-strain geometry, linear material properties (except in one case), and time-independence (i.e., no inertia or viscosity). The soil and footing are assumed to behave as a continuum and the metal liner is treated as a thin shell.

By grouping appropriate solutions, the effect of each parameter can be ascertained by inspecting the key responses—crown deflection, maximum thrust, and maximum moment in the liner wall.

PARAMETER INVESTIGATION

The long-span configuration chosen for the basic model is an 11.0-m (36-ft) high-profile arch with a 3.40-m (11-ft 2-in.) rise. Figure 3 portrays the basic idealization showing the in situ soil zone below the footing and the fill soil zone [18.9 kN/m^3 (120 lb/ft^3)] above the footing level. The soil zones, concrete footing, and metal liner are assumed to be bonded at material interfaces, and each zone is homogeneous with the elastic properties noted at the bottom of the figure.

The FEM discretization of the idealization is shown in Figure 4. Because of symmetry, only half of the system is modeled, with a total of 253 elements. Seventeen beam-column elements are connected to form the metal liner; the 17th element is buried in the concrete footing. The concrete footing (4 elements), in situ soil (90 elements), and fill soil (144 elements) are four-node quadrilateral or three-node triangular continuum elements with two degrees of freedom per node. In the CANDE program the continuum elements include high-order nonconforming displacement functions, whereas in the ADINA program they are standard isoparametric elements.

To accommodate the special features, the basic finite element mesh is altered slightly to model the thrust beam and soil bin. With regard to liner shape, only the bottom half of the mesh is changed to achieve a low profile or elliptical shape.

Large Deformation

This study illustrates the order of the error from using small deformation theory in the analysis of long-span systems. By considering the basic long-span model as a monolith, solutions for large and small deformation theories were obtained by means of the ADINA program (Run A-A and A-B, Table 1). The difference between solutions may be observed in Figure 5 by comparing deformed shapes of the metal liner. Deformed shapes are determined by adding (and magnifying) displacements to the corresponding points of the undeformed position after subtracting vertical rigid body movement of the footing.

The important observation is that the large deformation solution is not significantly different than the small deformation solution; the differences at most are 8 percent at the crown. As a general trend, the large deformation responses are slightly higher in magnitude than the small deformation responses.

For the large deformation theory, both Lagrangian and Eulerian coordinate descriptions give essentially identical results even though the same elastic properties are used in both descriptions. Therefore, it may be concluded that large strains do not come into play so that all differences between large and small deformation solutions are attributed to large rotations.

Figure 1 also illustrates a cross-check between the ADINA and CANDE programs (Run A-A and A, Table 1). The two solutions overlay each other with an error of less than 1 percent, thereby providing validation and confidence in the respective algorithms.

Monolith Versus Incremental

In this study a comparison is made between idealizing the long-span system as monolith versus an incremental system (Run A and B, Table 1). A monolith system may be imagined by assembling the long-span system

Figure 3. Description of basic model idealization.

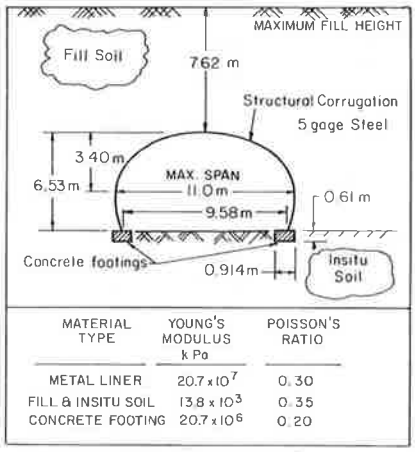

MATERIAL TYPE	YOUNG'S MODULUS k Pa	POISSON'S RATIO
METAL LINER	20.7×10^7	0.30
FILL & INSITU SOIL	13.8×10^3	0.35
CONCRETE FOOTING	20.7×10^6	0.20

Note: 1 m = 3.3 ft, 1 kPa = 0.15 lb/in^2.

Figure 4. FEM representation of basic model.

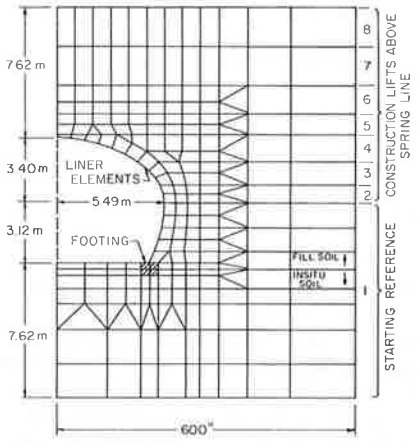

Note: 1 m = 3.3 ft.

Figure 5. Deformed shapes for small and large deformation theories.

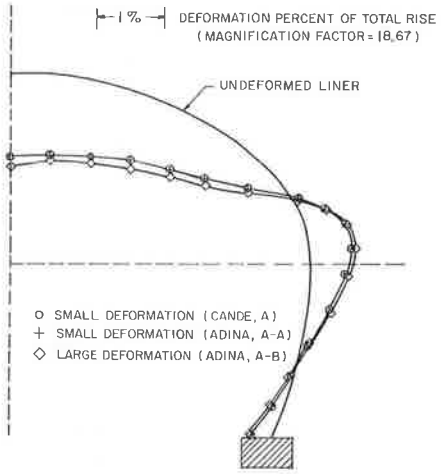

Figure 6. Influence of loading conditions on crown deflection.

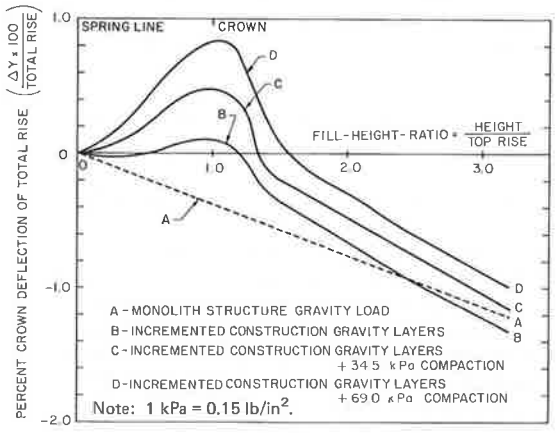

with gravity turned off. Once all the soil is in place, gravity is turned on and the system deforms under its own weight.

A more realistic modeling technique is incremental construction, which attempts to simulate the actual construction process. Here the soil system is divided into a series of soil lifts. Each lift is added into the system one at a time and the structural responses are accumulated.

Figure 4 illustrates the assignment of construction increments used in this study. The reference configuration (unloaded system) includes the liner, footing, in situ soil, and fill soil up to the springline, followed by seven gravity-loaded construction increments from the springline to the top. The reference configuration begins at the springline rather than at the footing level because construction increments placed between the footings and springline tend to hang from the liner in tension and give unrealistic results. [Special nonlinear soil models or interface elements may be used to correct this problem (12).]

The effect of monolith and incremental loading on crown displacement is shown in Figure 6 by curves A and B, respectively. Crown displacement is given as percentage of total rise (positive implies peaking), and is plotted as a function of fill-height ratio. Fill-height ratio is defined as fill height above springline divided by the top rise. Thus, if the fill-height ratio is 1, the current soil height is level with the crown.

Although the monolith structure (curve A) is not a function of intermediate fill heights, it is plotted as a straight line and the assumption is made that fill height corresponds to percentage of gravity so that full fill height implies full gravity.

The obvious difference between curves A and B is that the incremental solution shows a slight peaking when the fill height is near the crown, whereas the monolith solution is incapable of producing such a response. However, as the fill-height ratio increases beyond 2.0, the discrepancy becomes less pronounced. At full height, the crown displacement ratio is 0.92 (monolith/incremental). Other key response ratios at full height are thrust = 1.04 and moment = 1.08. Ratios are monolith divided by incremental evaluated at springline.

Effect of Compaction Loads

Compaction loads are all temporary loads that advertently or inadvertently compact the soil on the sides of the liner (e.g., vehicles, sheepsfoot rollers, heavy equipment, and hand compacters). Field observations indicate that compaction loads contribute more significantly to lateral movement and peaking than does the gravity weight of the soil layer.

A rigorous analytical model of compaction is very

Table 2. Key response ratios at full fill height.

Key Response Ratio	Parameter and Run Number											
	Compaction Loads		Soil Stiffness			Liner Thickness		Liner Shape		Special Features		
	A None	D Double	E One-Half	F Double	G Nonlinear	H Gage 10	I Gage 1	J Low Profile	K Ellipse	L Thrust Beam	M Soil Bin	N Stiff Ribs
Displacement ratio (crown)	1.15	0.85	1.99	0.52	0.88	1.02	0.99	0.83	2.17	0.99	1.09	0.85
Thrust ratio* (near springline)	1.02	0.98	1.01	0.98	0.99	0.99	1.00	0.95	0.90	1.02	1.01	1.01
Moment ratio (near springline)	1.02	0.98	1.69	0.58	0.89	0.69	1.23	1.09	0.71	1.06	1.00	12.1

Notes: For reference, values of run No. C are relative crown displacement = -7.62 cm (-3.002 in), maximum thrust = -15 516.8 kPa/cm (-5522 lb/in), and maximum moment = -17 257.1 N-m/m (-3878 in · lb/in).

*Both maximum moment and maximum thrust generally occured at first node above springline.

Figure 7. Effect of soil stiffness on crown deflection.

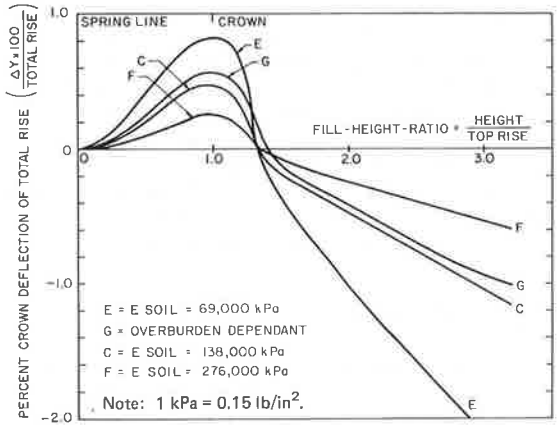

difficult because it requires describing the location, magnitude, and character of all temporary loads, including inertia effects. Moreover, a nonconservative soil model (e.g., plasticity model) must be used so that residual lateral stresses will remain after the compaction load is removed.

In this study a simplified compaction technique is used that simulates the effect of compaction and is applicable for both linear and nonlinear soil models. To start, a uniform pressure, which represents all compaction loads at this level, is applied along the surface of the first construction increment (except for the elements adjacent to the liner) and a solution obtained. Next, the second soil lift is added to the system and another uniform pressure applied to its surface. At the same time, the first pressure load is removed by applying an equal but opposite pressure. These pressures squeeze the second lift and increase lateral pressure on the liner via the Poisson effect. The process is repeated for each lift up to the crown. Above the crown the process is terminated by removing the last compaction pressure so that no compaction loads remain in the system.

The effect of applying this technique is illustrated in Figure 6 by curves B, C, and D (see Table 1), which represent no compaction, 34.5-kPa (5.0-lb/in^2), and 69.0-kPa (10.0-lb/in^2) compaction pressures, respectively. Note that as compaction pressure increases, maximum peaking increases substantially. Indeed, curves C and D are more representative of actual field behavior than curve B (for this reason run C was selected as standard).

As the fill height increases beyond the crown level, the differences between the curves begin to decrease. At full fill height, Table 2 compares ratios between crown displacements by using the basic model (run C) as standard. Each response ratio is formed by dividing the corresponding response of the run number by run C. In addition, comparison ratios are given for maximum moment and thrust located slightly above springline. It is observed that the final effect of compaction loads on maximum moment and thrust is negligible.

Effect of Soil Stiffness

The effect of soil stiffness is examined by specifying Young's modulus of the fill soil as 6900, 13 800, and 27 600 kPa (1000, 2000, and 4000 lb/in^2), corresponding to runs E, C, and F of Table 1. In addition, the effect of a rudimentary nonlinear model known as the overburden-dependent soil model (12) is investigated (run G, Table 1). Here the tangent Young's modulus increases with overburden pressure from a low of 6900 kPa (1000 lb/in^2) to 20 700 kPa (3000 lb/in^2) at full fill-height pressure. In all cases Poisson's ratio is held constant at 0.35 and the in situ soil stiffness is unaltered from the basic model.

Curves E, C, and F in Figure 7 depict the influence of elastic soil stiffness on crown deflection during the construction sequence. Maximum peaking and maximum flattening occur almost in inverse proportion to the soil stiffness. The comparison ratios in Table 2 reveal that thrust is practically unaffected by soil stiffness, whereas moment is influenced in the same manner as displacements but to a lesser degree.

The overburden-dependent model, curve G in Figure 7, shows greater peaking but less flattening than the basic model, curve C. This is expected since the stiffness changes from less than to greater than the basic model as fill height is increased. In summary, it is significant to note that deflection is directly controlled by soil stiffness, whereas thrust is not appreciably changed.

Effect of Liner Gage

The practical range of liner thicknesses for 15 × 5-cm (6 × 2-in) corrugation is gage 10 through 1. In this study, gage sizes 10, 5, and 1 are compared (i.e., runs C, H, and I of Table 1).

Section properties are shown in the insert of Figure 8, and curves C, H, and I show the history of crown deflection for each gage. Interestingly, deflection histories are practically unaffected by the gage even though

Figure 8. Effect of liner gage on crown deflection.

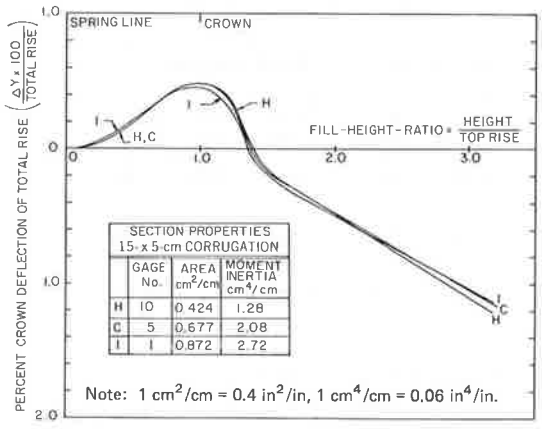

Figure 9. Effect of liner shape on crown deflection.

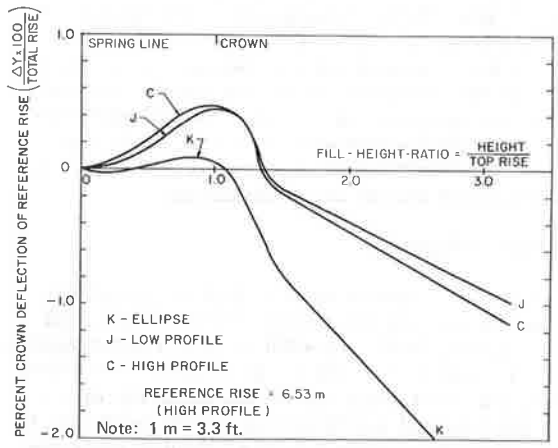

Figure 10. Effect of special features on crown deflection.

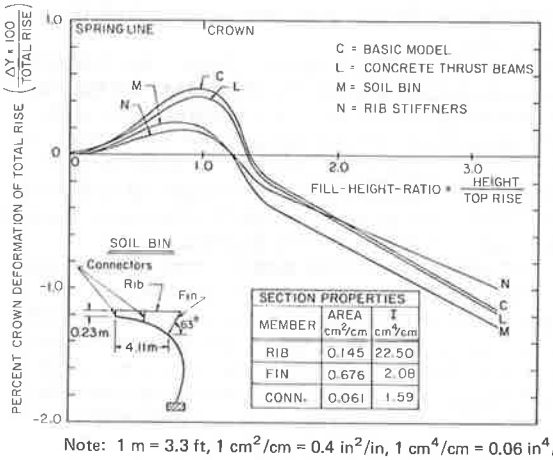

Note: 1 m = 3.3 ft, 1 cm²/cm = 0.4 in²/in, 1 cm⁴/cm = 0.06 in⁴/in.

bending stiffness (moment of inertia) is more than doubled. From the previous study one concludes that soil stiffness dominates liner stiffness and controls the deformed shape. Of course, in the early stages of construction, when the soil height is below the springline, this conclusion is not valid because the soil mass is too small to dominate the system. Here stiff liners are useful to maintain shape and provide lateral resistance for compaction. From Table 2, observe that thrust is unaffected by liner stiffness, whereas moment increases significantly with liner stiffness.

Effect of Liner Shape

Three fundamental shapes are compared: high-profile arch, low-profile arch, and ellipse, corresponding to runs C, J, and K in Table 1. All shapes have the same span and top rise so that the basic finite element mesh (Figure 4) is unaltered above the springline.

To model the ellipse, the bottom half of the basic mesh is replaced by a mirror image of the top half; thus, a horizontal ellipse is formed that has a total rise of 6.81 m (22.3 ft). For the low-profile arch, additional elements are added to raise the floor and footing of the basic mesh to 0.36 m (1.17 ft) below the springline so that the total rise is 3.76 m (12.3 ft). One liner element is used between the springline and the footing and the last element is anchored in the footing to provide continuity.

Figure 9 illustrates the history of crown deflection for each shape as a percentage of the common reference rise, 6.53 m (21.4 ft). Thus, the deflection histories may be compared directly. Note deflections of the high- and low-profile arches follow similar trends, but the high-profile arch is slightly more flexible. However, the ellipse exhibits very little peaking but excessive flattening, more than twice that of the high-profile arch.

Observe in Table 2 that the ellipse affords a moderate reduction of thrust and moment compared to the high-profile arch, whereas the low-profile arch exhibits a slight decrease in thrust and an increase in moment.

Effect of Special Features

The performance of special features (thrust beam, soil bin, and rib stiffeners) illustrated in Figure 2 are compared to each other and the basic model, corresponding to runs C, L, M, and N in Table 1. Note, however, that the finite element idealizations do not mimic all of the intended functions of each special feature. This must be kept in mind when interpreting the results.

To model the thrust beam, triangular continuum elements are added to the basic mesh forming a triangular concrete ear measuring 1.04 m (3.42 ft) on the horizontal leg and 0.71 m (2.33 ft) on the vertical leg. The acute angle is located 3.66 m (12.0 ft) off the center line. Material properties are the same as the concrete footing shown in Figure 3. The ear is assumed part of the initial configuration.

Modeling of the soil bin is approximated by superimposing a steel frame structure on the liner, as shown in the insert of Figure 10. The section properties of the rib and connection members represent smeared averages over the rib spacing interval, whereas the fin is continuous and has the same properties as the liner. Shaped rib stiffeners are easily incorporated into the basic mesh by increasing the sectional properties of the liner. Again section properties are approximated by a smeared average over the rib spacing interval. For this example, the composite liner moment of inertia is 82.0 cm⁴/cm (5.0 in⁴/in) and the composite liner area is 1.12 cm²/cm (0.44 in²/in). Properties approximate a curved I-beam (12WF36) spaced at 1.5-m (5-ft) intervals and bonded to the liner. Note that the stiffened liner is nearly 40 times stiffer in bending than the unstiffened liner.

Curves C, L, M, N in Figure 9 illustrate the effect of each special feature on the history of crown deflection. As might be expected, the rib stiffeners and soil bin substantially limit peaking (curves M and N). How-

ever, as fill height is increased, the soil bin structure exhibits slightly more flattening than the other structures. The thrust beam (curve L) provides a modest reduction in peaking but for the most part behaves like the basic model (curve C). At least one attribute of the thrust beam not modeled in this analysis is that higher compaction (soil stiffness) can be achieved in the soil adjacent to the thrust beam.

At full fill height, Table 2 shows that the maximum moment of the rib-stiffened structure is increased an order of magnitude due to the large increase in bending stiffness. However, other key responses are not significantly altered by the special features.

SUMMARY AND CONCLUSIONS

This study illustrates the influence of fundamental modeling assumptions in applying the finite element method to long-span systems. Based on these studies, the following findings, conclusions, and recommendations are offered:

1. Solutions that use large deformation theory do not differ appreciably from those that use small deformation theory; the discrepancy is less than 8 percent. This discrepancy is due to large rotations, not large strains. Therefore, small deformation theory and infinitesimal stress-strain laws may be used for analyzing long-span systems if the percentage of crown deflection remains within practical limits, say 2 percent.
2. At full fill height a monolith representation yields a solution in approximate agreement (10 percent discrepancy) with an incremented system. However, a monolith system is incapable of tracking the history of deformation such as maximum peaking, nor can it consider compaction loads. As a general rule monoliths have limited value in long-span analysis. Incremented techniques should be used.
3. Compaction pressure placed on each soil-layer increment produces peaking several times greater than the gravity weight of the soil. (This correlates with field observations.) Thus compaction loads should be included in long-span analysis.
4. Soil stiffness (Young's modulus) dictates the magnitude of the liner deformation (i.e., deformation is in inverse proportion to soil stiffness). Since liner deformation is primarily due to bending (as opposed to membrane contraction), the liner bending moments are also inversely proportional to soil stiffness. However, thrust is insensitive to soil stiffness. Evidently, the selection of a soil model (linear or nonlinear) is crucial for predicting the deformed shape of the liner.
5. Liner bending stiffness within the range of standard gage sizes for structural corrugation has negligible effect on controlling liner deformation when the fill soil is above the springline. In other words, the soil stiffness dominates the system so that the deformed shape is not changed when using a heavier gage. As a consequence, the maximum moment increases in proportion to the bending stiffness because the deformed shape does not change appreciably with gage. Thrust remains insensitive to liner gage, therefore thrust stress is reduced in proportion to the sectional area. Rather than conclude that increasing bending stiffness by heavier gage is of no value to reduce deflection, it is recognized that stiff liners are beneficial in early stages of construction to maintain shape and provide compaction resistance.
6. With regard to liner shape, high- and low-profile arches exhibit similar structural responses, but the high profile is slightly more flexible. In contrast, the ellipse exhibits very little peaking but shows excessive flattening due to the simultaneous deformation of top and bottom arches. Correspondingly, thrust is reduced by 10 percent due to increased soil arching.
7. Special features, thrust beam, soil bin, and rib stiffeners exhibit no marked difference in crown deflection at full fill height. However, during the incremental construction process, the circumferentially stiffened structures (soil bin and rib stiffeners) exhibit significantly less peaking than the less-stiffened structures.

The questions pursued in this study are fundamental. It is hoped the findings will provide a foundation or benchmark for other studies. Many more detailed areas of study and experimental programs need to be undertaken before a universally accepted long-span model is established. The area of singular concern is characterization of the soil because it controls the deformation of the entire system. When investigators come to agreement on a soil model, then agreement on an accepted modeling practice of long-span systems is not far behind.

ACKNOWLEDGMENTS

I wish to express appreciation to the Federal Highway Administration and the technical monitor, George P. Ring, for sponsoring this effort. This work is part of an ongoing research study in the Department of Civil Engineering, University of Notre Dame. Thanks are extended to Rene Orillac, research assistant at Notre Dame, for his support in this study.

REFERENCES

1. E. T. Selig, J. F. Abel, F. H. Kulhawy, and W. E. Falby. Review of the Design and Construction of Long-Span, Corrugated-Metal, Buried Conduits. Federal Highway Administration, Technical Rept. HRS-14, Oct. 1977.
2. M. G. Katona and J. M. Smith. A Modern Approach for Structural Design of Pipe Culverts. 2nd International Conference on Computers in Engineering and Building Design. IPC Science and Technology Press Limited, Guildford, Surrey, England, CAD76, 1976.
3. R. J. Krizek and others. Structural Analysis and Design of Pipe Culverts. NCHRP, Rept. 116, 1971.
4. C. B. Brown, D. R. Green, and S. Pawsey. Flexible Culverts Under High Fills. Proc., ASCE, Vol. 94, No. ST4, April 1968.
5. J. F. Abel and R. Mark. Soil Stresses Around Flexible Elliptical Pipes. Proc., ASCE, Vol. 99, No. SM7, July 1973, pp. 509-526.
6. J. M. Duncan. Finite Element Analysis of Buried Flexible Metal Culvert Structures. Laurits Bjerrum Memorial Vol., March 1975.
7. G. A. Leonards. Performance of Pipe Culverts Buried in Soil. Department of Civil Engineering, Purdue Univ., Lafayette, IN.
8. J. F. Abel, G. A. Nasir, and R. Mark. Stresses and Deflections in Soil-Structure Systems Formed by Long-Span Elliptic Pipe. Armco Steel Corp., Princeton Univ., July 1977.
9. J. M. Duncan. Design Studies for a 35-ft. Span Aluminum Culvert for Greenbrier County, West Virginia. Kaiser Aluminum, San Francisco, July 8, 1975.
10. J. M. Duncan. Behavior and Design of Long-Span Metal Culvert Structures. Journal of the Geo-

technical Engineering Division, Proc., ASCE, in press.
11. O. C. Zienkiewicz. The Finite Element Method in Engineering Science. McGraw-Hill Book Co., London, 1971.
12. M. G. Katona and others. CANDE: Engineering Manual—A Modern Approach for the Structural Design and Analysis of Buried Culverts. CANDE: System Manual. CANDE: User Manual. Repts. to the Federal Highway Administration, HRS-14, 1976.
13. K. J. Bathe. ADINA: A Finite Element Program for Automatic Dynamic Incremental Nonlinear Analysis. Acoustics and Vibration Laboratory, Department of Mechanical Engineering, MIT, Cambridge, Rept. 82448-1, 1975.

Publication of this paper sponsored by Committee on Subsurface Soil-Structure Interaction.